ALMA MATER STUDIORUM - Università di Bologna

Dottorato di Ricerca in

Meccanica e Scienze Avanzate dell'Ingegneria

Ciclo XXVII

Settore Concorsuale di afferenza: 09/A1 - INGEGNERIA AERONAUTICA, AEROSPAZIALE E NAVALE

Settore Scientifico disciplinare: ING-IND/03 - MECCANICA DEL VOLO

TITOLO TESI

DYNAMICS AND CONTROL ISSUES OF MULTI–ROTOR PLATFORMS

Presentata da: Gastone Ferrarese

Coordinatore Dottorato

Ch.mo Prof. Vincenzo Parenti Castelli

Relatore

Ch.mo Prof. Fabrizio Giulietti

Esame Finale Anno Terzo

Contents

List of Figures

List of Tables

List of Symbols

Greek Letters

$\boldsymbol{\alpha}$ Vector of Euler's Angles

ΔT Maneuver Time Duration for *Inverse Simulation*

Δt Time Integration Step

Δ Finite Variation

δ_t Throttle Valve Deflection

ϵ, χ Auxiliary Variables for *Inverse Simulation*

$\boldsymbol{\eta}$ Vector of Eigenvalues of $\mathbf{A}$

λ, μ, $\hat{w}$, $\hat{\eta}$ Rotor Velocities Non–Dimensional Ratii

$\boldsymbol{\Omega}$ Rotor Spin Rate Vector

$\boldsymbol{\omega}$ Angular Rate Vector

ϕ, θ, ψ Euler's Angles Small Variations

Φ, Θ, Ψ Euler's Angles

Π, Λ Rotor Aerodynamic Torque and Rolling Moment

ρ Air Density or Matrix Rank

Σ Input Thrust Parameter for *Inverse Simulation*

σ Rotor Solidity

τ Gear Ratio or Time Constant

θ Blade Pitch or Twist

ξ, Γ, δ Tilting, Dihedral and Azimuthal Angles of a Rotor

ζ Angle for Wind Orientation on Rotor Disk

Φ Electric Motor Coils Magnetic Flux

Roman Letters

$\mathbf{A}$, $\mathbf{B}$ *LTI* System Stability and Control Matrices

A Airframe Equivalent Flat Plate Area or Rotor Disk Area or State Matrix Element

b, h Rotor Arm Components

$\mathbf{C}$, $\mathbf{D}$ *LTI* System Output Matrices

C Cosine Function or Aerodynamic Coefficient

c Blade Section Chord

c.e.m.f. Counter Electromagnetic Force

$\mathbf{E}$ Angular Rate Transformation Matrix

$\mathbf{F}$ Vector of Forces

$\mathbf{g}$ Mapping Function for *Inverse Simulation*

g Gravity acceleration

$\mathbf{I}$ Inertia Tensor

LIST OF SYMBOLS

I Inertia Moment

i Electric Current

J Cost Function

K *LQR* Matrix Gain

K Motor Constant or *PID* Gain

L Angular Momentum

L Magnetic Inductance

L, M, N Components of Vector of External Moments

M Vector of Moments

m Aircraft Mass

P Position Vector or Controllability Matrix

N Number of Blades of a Rotor, without subscript, or Number of Rotors, with Subscript

N, E, D Position in *Earth Axis* Frame

P Engine Power

P, Q, R Angular Rates in *Body Axis* Frame

p, q, r Angular Rates Small Variations

q Quaternion vector

Q, **R** *LQR* Weighting Matrices

Q Motor or Engine Torque

R Rotor Radius or Electric Resistance

r Blade Span Coordinate

S Sine Function

s Laplace's Complex Variable

sgn Sign Function

$\mathbf{T}$ Generic Transformation Matrix

t Time

T, H Rotor Thrust and Drag

$\mathbf{U}$ Input Vector

$\mathbf{u}$ *LTI* System Input Vector

U Input Vector Component

U, V, W Velocities in *Body Axis* Frame

u, v, w Velocities Small Variations

$\mathbf{V}$ Velocity Vector

V Motor Input Voltage

v Generic Induced Velocity

$\mathbf{X}$ State Vector

$\mathbf{x}$ *LTI* System State Vector

X, Y, Z Components of Vector of External Forces

x, y, z Axes of a Generic Reference Frame

$\mathbf{y}$ *LTI* System Output Vector or Output Function for *Inverse Simulation*

Subscripts

0	Initial Condition or Trim Condition
α	Lift Curve Slope of Blade Section
Ω	Rotor or Shaft Spin Rate
a	Motor Armature Circuit
B	*Body Axis* Frame
c	Collective
col	Collective Command
E	*Earth Axis* Frame
eng, $engine$	Engine
e, t	Electric, Torque Subscripts
ext	External, referred to forces or moments
$gear$	Mechanical Transmission
i	Rotor Induction
j	Referred to j–th Rotor
lat	Longitudinal Command
l, d	Lift, Drag Blade Section Coefficient
lon	Lateral Command
P, I, D	Proportional, Integral, Derivative
R	*Rotor Axis* Frame
rot, $rotor$, $rotors$	Referred to One or More Rotors

rud Rudder Command

$shaft$ Motor or Engine Shaft Axis

tw Twist Angle

Superscripts

$*$ *Ad hoc* Quantity

af Airframe

$engine$ Engine

g Gravity

$gyro$ Gyroscopic

$motor$ Motor

r Rotor

Chapter 1

Introduction

1.1 Motivation

Among all Unmanned Aerial Vehicles (UAVs), multi–rotor aircrafts have enkindled great interest of research centers in recent times. Their activities have grown and developed fast in the first decade of the XXI century.
In civilian applications multi–rotors have proved to be perfect instruments for aerial monitoring and photography. Nowadays, indeed, many enterprises have been established that do business with these machines and on every TV channel it is possible to attest their efficiency, sooner or later appearing shots recorded with their on–board cameras. Sadly, by the way, the recent disaster that involved in 2011 the nuclear power plant of Fukushima, Japan, can be mentioned. Videos that witness the damages within that facility were shot with quad–rotors.
Ultimately, some of their capabilities make them preferable also to fixed–wing platforms. Multi–rotor UAVs can perform very easily hovering flight and vertical take–off and landing. These characteristics make them the optimal machine for indoor flight, for example, and for accessing dangerous locations with no harm for the pilot.
Multi–rotor platforms also are more employed than RC helicopters, for commercial applications. This is due to their overwhelming simplicity of

construction and greater ease of piloting.
In a word, multi–rotor aircrafts proved to be interesting machines and affordable technological solutions.

Figure 1.1: Hexa–copter for Environmental Monitoring

This thesis provides a deep insight in the dominion of multi–rotor UAVs flight dynamics. All the treatise is addressed to give the reader an analytical kit of equations, regarding the entire set of rotorcraft configurations, or at least the most common, for a comprehensive study of their behavior. Thus this work can certainly be considered as a general reference about flight mechanics and dynamics of multi–rotors platforms, but also a valid collection of theoretic instruments, that can direct some design concerns, avoiding rough and imprecise approaches in the making of these machines.

1.2 Literature Review and Thesis Objectives

Multi–rotor aircrafts, for their relative ease of construction, reliability, low dangerousness for humans, low–cost spares and maintenance, are extensively employed in academic institutes worldwide. They are indeed a valid test bed for control systems development, remote guidance techniques, etc. with the possibility of indoor or outdoor applications. They are exploited for the validation of all types of control strategies: from linear *SISO* control

to more sophisticated techniques, like *back–stepping control* or non–linear control through Lyapunov's functions, passing also through *MIMO LQ* regulators.

Various academic works can be mentioned. For example, one is the *OS–4* helicopter, designed and built within the laboratories of *EPFL* of Lausanne. This work is documented in [4] where the questions of modeling, design and control are treated. Another project is that developed by the *Australian National University* of Canberra [20]. There a very interesting configuration of multi–rotor has been built, with pushing propellers and mini teetering rotors, the *X4–Flyer*. Also, other important universities have been involved in the study on similar flying vehicles, as Stanford [10] and the *MIT* [5].

In all these works a mathematical analysis of the flying systems has not been neglected. More or less, for any machine, all the modeling issues have been faced. Also advanced problems like attitude stabilization, remote control have been treated.

However, notwithstanding the notable results achieved, what the author of the present thesis felt missing in all these projects, was a sort of theoretic foundation in the design of all machines and control systems. All the math tools provided in published works were only a mean to obtain description *a posteriori*, more or less precise, of an already existing aircraft.

For example, in the *EPFL* activity, all the dynamic modeling of the *OS–4* multi–rotor is accomplished in great detail. But, when it is the turn of the tuning of PID regulators, all that is done is a trial assignment of control gains. This signifies that all the analytical effort was not totally exploited to the definition of precise and *ad hoc* control laws.

The work presented in this thesis tries instead to circumvent this obstacle. The manner this is accomplished starts obviously from the mathematical study of multi–rotor aircraft dynamics, on the base of the results of helicopter theory.

This theoretic treatment is approached as usually it is done in the case of

fixed–wing aircrafts dynamics.

After brief hints on vector analysis, the rigid body equations of motion are introduced. The non–linear and the linear formulations are considered, as in all the text about airplanes flight dynamics.

Successively, the description of actions on a generic multi–rotor aircraft is treated. As before, the loads for non–linear modeling and for the linearized one are defined.

All this analytic tools are employed in different manners to appreciate the potentialities of a good mathematical description of multi–rotor behavior.

To the non–linear model, various expedients based on the experience of the author are included to make all the formulae in the text a serviceable tool for simulation. Infact non–linear models are the effective mean of analysis of complex systems like flying vehicles. They allow, for example, control laws validation, tuning of algorithm, pilot training. An interesting application of the non–linear model of dynamics is shown in this thesis for the study of an innovative configuration of quad–rotor.

The linear modeling represents the other great facet of theoretic formulation. The linear analysis has its own advantages. It allows the study of static and dynamic properties of flying vehicles and also it gives valid instruments for the study and design of control laws.

The problem of linear dynamics description for multi–rotor aircraft is here deeply considered. This has permitted the study of the influence of all the factors concerning multi–rotor dynamics, compared to already published works, in a very original way.

The results of this analysis are utilized then in various manners. The theoretic treatment of dynamic stability, or instability, of multi–rotor aircrafts is accomplished. The design of control system is addressed only with an analytical development. A study of controllability of a rotorcraft in case of actuator failure is tackled.

1.3 Outline

Chapter 2 starts with the definition of the rigid body equations of motion. Kinematics and dynamics equations are enounced, in the non–linear differential formulation.
Chapter 3 is centered on the definition of all the loads acting on a multi–rotor during flight. Obviously great care is put in the description of rotors aerodynamics. This chapter also treats the question of modeling of pilot's commands.
Chapter 4 provides general considerations to direct the writing of an effective simulation math model. This discussion faces also the problem of the resolution of the equations of motion and the problem of trim of the mathematical system.
Chapter 5 treats the linear modeling of dynamics of a multi–rotor aircraft. It contains also the definition of linearized aerodynamics of rotors and ends with the definition of the stability and control derivatives.
Chapter 6 is based on the result of the previous chapter and develops the analytic study of dynamic properties of multi–rotor aircrafts.
Chapter 7 addresses the problem of control laws design for multi–rotor on the source of the linear dynamics description provided in chapter 5.
Chapter 8 is an impressive application of all the instruments defined in the previous chapters. It aims at the analytical study of an innovative quad–rotor configuration to assess its enhanced performances with respect to classical quad–rotor.
All the work is enriched with proper numerical tests.

Chapter 2

Rigid Body Dynamics

In this chapter the mathematical instruments, utilized in the remainder of the text for the analytical study of the dynamics of motion of a rigid body in space, are described.
The chapter focuses on the exposition of the equations of motion for a rigid body, as they are generally treated for aerospace applications. Two approaches in the definition of the equations can be considered: the non–linear modeling, for the complete simulation of the motion of an aircraft, and the linear modeling around an equilibrium flight condition, for the study of aero–mechanical properties of a flying vehicle. Here only the non–linear modeling is treated. The linear one is the central argument of a following chapter.
To all this, brief considerations about reference systems are added.

2.1 Reference Axis Systems

To study the motion of a rigid body in space it is suitable a mechanical description in a reference frame fixed to the body itself. Also it is useful the knowledge of position and orientation of the body with respect to the Earth surface. A *reference frame*, in Mechanics problems, is generally a right–handed axis system, *i.e.* a triplet of directions in space with their relative

orientation definite and invariable – precisely any of three orthogonal to the other two – and whose origin is the intersection of is three axes. To simulate the motion of a multi–rotor aircraft in space two axis systems are needed, at least. One is the *Earth Axis* fixed frame chosen as inertial system: the first and the second axes of this frame are oriented to the North and to the East with the origin placed on or over the Earth surface. The second reference frame is the *Body Axis* reference frame whose origin is placed in the Centre of Gravity (C.G.) of the multi–rotor.
This choice of the two reference frames has two motivations. One is that the principles of Newtonian Mechanics must be applied to an inertial system, for writing the equations of motion of a rigid body. The second is that is very easier define all the actions generated by the aircraft components in a proper *Body Axis* system.
Moreover, in the following, other reference systems are considered. These systems are centered in the center of the rotors disks. Their definition and purpose will appear clearly along the discussion. To better understand the classification, one can refer to [6], where it is spoken about *Individual Element Reference Axis* (IERA) and *Individual Element Local System* (IELA) systems.

2.2 Transformation Matrices

Because in vector analysis the definition of a vector depends upon the chosen reference frame, the necessity incurs to describe a vector, representative of a mechanical or spatial quantity, with respect to different axis systems. This operation is generally called *vector resolution*.
The fundamental mathematical tool that permits this operation is the *Rotation Matrix* (or *Transformation Matrix*) of a vector between two axis systems.
In general two reference frames differ between them because of their unequal orientations. To know exactly this relative orientation, it is sufficient

to impose three sequential rotations about the three axes of a system, one after the other, to the starting frame. In Flight Mechanics problems these three rotations are effected in this order: first around the **z** (the third) axis of an angle α; then around the **y** axis (the second), as oriented after the first rotation, of an angle β; finally around the **x** axis (the first) of an angle γ. The three angles just defined are the notorious *Euler's Angles*. With these three angles the rotation matrix that can resolve a vector from an initial reference frame A to a final frame B can be written. This kind of matrix has the following expression.

$$\mathbf{T}_{BA}(\gamma,\beta,\alpha) = \begin{bmatrix} C_\beta C_\alpha & C_\beta S_\alpha & -S_\beta \\ S_\gamma S_\beta C_\alpha - C_\gamma S_\alpha & S_\gamma S_\beta S_\alpha + C_\gamma C_\alpha & S_\gamma C_\beta \\ C_\gamma S_\beta C_\alpha + S_\gamma S_\alpha & C_\gamma S_\beta S_\alpha - S_\gamma C_\alpha & C_\gamma C_\beta \end{bmatrix} \tag{2.1}$$

This operator allows to define a vector with respect to a frame B, when it is known instead in a frame A and the three Euler's angles are known too.

$$\mathbf{V}_B = \mathbf{T}_{BA}\mathbf{V}_A \tag{2.2}$$

2.3 Rigid Body Equations of Motion

The dynamical behavior of a multi–rotor aicraft can be conveniently represented by means of a set of rigid–body equations of motion, written in a set of body axes. The equations presented in this section are the results of the theory of flight dynamics already known from notorious specialized text. Here as primal reference [6] can be cited. First the non–linear equations of motion are described. After, from these same equations, the linearized equations of motions are obtained.

2.3.1 The State Vector

The equations permit, once integrated, to know the evolution of the dynamic and kinematic quantities of motion of the aircraft. As dynamic quantities the vector of the C.G. linear velocities $\mathbf{V}_B$ and the vector of the

angular rates $\boldsymbol{\omega}_B$ are considered, in the *Body Axis* system. As kinematic quantities, instead, the vector of position with respect to *Earth Axis* system $\mathbf{P}_E$ and the vector of the orientation angles $\boldsymbol{\alpha}_E$ are considered. The vector $\boldsymbol{\alpha}_E$ is the vector of the Euler's angles and, if necessary, it can be substituted by the vector of quaternion $\mathbf{q}$. Now it can be defined the state vector $\mathbf{X}$ of the dynamic system describing the quad–rotor dynamics and kinematics of motion.

$$\mathbf{X} = \begin{bmatrix} \mathbf{P}_E \\ \boldsymbol{\alpha}_E \\ \mathbf{V}_B \\ \boldsymbol{\omega}_B \end{bmatrix} \tag{2.3}$$

In the following chapters other components can be included in the definition of the state vector, depending upon the configuration of aircraft under study.

Now the elements of the state vector are:

1. Position: $\mathbf{P}_E = (N, E, D)$;
2. Attitude: $\boldsymbol{\alpha}_E = (\Phi, \Theta, \Psi)$;
3. Velocity: $\mathbf{V}_B = (U, V, W)$;
4. Angular rate: $\boldsymbol{\omega}_B = (P, Q, R)$.

2.3.2 Equations of Dynamics

Now the set of the non–linear equations of motions can be enounced. The formulation follows reference [6].

In the sequel, the *Body axes* are assumed to coincide with the principle axes of inertia of the aircraft. The longitudinal axis $\mathbf{x}_B$ can be considered parallel to one of the brackets of a quad–rotor configuration; the $\mathbf{z}_B$ axis is oriented towards the ground when the vehicle is in hovering and $\mathbf{y}_B$ completes a right–handed frame.

The mass of the multi–rotor is assumed constant in quantity and in distribution. The consequence of this assumption is that mass and inertia tensor are both constant.
The set of equations of the dynamics of a rigid body is given by

$$\begin{cases} m\dot{\mathbf{V}}_B + \boldsymbol{\omega}_B \times (m\mathbf{V}_B) = \mathbf{F}_{ext} \\ \\ \mathbf{I}\dot{\boldsymbol{\omega}}_B + \boldsymbol{\omega}_B \times (\mathbf{I}\boldsymbol{\omega}_B) = \mathbf{M}_{ext} \end{cases} . \tag{2.4}$$

The first equation of the system (2.4) defines the dynamics of translation in space of a rigid body, in a *Body Axis* reference frame. The second equation defines instead the dynamics of rotation in space of a rigid body, in the same *Body Axis* reference frame.
The inertial tensor is defined in eqn. (2.5).

$$\mathbf{I} = \begin{bmatrix} I_{xx} & 0 & 0 \\ 0 & I_{yy} & 0 \\ 0 & 0 & I_{zz} \end{bmatrix} \tag{2.5}$$

The two vector equations of dynamics of motion are equivalent to the set of six scalar equations (2.6).

$$\begin{cases} X = m(\dot{U} + QW - RV) \\ Y = m(\dot{V} + RU - PW) \\ Z = m(\dot{W} + PV - QU) \\ \\ L = I_{xx}\dot{P} + (I_{zz} - I_{yy})QR \\ M = I_{yy}\dot{Q} + (I_{xx} - I_{zz})PR \\ N = I_{zz}\dot{R} + (I_{yy} - I_{xx})PQ \end{cases} \tag{2.6}$$

In these equations

$$\mathbf{F}_{ext} = \begin{bmatrix} X \\ Y \\ Z \end{bmatrix} \tag{2.7}$$

and

$$\mathbf{M}_{ext} = \begin{bmatrix} L \\ M \\ N \end{bmatrix}. \tag{2.8}$$

$\mathbf{F}_{ext}$ and $\mathbf{M}_{ext}$ are the vector of the external forces and moments acting on the aircraft, defined in the *Body Axis* frame. Both vectors will be defined properly in next chapters.

2.3.3 Equations of Kinematics

The velocity in the inertial *Earth axis* reference frame is calculated from the velocity in the *Body axis* frame. The attitude variation is obtained from the angular rates vector $\boldsymbol{\omega}_B$.

$$\begin{cases} \dot{\mathbf{P}}_E = \mathbf{T}_{BE}^{-1}(\Phi, \Theta, \Psi)\mathbf{V}_B \\ \\ \dot{\boldsymbol{\alpha}}_E = \mathbf{E}^{-1}(\Phi, \Theta, \Psi)\boldsymbol{\omega}_B \end{cases} \tag{2.9}$$

The $\mathbf{T}_{BE}$ matrix is the rotation matrix that transforms a vector from the inertial *Earth axis* frame to the not inertial *Body axis* frame. The sequence of rotations is Ψ about z axis, Θ about y axis and then Φ about x axis.

$$\mathbf{T}_{BE}(\Phi, \Theta, \Psi) = \begin{bmatrix} C_\Theta C_\Psi & C_\Theta S_\Psi & -S_\Theta \\ S_\Phi S_\Theta C_\Psi - C_\Phi S_\Psi & S_\Phi S_\Theta S_\Psi + C_\Phi C_\Psi & S_\Phi C_\Theta \\ C_\Phi S_\Theta C_\Psi + S_\Phi S_\Psi & C_\Phi S_\Theta S_\Psi - S_\Phi C_\Psi & C_\Phi C_\Theta \end{bmatrix} \tag{2.10}$$

$\mathbf{E}^{-1}$ is the matrix that transforms the vector $\boldsymbol{\omega}_B$ in the vector of the time derivatives of the Euler's angles.

$$\mathbf{E}(\Phi, \Theta) = \begin{bmatrix} 1 & 0 & -\sin(\Theta) \\ 0 & \cos(\Phi) & \sin(\Phi)\cos(\Theta) \\ 0 & -\sin(\Phi) & \cos(\Phi)\cos(\Theta) \end{bmatrix} \tag{2.11}$$

It is also to remind that **E** is a matrix different from those defined in section (2.2).
Briefly, the equations (2.9) show the relation between inertial frame velocities and *Body axis* frame velocities and between *Body axis* frame rotation rates and rates of Euler's angles.

Attitude Representation

The inverse of **E** matrix presents a mathematical singularity for a value of Θ equal to $\pm\frac{\pi}{2}$ **rad**. If this orientation in pitch can be reached in simulation, then, it is necessary to choose, for attitude representation, the vector of quaternion **q**. The vector **q** is a vector of four elements that describes the rotation around a particular axis, the so called *Euler's axis*, and the orientation of this axis with respect to the inertial frame.

$$\mathbf{q} = \frac{1}{2}\begin{bmatrix} q_0 \\ q_1 \\ q_2 \\ q_3 \end{bmatrix} \tag{2.12}$$

It is necessary to define the equation of kinematics of the quaternion vector.

$$\dot{\mathbf{q}} = \frac{1}{2}\begin{bmatrix} -q_1 & -q_2 & -q_3 \\ q_0 & -q_3 & q_2 \\ q_3 & q_0 & -q_1 \\ -q_2 & q_1 & q_0 \end{bmatrix}\begin{bmatrix} P \\ Q \\ R \end{bmatrix} \tag{2.13}$$

If the quaternion vector is known, then the attitude representation through Euler's angles can be restored, given the relation between quaternion vector and attitude angles, passing through the matrix $\mathbf{T}_{BE}$.

$$\mathbf{T}_{BE} = \begin{bmatrix} q_0^2+q_1^2-q_2^2-q_3^2 & 2q_1q_2+2q_0q_3 & 2q_1q_3-2q_0q_2 \\ 2q_1q_2-2q_0q_3 & q_0^2-q_1^2+q_2^2-q_3^2 & 2q_2q_3+2q_0q_1 \\ 2q_1q_3+2q_0q_2 & 2q_2q_3-2q_0q_1 & q_0^2-q_1^2-q_2^2+q_3^2 \end{bmatrix} \tag{2.14}$$

Because the case of the singularity, in this text, is not considered, the attitude description with Euler's angles is maintained in the following.

2.3.4 Complete Differential Set of Equations

The two equations of dynamics and the two equations of kinematics can be rewritten, in an unique set of equations, isolating the derivatives of the elements of the state vector.

$$\begin{cases} \dot{\mathbf{P}}_E = \mathbf{T}_{BE}^{-1}(\boldsymbol{\alpha}_E)\mathbf{V}_B \\ \\ \dot{\boldsymbol{\alpha}}_E = \mathbf{E}^{-1}(\boldsymbol{\alpha}_E)\omega_B \\ \\ \dot{\mathbf{V}}_B = [\mathbf{F}_{ext} - \boldsymbol{\omega}_B \times (m\mathbf{V}_B)]/m \\ \\ \dot{\boldsymbol{\omega}}_B = \mathbf{I}^{-1}[\mathbf{M}_{ext} - \boldsymbol{\omega}_B \times (\mathbf{I}\boldsymbol{\omega}_B)] \end{cases} \tag{2.15}$$

This system is the set of non–linear differential equations of motion of a rigid body in space. It is apt to study and simulate operations of a flying vehicle in all its flight envelope, virtual testing of on–board systems of the aircraft under exam, virtual pilot training, etc.
The system can be written in a more compact form, considering the state vector $\mathbf{X}$. The vector $\mathbf{U}$ is the vector of the deterministic inputs (controls) of the system.

$$\begin{cases} \dot{\mathbf{X}} = \boldsymbol{f}(\mathbf{X}, \mathbf{U}) \\ \mathbf{X}_0 = \mathbf{X}(t_0) \end{cases} \tag{2.16}$$

The second equation defines the initial value of the state vector $\mathbf{X}_0$ at the initial time t_0, whose knowledge is necessary to start the integration of the equations of motion, being differential equations with time t as independent parameter.

2.4 Remarks

This chapter has dealt with the mathematical modeling of the dynamics and kinematics of motion of a rigid body, applicable also to the study

and simulation of the motion of multi–rotor vehicles. The problem has not been discussed in a lengthy manner, because these results are already available on various and notorious texts about flight mechanics or flight dynamics. Care has been put in the fact that the equations shown here could be those which can correctly and fully describe the dynamics of a multi–rotor aircraft in its complete flight envelope.
In the discussion, with regard to the mathematical aspect of the problem, the equilibrium point of the system was taken as an already known *datum*. However this is not true. The trim condition of the state vector $\mathbf{X}$ must be calculated. This problem is discussed in a dedicated chapter.

Chapter 3

External Actions Modeling

The motion dynamics of a multi–rotor is influenced by the external actions, due to aerodynamics and also to other effects. As it results from the previous chapter, this fact is witnessed by the presence in the equation of dynamics (2.15) of the vectors $\mathbf{F}_{ext}$ and $\mathbf{M}_{ext}$. Then, to complete the mathematical description of the mechanical behavior of the multi–rotor, it is necessary an accurate definition of all the forces and moments generated by the components of the aircraft.
This chapter focuses on this last argument. First it begins with the description of the atmospheric environment. Then all the components of a multi–rotor aircraft that can affect its dynamics are listed. The mathematical description of the actions imparted by each of these components are analyzed in detail. Finally the effects of the pilot's commands are considered .

3.1 Atmosphere

As any flying vehicle, a multi–rotor aircraft is subjected to aerodynamic loads due to the relative motion between its surfaces and the atmosphere. Every action of that type, also, is directly a function of some mechanical property of the air which the flying vehicle is sunken in.

The principal of this physical characteristics of the atmosphere is the air density ρ. ρ is a fundamental parameter for the evaluation of all types of aerodynamic actions, both of drag and of lift.
It is notorious that the value of ρ depends upon many factors. One of these is the altitude, generally to an increase in height from Earth's surface corresponding a decrease of ρ. Another is the Mach Number M of the air and another is the Temperature T.
However, multi–rotor aircrafts are vehicles that, during their operation, do not fly at velocities that imply high values of Mach Number, so that effects of compressibility do not occur in their flight envelope. Moreover, variations of altitude in flight for these machines are of the order of few ten meters.
All these considerations bring to assume that air density ρ is a constant that must be evaluated for the particular operative altitude of the multi-rotor.
Also in this thesis the problem of modeling of air disturbances, like wind gusts, is not dealt.
In a word, the only physical quantity of interest of the atmospheric environment for aerodynamic loads computation is the air density ρ, assumed always as a constant.

3.2 Loads on a Multi–rotor Aircraft

A multi–rotor aircraft is a flying vehicle whose rotors are the prime source of aerodynamic sustenance, propulsion and control. The lifting force that they generate has to oppose the gravitational force and drag effects. Moreover various other factors must be analyzed: aerodynamic torques of rotors, aerodynamic interferences, torques of the motors that spin the rotors blades, inertial torques on motors shafts, gyroscopic effects on rotors.
Thus, a first classification of external forces and moments acting on the aircraft can be stated. The external forces are due to gravitational effects,

aerodynamics of rotor and drag effects of the airframe. The external moments are due yet to the aerodynamics of rotors. In this vector gyroscopic effects and inertial torques of motors shafts are included for the sake of brevity, although they are not external loads.

$$\mathbf{F}_{ext} = \mathbf{F}^{(g)} + \mathbf{F}^{(r)} + \mathbf{F}^{(af)} \tag{3.1}$$

$$\mathbf{M}_{ext} = \mathbf{M}^{(r)} + \mathbf{M}^{(motor)} + \mathbf{M}^{(gyroscopic)} \tag{3.2}$$

Other than the analysis of the effects of gravity, airframe and motors, the rest of this chapter is dedicated to the study of aerodynamics of rotors, that, for the major importance on the dynamics of the aircraft, deserves the deepest and most detailed analysis. It is necessary to remind that the two previous vectors are defined in a *Body Axis* reference frame. This signifies that all the loads must be defined in the same reference axis system. If, some time in the treatment, this is not done, in those case the loads then must be resolved in the that frame, before integration of the equations of dynamics.

3.2.1 Gravity Force

Every body is characterized by its own mass m. A mass, plunged in the gravitational field of the Earth, is accelerated at a rate equal to the acceleration of gravity g. Thus the weight the mass is subjected to is equal, in magnitude, to mg. For the present study, it suffices to consider g as a constant, because a multi–rotor aircraft does not operate with significant variations of altitude, that can involve remarkable changes of the acceleration of gravity.

In the *Body Axis* frame the gravity force vector is the following.

$$\mathbf{F}^{(g)} = \mathbf{T}_{BE} \cdot \begin{bmatrix} 0 \\ 0 \\ mg \end{bmatrix} = \begin{bmatrix} -mg\sin(\Theta) \\ mg\sin(\Phi)\cos(\Theta) \\ mg\cos(\Phi)\cos(\Theta) \end{bmatrix} \tag{3.3}$$

The gravity force is applied at the multi–rotor C.G. and thus it does not generate any moment.

3.2.2 Forces Acting on the Airframe

Every body, that moves in a fluid or gas, is subjected to a force that opposes its motion. A force of this kind is called *drag*. Drag forces depend, in incompressible flows, on the shape of the body immersed in the fluid. The body shape, for drag assessment, depends, in its turn, on the direction of motion of the body itself, *i.e.*, for a multi–rotor aircraft in flight, on its attitude. Thus, the best way to quantify the drag would be to have a proper drag coefficient for any attitude of the multi–rotor. This knowledge, even though could be feasible, could prove excessive, with respect to approximated, but nevertheless affordable, solutions. Indeed an approximated and practical way is to assign a coefficient to each one of the reference axes of the fixed *Body Axis* frame. Any of this coefficient can be experimentally evaluated. In aircraft modeling this is done, assigning to every coefficient a value for some different orientations of the aircraft under exam. More details on this argument can be found in reference [6]. For multi–rotor modeling this last approach can be further simplified, having in mind what multi–rotor flying vehicles are able to do in flight (hovering, climbing, descending, horizontal flight with almost null attitude are their major capabilities). Drag is here defined with the assignment, to any principal axis of inertia of the body fixed *Body Axis* frame, an unique and constant aerodynamic coefficient.

More concisely, it is assumed that the forces acting on the multi–rotor airframe are the three components of the drag directed along the three axes of the body fixed reference frame. The distance between C.G. and

the aerodynamic center of the airframe is considered null. The drag forces are assessed with the equivalent flat plate area model [6].

$$\mathbf{F}^{(af)} = \begin{bmatrix} -\frac{1}{2}\rho A_x |U| U \\ -\frac{1}{2}\rho A_y |V| V \\ -\frac{1}{2}\rho A_z |W| W \end{bmatrix} \tag{3.4}$$

The three equivalent flat plate areas A_x, A_y, A_z are constant. The effect of the rotors induced velocities are neglected.
This drag forces in hovering, or near hovering flight, are practically negligible. Instead, at high velocities, drag forces act as a sort of damping effect that keeps the multi–rotor from getting out of control, at least in simulation.

3.2.3 Rotor Aerodynamics

For multi–rotors helicopters, as for any rotary wing machine, rotors are obviously the most important component in terms of flight performances. Indeed their action permit the aircraft to lift, hover, fly, be maneuvered and, necessarily, in a controlled and safe manner.
Because rotors are the device that produce lift forces, thrust and control actions, a precise analysis of the loads acting on rotors during flight is a necessary task for the understanding of the dynamic behavior both from a mathematical and from a physical point of view.
Although multi–rotor aircrafts prototypes [12] had been built before helicopters in the classical configuration (with a main rotor and a tail rotor), scientific research about aerodynamics of a rotor regarded principally, in the past century, the study of helicopter flight. This can be verified enumerating the various and remarkable texts in the specialized literature. However, since helicopters and multi–rotor UAVs rotors aerodynamics are

based on the same physical principles, the theoretic results obtained for helicopter rotors are liable to be applied to the study of multi–rotor aircrafts dynamics.

After this assumption, before starting the analytical treatment of the aerodynamics of a rotor, it is of obvious interest to describe the rotor as a "solid" device and the peculiarities of rotors for different rotary wing machines.

A rotor is a set of blades (two or more) attached to a rotating shaft and arranged as spokes of a wheel. Blades are wings, that is, beams with section shaped as an aerodynamic profile. They also might be twisted along their span, might be tapered or have variable chord.

In the case of manned helicopters, rotor blades are not rigidly attached to the hub of their shaft, but generally they are hinged to it. Then blades are free to rotate about an axis perpendicular to the shaft and to the blade span. This is the flapping motion of the blade. Moreover a second hinge permits the blade to rotate around an axis parallel to the shaft, to eliminate torques due to blade drag effects on their root and on the hub itself (lagging motion). A third hinge is the feathering hinge that commands the pitch of the blades (collective and cyclic). Rotors that possess all these hinges are named *articulated rotors*. Another type of rotor is the tethering rotor whose two blades are free to flap around an unique central hinge. In some rotors hinges are substituted by flexible elements (elastomeric bearings). This rotors are called semi–rigid rotors. All these expedients are necessary for not transmitting moments to the hub due to asymmetry of aerodynamic loads on the blades and for controlling the thrust and its direction through the pitch of the blades, by means of the collective and cyclic pitch controls. Indeed, through these inputs, flapping allows the flight control of a helicopter, because to flap the blades signifies to tilt the rotor disk, that is, the direction of the thrust itself. This last consideration must be united with the fact that helicopters rotors perform at almost constant rotational speed. A partial view of helicopter main

rotor is given in figure (3.1).

For details about rotors of helicopters and their working principles one can refer to classic texts [17, 2, 21, 15].

Figure 3.1: Main Articulated Rotor for a Manned Helicopter

All the considerations listed previously are valid wholly for helicopters rotors. A rotor for multi–rotor UAVs, although it is yet a device for producing thrust exploiting rotating blades, is more similar to a propeller of an airplane, for the majority of existing machines, as shown in figure (3.2).

The blades of these propellers are very short ones, with cambered profile, not rectilinear twist and a shape along blade span different from a linear tapering but instead comparable to that of blades for airplane propellers, with the maximum of chord about the half of the blade.

Blades for multi–rotor applications are made generally of wood, plastic material or carbon fiber. Especially if made of carbon fiber, they grant high stiffness and resistance against breaking in case of crash. They are characterized by very low weights, when blades for helicopters, instead, for hardest design requirements, are made of though metallic or composite materials.

Multi-rotor aircrafts usually are commanded with combined variations of their propellers rate and not with the changes of inclination of rotors disks by means of aerodynamic effects (flapping). Flapping effects for stabilization and pitch variations as control input have been included only in sporadic, although interesting, academic activities [5, 20]. Of course, ne-

glecting flapping and all rotor dynamics, the computation of aerodynamic loads on rotor is a less intricate problem but not, nevertheless, easy.

Figure 3.2: Multi–Rotor Propeller

At this point a question that should be answered is in what degree the aerodynamic models applied to helicopters rotors befit multi–rotor propellers. Indeed the first are, with respect to those of mini UAVs, very large rotors that during operations can reach velocities on the blades of the order of transonic speeds. Multi–rotors propellers instead remain far from this working conditions, as already stated. A comparison could be made evaluating the *Reynolds' numbers* for both types of rotor in some flight condition. Without proceeding in this analysis, it can be stated that multi–rotors UAVs propellers work at very lower values of Re, against higher Re of modern helicopters rotors [12]. This can signifies that the aerodynamic field around a multi–rotor propeller could be likely more distant from an ideal condition of rotor inflow with respect to a helicopter rotor flow field. This consideration could carry to the conclusion that aerodynamic models, that are enounced later, for large rotors could not be equally adequate for multi–rotor propellers analysis.

However, the aim of the present study is not to describe exactly the aerodynamic flow around the blade section of a propeller. Thus, regarding the assessment, although approximate, of the forces that are generated on a rotor globally, some other parameter can be chosen for a comparison.

The so called *Figure of Merit* [12] of a rotor is a quantity that relates the ideal power requited to a rotor to produce thrust divided by the power absorbed in induced and parasite drag effects on rotor blades, in hovering flight condition. If values of this parameter are similar for different rotors, it can be stated that, although the aerodynamic modeling can not give equally affordable results for wake description of rotors, from the point of view of global performances of rotors, in terms of forces and power absorption, the differences are less marked. For example in [28, 20] values of *F.M.* of the order of 70% and more are shown, in real applications. These values are comparable to those listed in [12, 15] for modern helicopters rotors. On this base it can be admitted that the mathematical modeling of aerodynamic loads utilized for helicopters rotors and described in the following pages is a still affordable instrument for multi–rotor analysis.

Hypotheses on Rotor Aerodynamics

After these considerations, some hypotheses have to be stated for the calculation of the aerodynamic loads. The assumptions permit to have analytical results available for dynamic simulations and dynamic stability characteristics assessment. Some of them regard the type of blades and these ones are the following:

1. blades are rigid beams;
2. blades are rigidly attached to the rotor shaft;
3. every section of the blades is a profile whose shape is the same along the blades span;
4. blades are not tapered and have linear twist along their span.

From these suppositions the next considerations derive. No flapping and rotor blades dynamic must be evaluated. Thus the rotor can be thought of as a rigid rotating disk (the *Rotor Disk*), whom a flow of air passes

through. The lifting characteristics of blades sections are constant along their span.
Linear aerodynamics of blades section are assumed. In particular:

1. $C_{l\alpha}$ is the lift curve slope of blades section;
2. C_d is the profile drag coefficient of the blades section and represent a mean value for all blades sections.

Because blades are wings of finite length, effects of induced velocity must be included in the aerodynamics analysis of the rotor. The induced velocity computation will be described in a successive section.

Aerodynamic Loads on Rotor

A detailed study of the aerodynamics of a helicopter rotor is available in texts like [17, 6], including effects of flapping, pitch of blades, etc. The assumptions made previously about rotor geometry, stiffness, and aerodynamic characteristics, permit to treat the aerodynamic load calculation in a way at all similar to that presented in [15], for the case of a rigid rotor in forward flight.
For the present case only few components of aerodynamic loads are sufficient to describe the actions on a propeller. Vectors $\mathbf{F}^{(r)}$ and $\mathbf{M}^{(r)}$ can be rewritten. These vectors now are defined with respect to a reference frame whose first axis is directed along the projection of velocity u_R of rotor center on the rotor disk itself. The third axis of this frame is directed orthogonal to the rotor disk plane, opposed to rotor thrust T, and the second axis is perpendicular to the other two. The origin of this frame is placed in the rotor disk center. Such a frame, called *Rotor Axis* frame, is indicated with a R subscript and can be oriented differently with respect to the *Body Axis* frame of the aircraft. In figure (3.3) a sketch of a rotor with its relative frame is depicted.
In this frame two components of the forces vector and two components of the moments vector, acting on the rotor, can be defined:

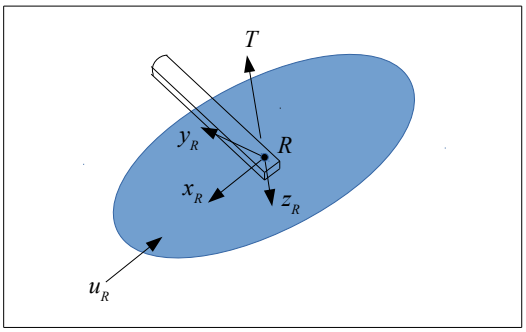

Figure 3.3: *Rotor Axis* Reference Frame

1. the thrust T;
2. the rotor drag H opposed to the velocity component u_R;
3. a rolling moment Λ around the direction of u_R;
4. a torque Π around the rotor disk axis.

$$\mathbf{F}_R^{(r)} = \begin{bmatrix} -H \\ 0 \\ -T \end{bmatrix} \tag{3.5}$$

$$\mathbf{M}_R^{(r)} = sgn(\Omega) \begin{bmatrix} \Lambda \\ 0 \\ -\Pi \end{bmatrix} \tag{3.6}$$

The sign of the not null two components of $\mathbf{M}_R^{(r)}$ depend on the sense of rotation of the rotor blades. Ω in this case is exactly the speed rate of the rotor. The sign of Ω follows the convention for a rotation in a right–handed frame.

In rotor aerodynamics it is usual to refer to non–dimensional coefficients instead of pure forces and moments. In this case the following coefficients can be defined.

$$\begin{aligned} C_T &= \frac{T}{\rho A \Omega^2 R^2} \\ C_H &= \frac{H}{\rho A \Omega^2 R^2} \\ C_\Lambda &= \frac{\Lambda}{\rho A \Omega^2 R^3} \\ C_\Pi &= \frac{\Pi}{\rho A \Omega^2 R^3} \end{aligned} \tag{3.7}$$

These coefficients can be referred to as the Thrust coefficient, the Drag coefficient, the Rolling Moment coefficient and the Torque coefficient, respectively. A is the rotor disk area and R is the rotor radius.

$$A = \pi R^2 \tag{3.8}$$

Induced Velocity on a Rotor

A rotor is a device that generates a force through its aerodynamic interaction with the surrounding air. For the Third Principle of Newtonian Dynamics, to the rotor lifting force (and also to the other) must correspond an equal and opposite force acting on the fluid that invests the propeller. This signifies that the flow passing through the rotor is subjected to an acceleration. This increase of the velocity of the air is the so called *induced velocity* v_i. From this hint it is clear that for knowing the forces generated by a rotor the calculation of this induced velocity is mandatory.
The induced velocity is distributed on the whole area swept by the rotor blades. This distribution cannot exactly been calculated. For details classic texts as [2, 17] can be referred to. Many simplifications must be made to have an analytical result apt to aerodynamic loads evaluation. Now an

induced velocity constant distribution is assumed all over the entire rotor disk. As shown in [2], this mean component of the induced velocity has the main influence on the rotor thrust. Thus, in this study, the induced velocity of a rotor in flight is assumed equal to its mean value on the whole rotor disk area.
The theory that permits the definition of the induced velocity in function of the rotor thrust is the *Momentum Theory* (MT). For details one can refer to [15, 6, 12]. This theory is based on several assumptions:

1. the rotor is modeled as a propeller with infinite number of blades (*actuator disk*);
2. the actuator disk operate on a streamtube that crosses the whole rotor area;
3. the airflow is incompressible and the induced velocity v_i is normal to the disk actuator;
4. through the actuator disk a leap in the airflow pressure, that is constant across any section of the streamtube and across the actuator disk area, is assumed.

Exploiting the Bernoulli theorem and defining the Momentum variation in the airflow through the actuator disk, the relation between the thrust T and the induced velocity v_i can be found. For the mathematical details [15, 6] can be consulted.

$$T = 2\rho A v_i \sqrt{U_R^2 + (W_R - v_i)^2} \tag{3.9}$$

This equation can be rewritten in the non–dimensional form.

$$C_T = 2\lambda_i \sqrt{\mu^2 + (\mu_z - \lambda_i)^2} \tag{3.10}$$

λ_i is the inflow ratio, μ is the advance ratio and μ_z is the climb ratio. All these quantities are obtained dividing the respective dimensional velocities by the blade tip velocity $|\Omega|R$.

The components of velocity in the previous expressions are depicted in figure (3.4).

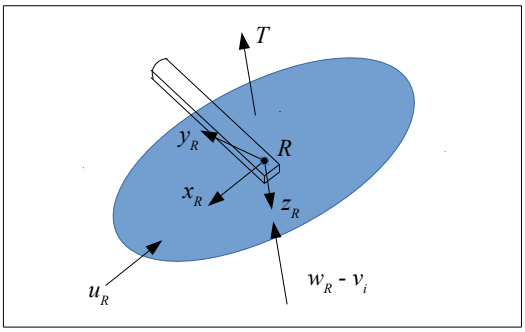

Figure 3.4: Air Velocity on a Rotor

Solving this equation is not a trivial matter. There is no analytical solution, except for the case of hovering flight, where the equations bring the following results.

$$v_i = \sqrt{\frac{T}{2\rho A}} \tag{3.11}$$

$$\lambda_i = \sqrt{\frac{C_T}{2}} \tag{3.12}$$

In a different flight condition, instead, an iterative approach is requited, assigning an initial value to the induced velocity or, alternatively, to the inflow ratio. The affordable and usual mathematical technique for this problem is the *Newton–Raphson* method. Now the formulation of the numerical process, as it appears in [6], is enounced. The following equations are those utilized for the simulations shown in this thesis.

$$v_i^* = \sqrt{\frac{T}{2\rho A}} = \sqrt{\frac{C_T(\Omega R)^2}{2}}$$

$$\begin{aligned} \hat{w} &= v_i / v_i^* \\ \hat{\mu} &= U_R / v_i^* \\ \hat{\eta} &= W_R / v_i^* \end{aligned} \tag{3.13}$$

Equation (3.9) can then be reformulated.

$$\hat{w}^2[\hat{\mu}^2 + (\hat{w} - \hat{\eta})^2] - 1 = 0 \tag{3.14}$$

With a truncated Taylor's series expansion the increment of $\hat{w}$ can be calculated.

$$\Delta\hat{w} = -\frac{f(\hat{w})}{F(\hat{w})}$$

$$f(\hat{w}) = \hat{w}^2[\hat{\mu}^2 + (\hat{w} - \hat{\eta})^2] - 1 \tag{3.15}$$

$$F(\hat{w}) = \frac{\partial f}{\partial \hat{w}} = 2\hat{w}[\hat{\mu}^2 + (\hat{w} - \hat{\eta})^2] + 2\hat{w}^2(\hat{w} - \hat{\eta})$$

Once the value of $\hat{w}$ has been updated, the iteration can go on.

$$\hat{w}_{new} = \hat{w}_{old} + \Delta\hat{w} \tag{3.16}$$

The process continues until the difference between two succeeding values of $\hat{w}$ becomes equal or inferior to a fixed tolerance (*e.g.*, this constraint can be chosen equal to 0.01). Thus the induced velocity v_i is achieved.

$$v_i = v_i^* \hat{w} \tag{3.17}$$

Another consideration, to the purpose of simulation, must be pointed out. The knowledge of thrust is necessary to start the calculation. But, as explained later, also the thrust must be defined in function of the induced velocity. Thus, to accomplish a numerical flight simulation through time,

what can be done is to compute the induced velocity at a precise instant, then to memorize this value of v_i and finally to transmit it at next time instant of the simulation. This little jump in time must be chosen to avoid divergence of the iterative process. This can be done with a trial and error procedure, within for example the $SIMULINK^{®}$ environment.
Other than this, the MT provides a relation that connects thrust of the rotor and the average induced velocity over the rotor disk. However there is some flight condition for whom its validity is no more granted. For this question the already cited texts can be the optimal reference.
In this work, all ground effects are neglected in the evaluation of the induced velocity of a rotor.
Moreover all the aerodynamic interferences that can arise between rotors wakes and between rotors wakes and airframe of the multi–rotor aircraft are neglected. This is due to the fact that, in the majority of multi–rotor platforms, propellers are mounted on their airframe in a way that all the various wakes substantially do not intercept other parts of the machine.

Calculation of the Rotor Aerodynamic Coefficients

Once the induced velocity or the inflow ratio is known, the computation of the aerodynamic actions defined in (3.2.3) is possible. To obtain the rotor forces and moments, including aerodynamic characteristics, pitch and geometry of the blades, it is necessary to make use of the so called *Blade Element Theory* (*BET*).
The approach of *BET* is to assume that every section of the rotor blades behaves exactly like an aerofoil. The air velocity over the blade section is the sum of the velocity due to rotation of blades about their shaft, of the speed of aircraft and of the induced velocity. From this quantities it is possible to evaluate the incidence of the aerofoil and then the lift and drag forces for unit length of every blade. After the integration along the blades span and around the rotor shaft axis, the rotor aerodynamic loads are computed, as averaged quantities for a 2π rotation of all the blades.

All these considerations and the hypotheses previously defined in section (3.2.3) on blades geometry and aerodynamic characteristics, permit to exploit the definitions of rotor aerodynamic coefficients presented in [15], as already stated, for the case of a rotor in forward flight, with also the effect of a linear blade twist and without inserting the cyclic commands.

$$\begin{aligned}
\frac{C_T}{\sigma C_{l\alpha}} &= [\theta_c(\frac{1}{6}+\frac{\mu^2}{4}) - \frac{\lambda_i-\mu_z}{4} - \frac{1}{8}(1+\mu^2)\theta_{tw}] \\
\frac{C_H}{\sigma C_{l\alpha}} &= [\frac{(\lambda_i-\mu_z)\mu}{4}(\theta_c - \frac{\theta_{tw}}{2}) + \frac{C_d\mu}{4C_{l\alpha}}] \\
\frac{C_\Lambda}{\sigma C_{l\alpha}} &= [\mu(\frac{\theta_c}{6} - \frac{\theta_{tw}}{8} - \frac{\lambda_i-\mu_z}{8})] \\
\frac{C_\Pi}{\sigma C_{l\alpha}} &= [(\lambda_i-\mu_z)(\frac{\theta_c}{6} - \frac{\theta_{tw}}{8} - \frac{\lambda_i-\mu_z}{4}) + \frac{C_d}{8C_{l\alpha}}(1+\mu^2)]
\end{aligned} \tag{3.18}$$

For clarity the twist angle of a blade for anyone of its sections, denoted with the coordinate r, is equal to $-\theta_{tw}\frac{r}{R}$. With this notation θ_{tw} is always positive, if the blade pitch is maximum at the root of the blade and minimum at the tip. θ_c is the collective pitch of the blades. For the case of multi–rotor rigid propellers θ_c and θ_{tw} are considered as fixed and constant parameters of the rotor. σ is the *solidity* of the rotor.

$$\sigma = \frac{Nc}{\pi R} \tag{3.19}$$

N is the number of blades of the rotor, c is the chord of the blades and R is equal to the span of the blades.

One doubt could arise now about the affordability of these coefficients. *BET* is developed for the analysis of the aerodynamics of the rotors of manned helicopters. These rotors, as already stated, have very different size, geometry and blade shape with respect to multi–rotor propellers, that adhere more precisely to the hypotheses under the *BET*. To briefly settle the question, a qualitative consideration can be added. A result of the

BET is that, for example, the total thrust of the rotor [2] is equal to the thrust generated by a rotor whose blades pitch is an average angle equal to that of the blade section at the 3/4 of blade span. It can be viewed that catalogues of propellers, as (`http://m-selig.ae.illinois.edu/props/propDB.html`), typically provide, as data, the diameter and the pitch of a particular section of the propellers blades. This section is generally that at around the 70% of blade span. This signifies that a correspondence betwixt the theoretic results and the real propeller aerodynamic behavior can be accepted.
Thus, the results of *BET* can be exploited, for propeller analysis, assuming, on the source of data coming from experimental campaigns, proper values of the various aerodynamic parameters of interest.
From the rotor coefficients the aerodynamic loads can be calculated, by means of equations (3.7). It is worth also remembering that these actions are calculated in a *Rotor Axis* frame. What is missing now, are the definitions of μ and μ_z. Aiming at this, some considerations must be added regarding the position and orientation of the rotor with rspect to the whole airframe of the multi–rotor vehicle.

Rotation Matrix for Rotor Orientation

For a multi–rotor aircraft any of its rotors possess its own precise displacement in the *Body Axis* reference frame. Moreover any of them could also be rotated so that the direction of thrust T could differ from the $\mathbf{z}_B$ axis. If the effects of their tilting angles must be accounted for, it is necessary insert those angles in the definition of forces and moments generated by the rotor. Indeed only when the orientation of a rotor is accurately defined, the velocity of the air that flows through the rotor is accurately known.
The mathematical tool available to this purpose is the *Rotation Matrix*. For each rotor, the rotation matrix is computed with three Euler's angles that describe the three sequential rotations that resolve a vector from the *Body Axis* frame to a frame fixed to the rotor disk itself

($\{\mathbf{0}_R, \mathbf{x}_{R1}, \mathbf{y}_{R1}, \mathbf{z}_{R1}\}$). The sequence of the rotations follow the same convention chosen for the transformation from Inertial to Moving frame for the equations of motions, as explained in section (2.2).

The first angle, called δ, is the angle that identifies the angular position of each rotor arm in the $\{(\mathbf{x}_B, \mathbf{y}_B)\}$ plane (*azimuth*). This rotation is around a direction parallel to the axis $\mathbf{z}_B$. The second angle, called Γ, is the angle that tilts the rotor disk so that a component of the rotor thrust T is directed along the rotor arm toward the C.G. of the rotorcraft. In a word, this axis of rotation lies on the $\{(\mathbf{x}_B, \mathbf{y}_B)\}$ plane and on the rotor disk. Γ is called *dihedral* angle, in analogy to the dihedral angle for a fixed–wing airplane. The third angle, called ξ, is the rotation around the local $\mathbf{x}$ axis. This rotation lets the thrust vector generate a component that is orthogonal to the local vertical plane containing the rotor arm. This last axis lies on the rotor disk plane. ξ is referred to as the *tilting* angle of the rotor. In figure (3.5) the tilting and the dihedral of a rotor are depicted.

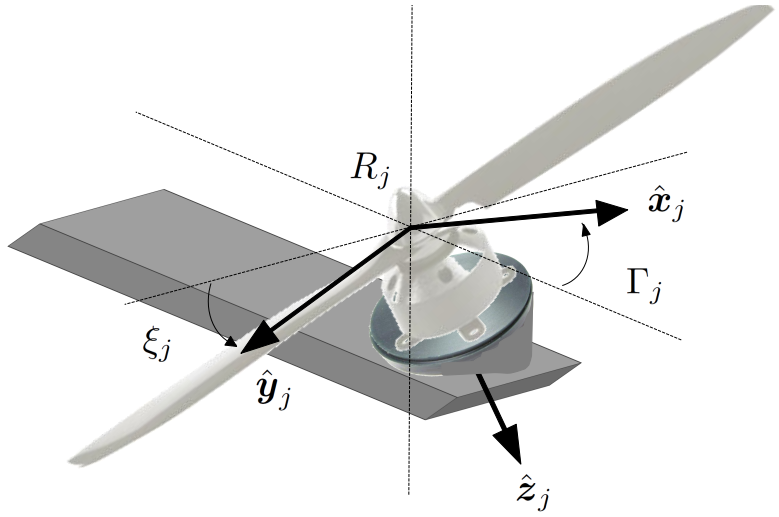

Figure 3.5: Rotor Orientation: *dihedral* and *tilting* angles

For a rotor the rotation matrix jut described is called $\mathbf{T}$.

$$\mathbf{T}(\xi,\Gamma,\delta) = \begin{bmatrix} C_\Gamma C_\delta & C_\Gamma S_\delta & -S_\Gamma \\ S_\xi S_\Gamma C_\delta - C_\xi S_\delta & S_\xi S_\Gamma S_\delta + C_\xi C_\delta & S_\xi C_\Gamma \\ C_\xi S_\Gamma C_\delta + S_\xi S_\delta & C_\xi S_\Gamma S_\delta - S_\xi C_\delta & C_\xi C_\Gamma \end{bmatrix} \tag{3.20}$$

Other than this matrix, for reasons that are pointed out successively, for any rotor a rotation matrix independent of the azimuth angle δ can be defined. This matrix is named $\tilde{\mathbf{T}}$.

$$\tilde{\mathbf{T}}(\xi,\Gamma,0) = \begin{bmatrix} C_\Gamma & 0 & -S_\Gamma \\ S_\xi S_\Gamma & C_\xi & S_\xi C_\Gamma \\ C_\xi S_\Gamma & S_\xi & C_\xi C_\Gamma \end{bmatrix} \tag{3.21}$$

These mathematical expressions are very helpful. They permit to pass from a configuration with tilted rotors to that without tilted rotors only changing the numeric value of the dihedral and tilting angles just defined. Also they allow to account for various numbers of rotors and their displacement with the angle δ.

Air Velocity on a Rotor

In equations (3.18) the quantities μ and μ_z are present. Through them the air velocity is included in the calculation of aerodynamic actions. Thus for the rotor the advance ratio and the climb ratio must be properly defined. Indeed, the velocity at which a rotor is moving can be different from the inertial velocity of the C.G. of the whole flying vehicle $\mathbf{V}_B$. Moreover the *Rotor Axis* reference frame utilized for rotor aerodynamics computation can have a diverse orientation with respect to the *Body Axis* system.
The factors that must be included in the air velocity definition are the following:

1. the rotor position in the *Body Axis* frame;
2. the orientation of the rotor.

As velocity of the rotor, that of the rotor disk center is assumed. This choice has been made in consideration of the fact that rotors for multi–rotor UAVs are generally of very small dimensions. Other than this, neglecting blades dynamics, under the hypothesis of linear aerodynamics of blade sections the effects of linear distribution velocities over the rotor disk due to angular rate ω_B are equal to the effects of the average velocity of the rotor disk center. The *BET* results of equations (3.18), because of the operation of integration over the rotor disk area, adhere exactly to this consideration.

Any rotor is hinged to the extremity of its own arm. The position of the propeller in the *Body Axis* frame on the plane $\{(\mathbf{x}_B, \mathbf{y}_B)\}$ can be described with two quantities: the distance b between the C.G. of the aircraft and the rotor disk center and its angular (*azimuth*) position, named δ, around the $\mathbf{z}_B$ axis. b is always positive definite. The distance between the C.G. and the rotor center along the $\mathbf{z}_B$ axis is indicated with h and its sign depends by the rotor displacement. Any j–th rotor of a multi–rotor aircraft is identified by its δ_j angle. b and h, in any numerical case, are considered equal for all the propellers of the same rotorcraft. b, h and δ_j can be visualized in figure (3.6).

At this point for the rotor what can be calculated is the rotor velocity in a reference frame with axes parallel to those of the *Body Axis* frame. This vector can be called $\mathbf{V}_B^{(r)}$.

$$\mathbf{V}_B^{(r)} = \mathbf{V}_B + \boldsymbol{\omega}_B \times \begin{bmatrix} bC_\delta \\ bS_\delta \\ h \end{bmatrix} \tag{3.22}$$

Now, by multiplying the matrix $\mathbf{T}$ to vector $\mathbf{V}_B^{(r)}$, what can be obtained is a velocity vector with two components that lie on the rotor disk plane. This vector can be called $\mathbf{V}_{R*}^{(r)}$.

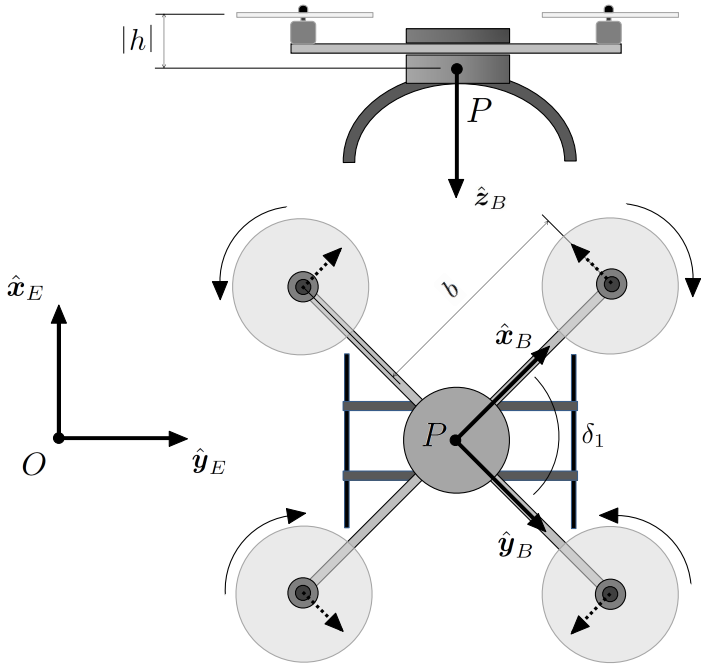

Figure 3.6: Rotor Displacement: b, h and δ_j angle are shown; P is the C.G. of the aircraft and O the origin of the Inertial Frame

$$\mathbf{V}_{R*}^{(r)} = \mathbf{T}\mathbf{V}_{B}^{(r)} = \begin{bmatrix} U_{R*} \\ V_{R*} \\ W_{R*} \end{bmatrix} \tag{3.23}$$

However this is not yet the vector needed for rotor aerodynamic coefficients calculation. It is necessary another operation of vector resolution that could transform $\mathbf{V}_{R*}^{(r)}$ in a new vector of the form $[u_R, 0, w_R]^T$. This operation can be effected with another rotation matrix. This matrix can be defined in the following manner.

$$\mathbf{T}_\zeta(0,0,\zeta) = \begin{bmatrix} C_\zeta & -S_\zeta & 0 \\ S_\zeta & C_\zeta & 0 \\ 0 & 0 & 1 \end{bmatrix} \tag{3.24}$$

The angle ζ is a function of the first two components of $\mathbf{V}_{R*}^{(r)}$.

$$\zeta = \arctan\left(\frac{v_{R*}}{u_{R*}}\right) \tag{3.25}$$

Finally the velocity vector of the rotor disk center in the *Rotor Axis* frame can be defined.

$$\mathbf{V}_{R}^{(r)} = \begin{bmatrix} U_R \\ V_R \\ W_R \end{bmatrix} = \mathbf{T}_\zeta \mathbf{V}_{R*}^{(r)} \tag{3.26}$$

The air velocity of the rotor can be obtained summing to this last vector the induced velocity v_i of the rotor itself, that is always directed along the third axis of the *Rotor Axis* frame and opposed to the thrust T.
From the vector defined by the expression (3.26) the advance and the climb ratii can be computed. Now there is all to compute the rotor aerodynamic coefficients. It is worth noticing that in the hovering flight condition the frame $\{(O_R, \mathbf{x}_R, \mathbf{y}_R, \mathbf{z}_R)\}$ and the frame $\{(O_{R*}, \mathbf{x}_{R*}, \mathbf{y}_{R*}, \mathbf{z}_{R*})\}$ coincide.
The aerodynamic actions of the rotor defined in this way are referred not to the *Body Axis* frame. To have the forces and moments resolved to the axis

system with respect to which the equations of Dynamics (2.4) are written, the next passage must be done, reminding that, for the properties of the rotation matrices, the inversion and the transpose operations coincide.

$$\mathbf{F}^{(r)} = (\mathbf{T}_\zeta \mathbf{T})^{-1} \mathbf{F}_R^{(r)} = \mathbf{T}^T \mathbf{T}_\zeta^T \mathbf{F}_R^{(r)} \tag{3.27}$$

$$\mathbf{M}^{(r)} = (\mathbf{T}_\zeta \mathbf{T})^{-1} \mathbf{M}_R^{(r)} = \mathbf{T}^T \mathbf{T}_\zeta^T \mathbf{M}_R^{(r)} \tag{3.28}$$

In a complete multi–rotor mathematical model, vectors $\mathbf{F}^{(r)}$ and $\mathbf{M}^{(r)}$ are obviously the sum of the contributions given by all the propellers.
The analytical treatment of rotor aerodynamics is thus terminated.

3.2.4 Rotor Gyroscopic Effects

A rotor is a body rotating about its own shaft axis and moving in space. The combination of its spinning motion and the rotation of the airframe of the multi–rotor generate gyroscopic effects on it.
The rotor can be considered as a body whose inertia matrix $\mathbf{I}_{rotor}$, defined with respect to a reference frame whose third axis is the spinning axis, is diagonal, like that of a disk. With this analogy, the moments of inertia along the axes different from that of spin are equal. So, a rotor can be adequately viewed as a *gyroscopic body*.
Like for any rotating body, the gyroscopic torque can be calculated considering the variation of its angular momentum $\mathbf{L}$. In the case of a rotor $\mathbf{L}$ is the product of the inertia matrix $\mathbf{I}_{rotor}$ and the spinning vector $\mathbf{\Omega}$.

$$\mathbf{L} = \mathbf{I}_{rotor}\mathbf{\Omega} = \mathbf{I}_{rotor} \begin{bmatrix} 0 \\ 0 \\ \Omega \end{bmatrix} \tag{3.29}$$

Calling I_{rotor} the third element of the diagonal of $\mathbf{I}_{rotor}$, the angular momentum of the rotor is equal to the following vector.

$$\mathbf{L} = \begin{bmatrix} 0 \\ 0 \\ I_{rotor}\Omega \end{bmatrix} \tag{3.30}$$

Now, the variation of $\mathbf{L}$ can be defined with its derivative with respect to time, with the aid of the Coriolis's theorem.

$$\frac{\mathbf{dL}}{\mathbf{d}t} = \frac{\partial \mathbf{L}}{\partial t} + (\mathbf{T}\boldsymbol{\omega}_B) \times (\mathbf{I}_{rotor}\boldsymbol{\Omega}) \tag{3.31}$$

The vector $\boldsymbol{\omega}_B$ has been multiplied by matrix $\mathbf{T}$ to account for rotor orientation.

The second term of the right hand side of this last equation represents the gyroscopic effect on the rotor. Vector $\mathbf{M}^{(gyroscopic)}$ for a single rotor can be defined, noting that to the airframe the rotor transmits this torque with the opposite sign.

$$\mathbf{M}^{(gyroscopic)} = -\mathbf{T}^T[(\mathbf{T}\boldsymbol{\omega}_B) \times (\mathbf{I}_{rotor}\boldsymbol{\Omega})] \tag{3.32}$$

3.2.5 Motors and Engine Dynamics

A rotor is a propeller made up of two or more blades that are clutched to a rotating shaft. The rotor angular rate is another fundamental parameter to be known for the evaluation of aerodynamic loads generated by the rotor. The rotation of the shaft is granted by the torque provided by a motor connected to the shaft or to another shaft that is linked by means of a mechanical transmission to the rotor shaft. The rotor spin is therefore enhanced or decreased with a proper command to the motor.

Thus, for completing the calculation of rotor aerodynamics, it is necessary to describe the dynamics of the rotor shaft and, then, of the motor.

The motors usually applied in multi–rotor applications are electric motors. Generally one motor is associated to any propeller. However, a chapter of

this thesis is dedicated to the study of an innovative configuration of multi–rotor helicopter, that is featured with a single internal combustion engine. For this reason, in the present section, the description of the dynamics both of electric motors and of an *I.C.E.* to be installed on a mini-UAV flying vehicle is discussed. First is presented the case of an electric motor and then the case of an *I.C.E.*

Electric Motor Dynamics

The electric motors mounted on multi–rotors frames, generally, are D.C. brushless electric motors. For details around this electric machines one can refer to [11].
In the case of electric motors, *i.e.* of electric machines, it is necessary to define the corresponding electromagnetic circuit, including all the electric and magnetic effects. Without a deep sinking in the description of the physical principles concerning the behavior of these motors, in the electric circuit, represented in figure (3.7), can be included:

- an electric resistance R_a;
- a magnetic inductance L_a;
- a counter electromotive force ($c.e.m.f.$);
- an armature voltage V_a (input to the motor) and the armature current i_a.

For clarifications, the recommended reference is still [11].
The equation of the electric equivalent circuit is the following.

$$V_a = R_a \; i_a + L_a \; \frac{di_a}{dt} + c.e.m.f. \tag{3.33}$$

The $c.e.m.f.$ is proportional to variation of the magnetic flux Φ that crosses the motor rotating coils. It can be also demonstrated that it is proportional to the motor angular speed Ω. K_e is the electric constant of the motor.

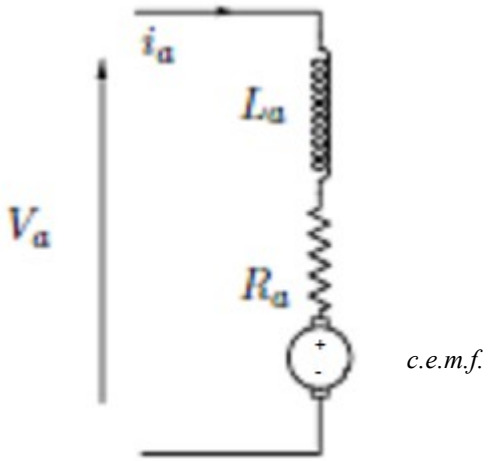

Figure 3.7: Brushless Motor Electric Circuit

$$c.e.m.f. = K\ \Phi\ \Omega = K_e\ \Omega \tag{3.34}$$

In the case of small D.C. brushless motors the inductance effects are not so relevant and also to simplify the equation L_a can be neglected.
From equation 3.33, the armature current can be calculated given a voltage input V_a.

$$i_a = \frac{(V_a - K_e\Omega)}{R_a} \tag{3.35}$$

The knowledge of the armature current i_a permits to find the torque generated by the electromagnetic circuit on the motor shaft. This torque is proportional to the same current i_a. K_t is the so called motor torque constant.

$$Q_{motor} = K_t\ i_a \tag{3.36}$$

K_t is a quantity that is strongly tied to the electromagnetic characteristics

of the non rotating part (stator) of the motor. For D.C. brushless motors the following relation between electric and torque constants can be stated [11].

$$K_t = \sqrt{3} K_e \tag{3.37}$$

If between propeller and motor shaft there is no gear or any transmission other than the motor shaft, the propeller speed is the same speed of motor. If this is not the case, then the load of the propeller must be multiplied to the gear ratio τ. The dynamics of motor is given by the difference between driving torque of motor and the aerodynamic torque of rotor.

$$I_{shaft}\, \dot{\Omega} = Q_{motor} - Q_{rotor}\tau \tag{3.38}$$

$$Q_{rotor} = \Pi \tag{3.39}$$

Every part of the multi–rotor aircraft, that is accelerating with respect to the remainder of the whole vehicle, imparts to the vehicle structure a torque proportional and opposite to its own acceleration. So in the case of electric driven propellers, the inertial torques of all the shafts must be accounted for in the equilibrium of rotational momentum. It is supposed that all the shafts have the same rotational inertial moment with respect to their own axis of revolution.

$$\mathbf{M}^{(motor)} = \left\{ \begin{array}{l} 0 \\ 0 \\ -I_{shaft} \sum_{j=1}^{N_{rot}} \dot{\Omega}_j \end{array} \right\} \tag{3.40}$$

The rotational inertia that opposes the spin of the motor, if τ is different from 1, must be calculated.

$$I_{shaft} = I_{rotor}\tau^2 \tag{3.41}$$

A brief annotation must be included. The dynamic behavior of an electric motor is far from be really represented by this equation. Every motor, truly, does not receive, as input, simply a voltage from the pilot for bringing the propeller to the desired spin rate. There are other phenomena and principles that must be dug. Still reference [11] remains an optimal support. The aim of this modeling is to have a mathematical approximated expression of the transients of the rate of rotors, instead of even more unrealistic step input responses. Moreover, notably, there is the fact that every motor, in real applications, is generally driven by a control system that this dynamic modeling does not include.

Internal Combustion Engine Dynamics

As mentioned before, in this text an innovative mock-up of quad–rotor with rotors driven by a single *I.C.E.* is discussed in detail in a following chapter. So, a mathematical model of the dynamics of this engine must be defined.
The quad–rotor engine is a two stroke combustion engine. The rate of the shaft Ω is proportional to the velocity of the rotors. The gear ratio is τ.
To determine the dynamics of rotors and the counter–torque applied to the airframe by the engine itself it is necessary to describe the dynamics of the shaft of the engine.
The performances of an *I.C.E.* can be assessed with direct measurement of the torque absorbed on a test bench and of its angular speed. The results of this data collections are available by engines constructors in diagrams known as power curves. From these diagrams one can establish empirical relations between rotation speed of the shaft, torque and also power, fuel consumption, etc. in function of other parameter as, for example, the valve deflection (throttle position), that is, in general, the input for engine regulation. An interesting example regarding the modeling of a helicopter engine is given in [24]. A similar approach is utilized here.
The shaft dynamics of the *I.C.E.* is described by the following equation.

The effects of $\dot{r}$ are neglected, for simplicity.

$$I_{shaft}\dot{\Omega} = Q_{engine} - Q_{rotors} \tag{3.42}$$

Q_{rotors} is the sum of the aerodynamic torques of the four rotors multiplied by the gear ratio. Π_j is the aerodynamic torque acting on the j-th rotor.

$$Q_{rotors} = \sum_{j=1}^{N_{rot}} (\Pi_j \tau) \tag{3.43}$$

Q_{engine} is the torque provided by the engine.
It is assumed that the engine works at nearly constant speed. The power provided by the engine can be considered function only of the throttle position, that is the fuel flow. Thus the control variable of the engine is the throttle valve deflection (δ_t). The power of the engine is assumed proportional to the valve deflection itself. The value of δ_t must be comprised between 0 and 1.

$$P_{engine} = (P^{max}_{engine,\delta_t} - P^{min}_{engine,\delta_t})\delta_t \tag{3.44}$$

$$Q_{engine} = \frac{P_{engine}}{\Omega} \tag{3.45}$$

Shaft acceleration or deceleration determine a torque acting on the airframe.

$$\mathbf{M}^{(engine)} = \left\{ \begin{array}{l} 0 \\ 0 \\ -I_{shaft}\dot{\Omega} \end{array} \right\} \tag{3.46}$$

In the case of *I.C.E.* driven propellers the definition of $\mathbf{M}_{ext}$ slightly changes.

$$\mathbf{M}_{ext} = \mathbf{M}^{(r)} + \mathbf{M}^{(engine)} + \mathbf{M}^{(gyroscopic)} \tag{3.47}$$

In the case of a single engine driving all the propellers of the rotorcraft, the inertia of the shaft must include the inertia of all the rotors and of the mechanical transmission.

$$I_{shaft} = I_{gear} + \Sigma_{j=1}^{N_{rot}} I_{rotor} \tau^2 \tag{3.48}$$

As for the case of electric motors, this engine modeling is conceived with the purpose of giving to the entire mathematical modeling of dynamics of a multi–rotor aircraft an approximated description of the transients of the rotation rate of propellers. This engine dynamics description is far from covering the whole knowledge of an engine behavior.

3.3 Controls

The actions that permit to control the multi–rotor aircraft during its operations must be accounted for in the modeling. Indeed, to a mathematical model it can reasonably be requested the simulation of remote controllers or human pilot's commands. The subject of this section is the insertion of the pilot's actions in the mathematical model.

3.3.1 Multi–Rotor Inputs

A multi–rotor in flight can be maneuvered with simultaneous changes of the spin rates of their rotors. In the majority of the existing platforms any rotor is driven directly by its own electric motor. This implies that there is no actuators action to be modeled, other than the dynamics of the motors shaft, as described in section (3.2.5).
The action of a remote pilot requires some further considerations. A human pilot is capable of guiding the aircraft imposing rotors spin variations by means of a transmitter. The transmitter sends an electromagnetic signal to the receiver of the multi–rotor. The aircraft on–board computer, on the source of the information obtained by that signal, through its algorithms, effects a mixing operation to regulate the electric input of each motor. At

this point the rate of the rotors can vary, following the dynamics of their motors.
From these few words it is clear that the modeling of the control actions concern first the choice of what quantity the pilot really masters.
Obviously the modeling of pilot actions must be suitable to the simulation purpose. Because the argument of this thesis regards more the dynamic aspect of multi–rotor behavior, the electric motor voltage input V_a or the spin rate of rotors Ω can be conveniently chosen as the control input of all the simulation model, for the case of electric driven multi–rotor aircrafts. To all this appropriate considerations have to be added about the concept of control mixing and the particular configuration of multi–rotor vehicle.

3.3.2 Pilot Action Modeling

A multi–rotor aircraft in flight can be maneuvered with variations of the spin rates of its rotors. Any control action does not cause the acceleration or the deceleration of a single rotor. Otherwise unbalanced torques would be generated that would risk the flight.
To allow the aircraft to be safely handled, it is necessary to change the speed of all or some of the rotors together. This fact can be referred to as *control mixing*. The combination of rotors for any control action depends upon:

- the number of rotors;
- the rotors arrangement;
- the type of maneuver.

Any multi-rotor aircraft has its own number of propellers (4, 6 or 8). These are positioned, generally, with respect to the airframe, giving an axisymmetric look to the whole machine. Moreover, the orientation of the "nose" of the aircraft marks also two types of configuration. The so called

X-shape configuration is the one in which the reference axis $\mathbf{x}_B$ is directed between two rotors arms. The other configuration is the *Cross-shape* type, where the reference axis coincide with one of the rotor arms. The sketches (3.8) and (3.9) represent the two possibilities, for an hexa–copter.

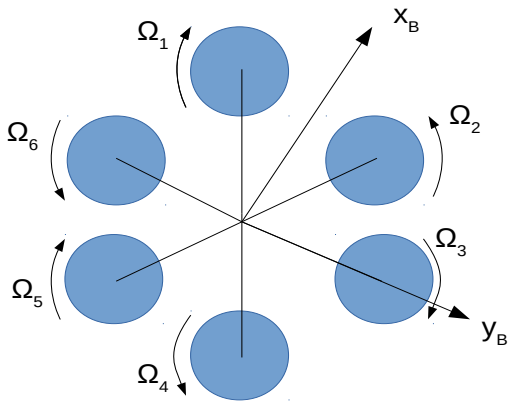

Figure 3.8: *X–Shape* Configuration

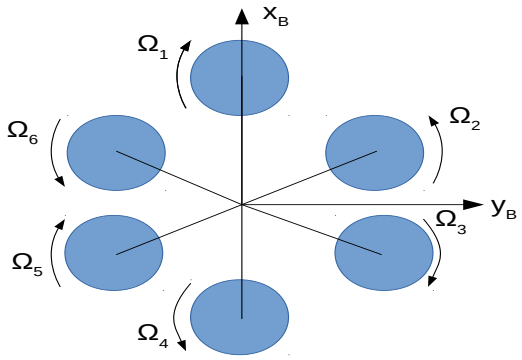

Figure 3.9: *Cross–Shape* Configuration

Once the mock–up of the multi–rotor is precisely defined, for any maneuver, the set of rotors to be driven can be selected. Normally, a multi–rotor

characteristic is to have 4 possibilities of motion in space (4 degrees of freedom). These are:

- the translation along the $\mathbf{z}_B$ axis (vertical flight), analogous to the response to a collective command for helicopters u_{col};
- the rotation about the $\mathbf{x}_B$ axis (lateral flight), analogous to a lateral cyclic command u_{lon} response;
- the rotation about along the $\mathbf{y}_B$ axis (forward and backward flight), analogous to a longitudinal cyclic command u_{lat} response;
- the rotation around the $\mathbf{z}_B$ yawing axis (heading maneuver), analogous to a rudder command u_{rud} response.

Vertical flight can be effected with a simultaneous acceleration or deceleration of all the rotors. This command has an effect on the velocity W.
Lateral flight is imposed with an acceleration of the rotors on the right of the $\mathbf{x}_B$ nose axis and an acceleration of the opposite sign of the other rotors. This command acts on V, W and Φ variables.
Forward flight is imposed with the decrease of spin rate of the rotors whose arms point along the positive verse of the $\mathbf{x}_B$ axis, together with the increase of speed of the other rotors. This command acts on U, W and Θ variables.
A yawing rate is commanded by means of the variation of the rate of rotors that spin in one sense of rotation with the contemporary opposite rate variation of the other rotors. This command acts only on r.
It is worth noticing that horizontal flight is always coupled to an attitude variation. This is why electric driven multi–rotor helicopters are classified as under–actuated systems.
Once that the control action mixing is devised, for any of the 4 commands of the pilot, a linear relation between the range of stick position on the pilot's transmitter and the range of motors voltage or spin rate of propellers

can be established. The stick limit positions can be conveniently put equal to 0 and 1 or to -1 and 1.
For example a collective command u_{col} can be forced to impose to the rotor 1 of figure (3.9) a spin rate as expressed in the next formula [6].

$$\Omega_1 = \Omega_{1,min} + (\Omega_{1,max} - \Omega_{1,min}) \frac{u_{col} - u_{col,min}}{u_{col,max} - u_{col,min}} \tag{3.49}$$

In terms of voltage V_a for rotor 1 in the same figure it can be written an equivalent relation.

$$V_{a1} = V_{a1,min} + (V_{a1,max} - V_{a1,min}) \frac{u_{col} - u_{col,min}}{u_{col,max} - u_{col,min}} \tag{3.50}$$

Another example is the case of a longitudinal command u_{lon}. The rotors spin rates for a cross-shape configuration, considering rotors 1 and 4 of figure (3.9), are the following.

$$\Omega_1 = \Omega_{1,min} - (\Omega_{1,max} - \Omega_{1,min}) \frac{U_{lon} - U_{lon,min}}{U_{lon,max} - U_{lon,min}} \tag{3.51}$$

$$\Omega_4 = \Omega_{4,min} + (\Omega_{4,max} - \Omega_{4,min}) \frac{U_{lon} - U_{lon,min}}{U_{lon,max} - U_{lon,min}} \tag{3.52}$$

Similarly the pilot actions on all the rotors for the possible commands can be easily defined.
The influence on control actions due to the signal transmission between pilot transmitter and the aircraft on–board computer are not here considered. However a very rapid and simple way to consider them could be that of a lag effect. This lag can be modeled with a transfer function with proper values for gain, damp, overshoot [6].

The Input Vector

Now it is defined how the pilot can affect the dynamics of the multi–rotor aircraft. Referring to the *state equation* expression (2.16) of a dynamic system, the *input vector* **U** can be finally defined.

$$\mathbf{U} = [U_{col}\ U_{lon}\ U_{lat}\ U_{rud}]^T \tag{3.53}$$

This is, as always, only a possible choice. The input vector just introduced is proposed for the configuration of multi–rotor platform examined above. For any other configuration or also for this same one other definitions of the **U** vector can be elected.

3.4 Remarks

In this chapter a mathematical description of all the actions to whom a multi–rotor aircraft is subjected during flight is provided in detail. All the formulae are useful to complete a non-linear math model of multi–rotor dynamics of motion. The problem of linear modeling of dynamics of motion is dealt with in a following chapter, because it requires some introductory consideration about the trim condition evaluation.
Great care has been put in the definition of rotor aerodynamics, for obvious reasons. All the results are principally collected from the theory of aerodynamics of helicopters rotors. Proper assumptions and simplifications has been done to obtain instruments apt to the modeling of multi–rotor UAVs aerodynamics.
Moreover, various considerations and personal mathematical expedients are included to render all the equations actually a practical and serviceable tool for simulation in a proper electronic calculation environment, as it can be the $MATLAB^{®}$.
This chapter also suggests a method to insert the action of the pilot in the mathematical modeling of multi–rotor dynamics. It must be pointed out that the results listed here are not the ultimate possibility. They are defined, as all the rest in this thesis, to be functional to the development of the arguments in next chapters.

Chapter 4

Solution of the Equations of Motion

In the previous chapters all the equations needed to analyze the behavior of a multi–rotor aircraft in flight have been provided, after the description of the various phenomena that must be accounted for.
This chapter contains a periphrasis about the approach in the usage of the previous results, from a practical point of view. Also the problem of the integration of the equations of motion and their initialization are treated. This last argument falls in the study of the trim of a multi–rotor aircraft.

4.1 Modeling Objectives and Issues

Till now only a heap of equations has been shown. These equations are only the bricks which the house can be built with.
The mathematical model of the dynamics of an aircraft is a way to analyze a certain behavior of a real physical system. In terms of Systems Theory, this analysis corresponds to the study of the evolution through time of certain quantities, the *state variables*, tied together by a set of equations, that, in vector form, corresponds to the *state equation*. These concepts have already been introduced in sections (2.3.1) and (2.3.4). In those

sections also the notion of *input vector* has been included.

A methodology to write the state equation of a dynamic system, as it is a multi–rotor aircraft, has been addressed. Obviously, the analysis of a dynamic system could be liable to be effected in different manners, admitting different purposes or types of information that have to be reckoned. Other variables or physical aspects could be introduced, but all the efforts, however, must be directed to a precise target.

To clarify, a more practical example can be cited. In the study of a dynamic system it is of paramount importance the choice of the components of the state vector and of the input vector. This choice is directed by the characteristics of the system that have to be analyzed. The number of components of the state and input vectors, and so the complexity of the problem, are strictly dependent upon this consideration. As a paradigmatic case, the angular speed of rotors is worth mentioning. Indeed, the rate of the propellers can be taken both as an element of the state vector or of the input vector. The first case can be that of the direct analysis of the pilot action on the multi–rotor dynamics, where the dynamics of the rotors are required. The second case can be represented by the study of the aerodynamic effect of propellers on the dynamic stability of the multi–rotor aircraft. In this problem the rate of rotors can be seen instead as an input of the system. In following chapters these considerations are applied.

Other than this, the aim of a mathematical model could be also the study of a quantity that is not part of the state vector, like the induced velocity of rotors or the power consumption of motors.

These few words to show that the analytical description of a dynamic system does not have an unique solution. What has been proposed in previous chapters is the one that has been considered suitable to obtain the results that are presented in the following.

Also, the analytical description of the system can not precede the deep examination of the flying machine, viewed as a "solid" subject. This knowledge concerns indeed aspects as number of rotors, mass properties, control

systems, motors curves, energy supplies, payloads, etc. For example, the hypothesis of principle axes of inertia introduced in section (2.3.2) is only an approximation, due to the more or less axisymmetric mock–up of the majority of existing multi–rotor aircraft. The same hypothesis of rigid body could be questioned, thinking about a payload that has some degree of freedom with respect to the airframe of the aircraft.
Lastly, all phenomena could be considered in the modeling, the degree of precision that can be attained in the modeling goes side by side with its complexity and the more great difficulty in the resolution of the equations of motion. So, before writing all the equations, it is worth considering whether the depth of the modeling could bring an effective bargain in the results.
Once the state equation of the dynamic system has been completely written, it is time to deal with the solution of it. This problem is addressed in the next sections.

4.2 Integration of the Equations of Motion

In section (2.3.4) it is stated that the mathematical formulation of the equations of motion provides an expression like that of equation (2.16). This is a system of differential equations. The time t represents the independent parameter, with respect to which the derivatives of the state vector elements are defined. Unfortunately, the solving of such a set of equations does not provide an analytical result available by means of an hand calculation. What can be done is proceeding with a numerical method of resolution.
The solution of a differential equation corresponds to the integration of it. Because the integration is made with respect to time t, the first step is to define the value of the state vector X_0 at the starting time of integration t_0. This is due to the fact that this mathematical problem corresponds to a Cauchy problem, or better to an initial value differential problem. Once

the initial condition of the state vector is known, a numerical integration of the equations can start.
The numerical methods of integration substitute to the analytical solution, at discrete instants of time, an increment of the function to be integrated that is an average of the derivative of the same function in some precise instants of time multiplied by an increment of time Δt. How that average of the derivative through time is calculated, defines a particular method of numerical integration. Any of them has its own performance characteristics, in terms of error in the solution and propagation of the error.
Classical methods of numerical integration are the *Runge–Kutta* methods. For the simulation results shown in this text, the fourth order *Runge–Kutta* explicit method $RK4$ has been utilized, because in the $MATLAB^{®}$ environment it can be easily implemented. The time increment for integration must be chosen so that the results are affordable. This has been done with various attempts. If not declared, in the following the time increment Δt for integration is put equal to 0.01 **s**, reminding also what stated in section (3.2.3).

4.3 The Problem of Trim

In the previous section it is stated that to start the integration of the equations of motion, that is to say a numerical simulation, the knowledge of the initial value of the state vector is mandatory. In section (5.1) it has been assumed that in this work the initial value of the state vector will always coincide with a trim condition, that is a flight equilibrium point. Valid motivations for this choice can be cited from [6]. For example, the trim condition evaluation permits to study the stability and controllability properties of the aircraft. In this case the value of the state vector is necessary to define the linear model that includes all the aerodynamic derivatives. Other reason to find the trim condition is that, to simulate a mission for pilot training, an equilibrium starting point is the preferable

way of initialization.
The solution of the trim problem coincides, on the mathematical point of view, with the definition of the state $\mathbf{X}$ and input $\mathbf{U}$ vectors elements that yield a state vector derivative $\dot{\mathbf{X}}$ equal to zero. Thus, what is to do, is to resolve the equations of the differential system (2.15) with all the left hand sides put equal to zero. In vector form the equation is the following.

$$0 = \boldsymbol{f}(\mathbf{X}, \mathbf{U}) \tag{4.1}$$

The mathematical formulation of the problem shown in the previous chapters is such that the value of the vector of position $\mathbf{P}_E$ does not affect the trim condition calculation. Thus, the only state variables considered in the remainder of the chapter are the attitude $\boldsymbol{\alpha}_E$, velocity $\mathbf{V}_B$ and angular rate $\boldsymbol{\omega}_B$ variables.
Moreover, the solution of the trimming problem it is not more the solution of a differential system, but instead the solution of an algebraic one. However this does not signify that the result can be found easily.

4.3.1 Numerical Trim Solution

The trim equation (4.1) does not in general posses an analytical solution. To solve it, for a general flight trim condition, it is necessary to make use of an numerical (iterative) method.
Some interesting methods of resolution can be listed from literature.
In [17] an iterative process is explained, for the trim of an helicopter, where, beginning with the imposition of very few variables, the value of the other state elements are found, trying to satisfy, step after step, some ulterior constraint. If the iteration does not give acceptable results at some point, the entire process must newly start from the beginning, with new values for the initial constraints. This methodology is referred to, elsewhere, as *Sequential Correction* [6]. In a word this is a procedure that, at any step, tempts to find the equilibrium for any degree of freedom of the system.

Another way is the numerical resolution of the trim equation (4.1). For example, the *Jacobian method*, shown in [6], is a valid one.
First of all, the value of the state vector must be assigned properly or at least with some constraints on its components. Also an initial value to the input vector must be imposed. Then, after a linearization of the equations of motion around the equilibrium point, a linearized model of the perturbation of the state vector is obtained. This small perturbation vector is a linear function of the input small perturbations. If the initial guess of the input vector does not provide a null value of the state vector acceleration perturbation, a new value of the control vector is calculated, in iterative way, until the perturbation of the derivative of state vector is zero or sufficiently near to zero. This method corresponds to the expansion of the *Newton–Raphson* method utilized in section (3.2.3) for vector equation resolution.
In $MATLAB^{®}$ a numerical method for the trim of a dynamic system is implemented. This method has not the same formulation of the *Jacobian method*, but it is an iterative process, too, that exploits the theory of the Lagrangian multipliers (`http://it.mathworks.com/help/simulink/slref/trim.html`). The $MATLAB^{®}$ function named *trim* recalls this numerical method. This function has been cited because in the following section it is used for numerical validation of a special trim calculation.
Anyone of the aforementioned methods can be utilized for the calculation of the trim values of the state vector and of the input vector.

4.3.2 Analytical Trim Solution

In opposition to what has been just asserted, for multi–rotor platforms it exists an equilibrium flight condition that allows an analytical result of the equations of motion.
All rotary wing aircrafts possess, within their flight envelope, the capability of hovering flight. This is a particular flight condition characterized by null values of all the components of the velocity vector $\mathbf{V}_B$ and of the angular

rate vector $\boldsymbol{\omega}_B$. Moreover for a multi–rotor aircraft, due to symmetry of its airframe, the attitude vector $\boldsymbol{\alpha}_E$ can be considered equal to zero in this same equilibrium flight condition. In addition, the condition of zero translational velocity in hovering flight allows to assume null all the drag forces acting both on the rotors and on the airframe, too, and also the rolling moments due to a component in the velocity that could lie on the rotors disks planes.

All these assumptions permit to eliminate, in the equation of motions, a lot of terms that cause various coupling effects between the diverse degrees of freedom of the multi–rotor aircraft, granting a relatively ease of resolution.

Before starting the mathematical demonstration, it is necessary to give some information on the type of aircraft to be trimmed. In this case it is considered a multi–rotor UAV with N_{rot} propellers, driven by electric motors. However the trim calculation will be extended to a different test case in this text with little effort.

Thus the object of the trim calculation is that of finding the spin of the rotors Ω_0 at the equilibrium point of the flight envelope and successively the voltage input V_a of all the motors.

Some assumptions can be made. Particularly, it can be thought that all the rotors, being all immersed in an equal aerodynamic field, must rotate at the same speed and consequently that the motors inputs are the same. Also it is supposed that, for reasons of equilibrium of forces, it can be assumed that the thrust in the trim condition T_0 of each rotor should be equal to the weight of the whole aircraft, divided by the total number of rotors N_{rot} and by a term due to the tilting angle ξ and to the dihedral angle Γ of the rotors themselves.

$$N_{rot}\ T_0\ \cos(\xi)\cos(\Gamma) = mg \tag{4.2}$$

$$T_0 = \frac{mg}{N_{rot}\cos(\xi)\cos(\Gamma)} \tag{4.3}$$

In this last formula, it is supposed that the rotors possess the same dihedral angles and that the tilting angles are equal in *modulus* but differ in sign between adjacent rotors. The reason for this choice will be explained in a following chapter.
The hypothesis of equal rotors spins grants also the equilibrium around the yaw axis $\mathbf{z}_B$.
Having the thrust of any of the rotors, it is also possible, through the formula (3.11), to obtain the induced velocity of each rotor.

$$v_{i0} = \sqrt{\frac{T_0}{2\rho A}} \tag{4.4}$$

Considering now the expression of the thrust coefficient given in equation (3.7) and that in hovering flight $\mu = \mu_z = 0$, the following result is achieved.

$$\frac{T_0}{\rho A \Omega_0^2 R^2} = \frac{\sigma C_{l\alpha}}{2}\left(\frac{\theta_c}{3} - \sqrt{\frac{T_0}{2\rho A}}\frac{1}{2\Omega_0 R} - \frac{\theta_{tw}}{4}\right) \tag{4.5}$$

This last equation is obtained given the definition of the inflow ratio at hover.

$$\lambda_{i0} = \frac{v_{i0}}{\Omega_0 R} \tag{4.6}$$

Provided Ω_0 is the unknown variable, a quadratic equation can be derived from equation (4.5).

$$\left(\frac{\theta_c}{3} - \frac{\theta_{tw}}{4}\right)\Omega_0^2 - \frac{1}{2R}\sqrt{\frac{T_0}{2\rho A}}\,\Omega_0 - \frac{2T_0}{\sigma C_{l\alpha}\rho A R^2} = 0 \tag{4.7}$$

The positive solution provides the magnitude of the rotor spin rate in hovering flight.

$$\Omega_0 = \frac{1}{4R}\sqrt{\frac{T_0}{2\rho A}}\left[\frac{1 + \sqrt{1 + \dfrac{64}{\sigma C_{l\alpha}}\left(\dfrac{\theta_c}{3} - \dfrac{\theta_{tw}}{4}\right)}}{\dfrac{\theta_c}{3} - \dfrac{\theta_{tw}}{4}}\right] \tag{4.8}$$

Once that the speed of the rotors is defined, it is possible to compute also the input voltage of the electric motors V_a, that, as already stated, is supposed to be the same for all the motors.
At the equilibrium point, the shafts of the motors must not be subjected to some acceleration. Thus, from equation (3.38), the identity of torque furnished by the coils of each motor and of the aerodynamic torque of the respective rotor must be granted.

$$Q_{motor} = Q_{rotor}\tau \tag{4.9}$$

In the hovering flight condition, from equations (3.7), it can be shown the following relation between the thrust coefficient and the torque coefficient.

$$C_{\Pi 0} = C_{T0}\lambda_{i0} + \frac{\sigma C_d}{8} \tag{4.10}$$

$$C_{T0} = \frac{T_0}{\rho A(\Omega_0 R)^2} \tag{4.11}$$

Thus, the aerodynamic torque due to the rotor can be computed.

$$Q_{rotor} = \left(\frac{T_0}{\rho A(\Omega_0 R)^2}\frac{v_{i0}}{\Omega_0 R} + \frac{\sigma C_d}{8}\right)\rho A(\Omega_0 R)^2 R \tag{4.12}$$

From equation (3.36) the armature current at hover can be found.

$$i_{a0} = \frac{Q_{rotor}\tau}{K_t} = \frac{\left(\frac{T_0}{\rho A(\Omega_0 R)^2}\frac{v_{i0}}{\Omega_0 R} + \frac{\sigma C_d}{8}\right)\rho A(\Omega_0 R)^2 R\ \tau}{K_t} \tag{4.13}$$

And finally from equation (3.35) the trim input voltage is achieved.

$$\begin{aligned} V_{a0} = &\quad R_a i_{a0} + K_e\Omega_0 = \\ &= \frac{\left(\frac{T_0}{\rho A(\Omega_0 R)^2}\frac{v_{i0}}{\Omega_0 R} + \frac{\sigma C_d}{8}\right)\rho A(\Omega_0 R)^2 R\ \tau}{K_t} + K_e\Omega_0 \end{aligned} \tag{4.14}$$

With this last result all the data necessary to start the simulation of a mission are obtained.

Numerical Test

Exploiting the $MATLAB^{®}$ function mentioned before, it is possible a numerical validation of the trim calculation method for hovering flight. Now it is considered the case of a hexa–copter driven by electric motors. With the formulae of the previous section and the data contained in table (4.3), supposing $\mathbf{V}_B = 0$ **m** $\mathbf{s}^{-1}$, $\boldsymbol{\omega}_B = 0$ **rad** $\mathbf{s}^{-1}$ and $\boldsymbol{\alpha}_E = 0$ **rad**, the following values for Ω_0, $v_i 0$ and V_{a0} can be computed.

Ω_0	461.9230 **rad** $\mathbf{s}^{-1}$
V_{a0}	2.4159 **V**
v_{i0}	6.1725 **m** $\mathbf{s}^{-1}$

Table 4.1: Hovering Flight: Trim Analytical Results

Using the numeric resolution method implemented in $MATLAB^{®}$, the components of the state vector are calculated, for the hovering flight condition. The input of any motor, the spin rate and the induced velocity for any of the rotors are also computed.
The numeric results are identical for both the trimming problem solutions. Through another simulation during a finite period of time, it can be seen that this flight condition is perfectly maintained by the multi–rotor aircraft.

4.4 Remarks

This chapter has started with a brief discussion about the approach in the analysis of dynamic systems. This to have an insight in the usage of the mathematical expressions till now described, in a complex simulation environment. Attention has been paid also to the identification of the real

$\boldsymbol{\alpha}_E$ [rad]	$\mathbf{V}_B$ [m s^{-1}]	$\boldsymbol{\omega}_B$ [rad s^{-1}]
-0.0000	0.0000	0.0000
-0.0000	0.0000	0.0000
-0.0000	0.0000	0.0000
Ω_0 [rad s^{-1}]	V_{a0} [V]	v_{i0} [m s^{-1}]
461.9230	2.4159	6.1725
461.9230	2.4159	6.1725
461.9230	2.4159	6.1725
461.9230	2.4159	6.1725
461.9230	2.4159	6.1725
461.9230	2.4159	6.1725

Table 4.2: Hovering Flight: Trim $MATLAB^{®}$ Results

Type	Value	Unity	Type	Value	Unity
ρ	1.2235	kg m^{-3}	g	9.81	m s^{-2}
m	4	kg	I_{xx}	0.044	kg m^2
I_{yy}	0.044	kg m^2	I_{zz}	0.098	kg m^2
N_{rot}	6		R	0.15	m
N	2		θ_c	15	^{o}
θ_{tw}	2	^{o}	$C_{l\alpha}$	5.5	rad^{-1}
C_d	0.003		c	0.04	m
I_{rotor}	10^{-4}	kg m^2	b	0.68	m
h	-0.3	m	R_a	0.01	Ω
K_e	0.005	N m A^{-1}	ξ	5	^{o}
Γ	5	^{o}	τ	1	

Table 4.3: Hexa–Copter Data for Trim Calculation

system and on the choice of the behaviors of interest.
After this, some questions around the mathematical aspects of simulation of dynamic systems has been faced. Hints about the resolution of the equations of motion have been mentioned. Finally the problem of the initial condition for the integration of the equations has been discussed and an analytic solution to the problem of trim of the multi–rotor aircraft has been described.
The knowledge of the equilibrium flight condition is not only usable for direct integration of the equations of motion. All the results just found are necessary to the definition of linearized model of dynamics of motion, as already discussed in section (5.1). As it is testified in the remainder of this thesis, the trim point evaluation permits to affront the problem of stability and controllability of the type of air vehicles under study, in a purely analytic way. From now on, the condition of hovering flight is assumed as the trim –or equilibrium– flight condition.

Chapter 5

Multi–Rotor Dynamics Linear Modeling

In chapter (2) only the non–linear modeling of dynamics has been considered.

This chapter deals instead with the linear modeling of dynamics. It starts with the definition of the linearized equations of motion. Then it proceeds with the linearization of the rotor aerodynamic loads. After, all the aerodynamic and control derivatives are computed and the stability and control matrices are defined.

5.1 Linearized Equations of Motion

The other classical approach in the study of the dynamic characteristics of a system like a flying vehicle is based on the linear analysis of its behavior in the proximity of a trim condition of its flight envelope. The trim condition represents an equilibrium point of the differential equations system (2.16), that is a value of $\mathbf{X}$ for whom its time derivative $\dot{\mathbf{X}}$ is null.

The linearized equations of dynamics can be written in the following classical form.

$$\begin{cases} \dot{\mathbf{x}} = \mathbf{A}\mathbf{x} + \mathbf{B}\mathbf{u}, \quad \mathbf{x}(t_0) = \mathbf{x}_0 \\ \mathbf{y} = \mathbf{C}\mathbf{x} + \mathbf{D}\mathbf{u} \end{cases} \tag{5.1}$$

$\mathbf{x}$ is still the state vector, but now it represents the small perturbation of the state variables from the equilibrium point. $\mathbf{y}$ is the output vector. $\mathbf{u}$ is the vector of small variations of the inputs of the system. This vector will assume a proper definition for any of the configurations of multi–rotor analyzed in the next chapters. $\mathbf{A}$ is called *stability matrix* or *state matrix* and $\mathbf{B}$ is the *control matrix*. $\mathbf{C}$ and $\mathbf{D}$ are the observability matrices of the state and of the inputs. In this work only the study of the first equation of the system (5.1) is considered.

As before, $\mathbf{x}_0$ is the state vector at the initial time t_0 and it represents also the trim condition. From now on the notations for a trim flight condition and the initial condition for a flight simulation will be the same, because they will always coincide. In the trim condition, the previous differential system reduces to the following set of algebraic equations.

$$\begin{cases} 0 = \mathbf{A}\mathbf{x}_0 + \mathbf{B}\mathbf{u}_0, \quad \mathbf{x}_0 = \mathbf{x}(t_0) \\ \mathbf{y}_0 = \mathbf{C}\mathbf{x}_0 + \mathbf{D}\mathbf{u}_0 \end{cases} \tag{5.2}$$

The relation between state vector $\mathbf{X}$ and state vector $\mathbf{x}$ is stated by the next system of equations.

$$\begin{cases} \mathbf{X} = \mathbf{X}_0 + \mathbf{x} \\ \dot{\mathbf{X}} = \dot{\mathbf{X}}_0 + \dot{\mathbf{x}} = \dot{\mathbf{x}} \end{cases} \tag{5.3}$$

In the present work, in the linearized modeling of dynamics of a rigid body, from the state vector $\mathbf{x}$, the perturbations of the variables of position N, E, D are excluded, because they are not decisive in the questions of dynamic stability discussed in following chapters. The state vector can be defined as follows.

$$\mathbf{x} = [\phi, \theta, \psi, u, v, w, p, q, r]^T \tag{5.4}$$

The linearized equations of motion are obtained, as the name suggests, from an operation of linearization of the non–linear equations of motion around a trim condition. With this consideration the **A** and **B** matrices can be defined in terms of *Jacobian* of the vector function $\boldsymbol{f}$ (eqn. 2.16), neglecting the equation of kinematics of position.

$$\mathbf{A} = \frac{\partial \boldsymbol{f}}{\partial \mathbf{X}}, \quad \mathbf{B} = \frac{\partial \boldsymbol{f}}{\partial \mathbf{U}} \tag{5.5}$$

In the equations of system (5.1) the dynamics of the state vector are written in compact form. The linearized dynamics of the state vector $\mathbf{x}$ can be expressed in a more explicit way, bringing to the writing of a system of scalar differential equations. The 0 subscript indicates the trim condition and the Δ indicates the small finite excursion of the related variable.

$$\begin{cases} m\dot{u} = \Delta X - mqW_0 + mrV_0 - mg\cos(\Theta_0)\Delta\Theta \\ m\dot{v} = \Delta Y - mrU_0 + mpW_0 - mg\cos(\Phi_0)\Delta\Phi \\ m\dot{w} = \Delta Z - mpV_0 + mqU_0 - mg\sin(\Theta_0)\Delta\Theta \\ I_{xx}\dot{p} = \Delta L \\ I_{yy}\dot{q} = \Delta M \\ I_{zz}\dot{r} = \Delta N \\ \dot{\phi} = p \\ \dot{\theta} = q \\ \dot{\psi} = r \end{cases} \tag{5.6}$$

These equations are the equations of linearized dynamics of an aircraft with respect to a *Body Axis* reference frame. This differential system is referred to an equilibrium point for the state vector of the complete dynamics, namely, $\mathbf{X}_0$.

$$\mathbf{X}_0 = [\Phi_0, \Theta_0, \Psi_0, U_0, V_0, W_0, 0, 0, 0]^T \tag{5.7}$$

$\mathbf{X}_0$ can represent a general condition of trimmed horizontal or vertical flight for a multi–rotor aircraft.

Noting that $\Delta\Theta = \theta$ and that $\Delta\Phi = \phi$ and isolating the time derivatives, the linearized system can be rewritten.

$$\begin{cases} \dot{u} = \Delta X/m - qW_0 + rV_0 - g\cos(\Theta_0)\Delta\Theta \\ \dot{v} = \Delta Y/m - rU_0 + pW_0 - g\cos(\Phi_0)\Delta\Phi \\ \dot{w} = \Delta Z/m - pV_0 + qU_0 - g\sin(\Theta_0)\Delta\Theta \\ \dot{p} = \Delta L/I_{xx} \\ \dot{q} = \Delta M/I_{yy} \\ \dot{r} = \Delta N/I_{zz} \\ \dot{\phi} = p \\ \dot{\theta} = q \\ \dot{\psi} = r \end{cases} \tag{5.8}$$

This formulation of the equations of the linearized dynamics coincide with the first equation of the system (5.1).

The vectors $\Delta\mathbf{F} = [\Delta X, \Delta Y, \Delta Z]^T$ and $\Delta\mathbf{M} = [\Delta L, \Delta M, \Delta N]^T$ define the perturbations of the external forces and moments. They are computed as the sum of the perturbations due to every component of both the state vector $\mathbf{x}$ and the control vector $\mathbf{u}$, by means of the first terms of a Taylor's series expansion. For example, $\Delta X = X_u\Delta u + X_v\Delta v + ... + X_{u_i}\Delta u_i + ...$, where u_i is the i–th element of the vector $\mathbf{u}$. Every term of the sum is the first term of the Taylor's series expansion of X associated to the variable in subscript. They are generally known as aerodynamic derivatives. All the aerodynamic derivatives permit to define all the elements of the stability matrix $\mathbf{A}$ and those of the control matrix $\mathbf{B}$. The elements of $\mathbf{A}$ are the stability derivatives and the elements of $\mathbf{B}$ are the control derivatives. Their definitions are discussed in following chapters, once all the external actions on the multi–rotor are defined too.

5.2 Rotor Linearized Aerodynamics

To define precisely the aerodynamic derivatives of the linearized model of dynamics, some considerations about linearization of aerodynamic loads of rotors must be added.

The linearized model of the dynamics of a system is characterized, as in expression (5.1), by the *Stability matrix* **A** and the *Control matrix* **B**. The components of these matrices represent, for a multi–rotor aircraft, the perturbations of forces and moments acting on it, due to little variations of the state variable and of the control inputs. In section (5.1) it has been stated that these small perturbations can be computed by means of an operation of differentiation of the various loads.

The forces and moments acting on the aircraft depend all on the state vector variables (attitude, velocity and angular rates) other than the control inputs. In the 6 D.O.F. math model this relations are included and defined. To obtain the aerodynamic derivatives, all these relations must be considered in the differentiation. In particular great care is necessary for the definition of the derivatives of the aerodynamic actions of the rotors, described by their relative aerodynamic coefficients. The coefficients are those defined in equation (3.7).

In the formulae of the coefficients quantities as the advance ratio, the climb ratio, the inflow ratio and blade pitch are included, besides the aerodynamic and geometric parameters of rotors. All these quantities depend on the state variables themselves.

Also, a particular attention must be paid to the presence of the induced velocity, that is itself dependent on rotor thrust and velocities.

In the academic literature about helicopters flight theory, useful results are again available. Thus, helicopters aerodynamics is yet the starting point. The equations shown in this section are extracted directly from [2] or derived from the results described in the same text.

The next formulae are relative to the hovering flight condition.

θ_{c0} is the blades pitch of a rotor in the hovering flight condition.

$$\frac{\partial \lambda_i}{\partial \mu} = 0 \tag{5.9}$$

$$\frac{\partial (\lambda_i - \mu_z)}{\partial \mu_z} = -\frac{8\lambda_{i0}}{16\lambda_{i0} + C_{L\alpha}\sigma} \tag{5.10}$$

$$\frac{\partial C_T}{\partial \mu} = 0 \tag{5.11}$$

$$\frac{\partial C_T}{\partial \mu_z} = \frac{2\sigma C_{L\alpha}\lambda_{i0}}{16\lambda_{i0} + C_{L\alpha}\sigma} \tag{5.12}$$

$$\frac{\partial C_T}{\partial \theta_c} = \frac{\frac{8}{3}\sigma C_{L\alpha}\lambda_{i0}}{16\lambda_{i0} + C_{L\alpha}\sigma} \tag{5.13}$$

$$\frac{\partial \lambda_i}{\partial \theta_c} = \frac{1}{2}\frac{\lambda_{i0}}{C_{T0}}\frac{\partial C_T}{\partial \theta_c} \tag{5.14}$$

$$\frac{\partial (\lambda_i - \mu_z)}{\partial \theta_c} = \frac{\partial \lambda_i}{\partial \theta_c} \tag{5.15}$$

From these equations it can be defined the derivative of the inflow ratio with respect to the pitch of the blades.

$$\frac{\partial \lambda_i}{\partial \theta_c} = \frac{2}{3}\left(\frac{C_{L\alpha}\sigma}{8\lambda_{i0} + C_{L\alpha}\sigma}\right) \tag{5.16}$$

Now the other derivatives necessary to the definition of the linearized rotor aerodynamics can be obtained. The missing derivatives are $\partial C_\Pi/\partial \mu$, $\partial C_\Pi/\partial \mu_z$, $\partial C_\Pi/\partial \theta_c$ and the derivatives of C_H and C_Λ coefficients.
Noting that μ_z is independent of μ, the next relation stands.

$$\frac{\partial (\lambda_i - \mu_z)}{\partial \mu} = \frac{\partial \lambda_i}{\partial \mu} = 0 \tag{5.17}$$

Thus, it can be shown that $\partial C_\Pi/\partial \mu = 0$.

$$\frac{\partial C_\Pi}{\partial \mu} = \sigma C_{L\alpha}\left[\frac{\partial(\lambda_i-\mu_z)}{\partial \mu}\left(\frac{\theta_c}{6}-\frac{\theta_{tw}}{8}-\frac{\lambda_i-\mu_z}{4}\right)- -(\lambda_i-\mu_z)\frac{1}{4}\frac{\partial(\lambda_i-\mu_z)}{\partial \mu}+\frac{C_d}{8C_{l\alpha}}(2\mu)\right] \tag{5.18}$$

In hovering flight $\mu, \mu_z = 0$.

$$\frac{\partial C_\Pi}{\partial \mu} = \sigma C_{L\alpha}\left[\frac{\partial \lambda_i}{\partial \mu}\left(\frac{\theta_c}{6}-\frac{\theta_{tw}}{8}-\frac{\lambda_i}{4}\right)-\lambda_i\frac{1}{4}\frac{\partial \lambda_i}{\partial \mu}+0\right]=0 \tag{5.19}$$

For the $\partial C_\Pi/\partial \mu_z$ derivative the chain rule must be used in the differentiation.

$$\frac{\partial C_\Pi}{\partial \mu_z} = \frac{\partial C_Q}{\partial(\lambda_i-\mu_z)}\frac{\partial(\lambda_i-\mu_z)}{\partial \mu_z} \tag{5.20}$$

$$\frac{\partial C_\Pi}{\partial(\lambda_i-\mu_z)} = \sigma C_{L\alpha}\left[\left(\frac{\theta_c}{6}-\frac{\theta_{tw}}{8}-\frac{\lambda_i-\mu_z}{4}\right)-\frac{\lambda_i-\mu_z}{4}\right] \tag{5.21}$$

Combining this result with the derivative of the downwash ratio $(\lambda_i-\mu_z)$, the derivative can be calculated.

$$\frac{\partial C_\Pi}{\partial \mu_z} = \frac{-4\sigma C_{L\alpha}}{16\lambda_{i0}+\sigma C_{L\alpha}}\left(\frac{\theta_{c0}}{3}-\frac{\theta_{tw}}{4}-\lambda_{i0}\right) \tag{5.22}$$

The derivative $\partial C_\Pi/\partial \theta_c$ can be calculated as a sum of derivatives.

$$\frac{\partial C_\Pi}{\partial \theta_c} = \sigma C_{L\alpha}\left[\frac{(\lambda_i-\mu_z)}{6}+\frac{\partial(\lambda_i-\mu_z)}{\partial \theta_c}\left(\frac{\theta_c}{6}-\frac{\theta_{tw}}{8}\right)-\frac{1}{4}\frac{\partial(\lambda_i-\mu_z)^2}{\partial \theta_c}+0\right] \tag{5.23}$$

For the rule of differentiation of a composed function it can be obtained the following expression.

$$\frac{\partial(\lambda_i-\mu_z)^2}{\partial \theta_c} = 2(\lambda_i-\mu_z)\frac{\partial(\lambda_i-\mu_z)}{\partial \theta_c} \tag{5.24}$$

Finally $\partial C_\Pi/\partial \theta_c$ can be calculated.

$$\frac{\partial C_\Pi}{\partial \theta_c} = \sigma C_{L\alpha}\left[\frac{\lambda_{i0}}{6} + \frac{2}{3}\frac{C_{L\alpha}\sigma}{8\lambda_{i0} + C_{L\alpha}\sigma}\left(\frac{\theta_{c0}}{6} - \frac{\theta_{tw}}{8}\right) - \frac{\lambda_{i0}}{3}\frac{C_{L\alpha}\sigma}{8\lambda_{i0} + C_{L\alpha}\sigma}\right] \tag{5.25}$$

The derivatives of C_H and C_Λ are very easy to compute. Thus the demonstration is omitted.

$$\frac{\partial C_H}{\partial \mu} = \sigma C_d/4 \tag{5.26}$$

$$\frac{\partial C_H}{\partial \mu_z} = 0 \tag{5.27}$$

$$\frac{\partial C_H}{\partial \theta_c} = 0 \tag{5.28}$$

$$\frac{\partial C_\Lambda}{\partial \mu} = \sigma C_{L\alpha}\left(\frac{\theta_{c0}}{6} - \frac{\lambda_{i0}}{2} - \frac{\theta_{tw}}{8}\right) \tag{5.29}$$

$$\frac{\partial C_\Lambda}{\partial \mu_z} = 0 \tag{5.30}$$

$$\frac{\partial C_\Lambda}{\partial \theta_c} = 0 \tag{5.31}$$

Although all the derivatives are calculated in the case of hovering flight, for easing the writing, the subscript 0 is not included.

5.2.1 The Rotor Rate Derivatives

The motor or engine speed perturbation can be a component of the state vector. Then the derivatives with respect to this variable must be computed. In this case the hypothesis of constancy of the rotors aerodynamic coefficients during motor or engine acceleration is applied. For example, with that assumption, the variation of thrust of a rotor can be evaluated in the following way.

$$\Delta T = T_\Omega \Delta\Omega = C_T\ \rho A\ (\tau R)^2\ 2\Omega_0\ \Delta\Omega \tag{5.32}$$

5.3 Stability and Control Matrices Computation

In this section the linearized model of dynamics is completed with the calculation of the elements of the **A** and **B** matrices. The results of the previous sections are the base for the following treatment. Numerical tests permit to evaluate the goodness of the linear modeling, in association with the non–linear one. Here it is considered a multi–rotor traditional configuration with electric driven propellers, exactly that of section (4.3.2).

5.3.1 Premise

In section (5.1) an implicit formulation of the linear equations of motion is shown. The so called *state equation* is characterized by the two matrices **A** and **B**. This equation can be used to describe the dynamics of a multi–rotor aircraft in the neighborhood of an equilibrium flight condition, in terms of small variations of the state variables.
For completing the non–linear modeling of dynamics, the definition of vectors of external forces and moments has been executed. Similarly, for the linear equations of motion (5.8) the perturbations of the external actions must be computed.
The definition of the linearized model of an aircraft can be done either in an experimental or a mathematical way. The experimental way is the so called *System Identification* methodology [26, 14]. The other way is to directly compute the values of the derivatives, with a numerical differentiation or with the analytical differentiation of the non linear equations of motion [17].
In this thesis the expression of the matrices is found by differentiation of the equations. The calculation can be made in both manners, numerical and analytical, to compare the two results, as a first check for the analytic differentiation. The numerical differentiation can be done with the $MATLAB^{®}$ functions. The analytic differentiation is explained in detail in the following, both for the stability matrix and for the control matrix.

5.3.2 Conventions

When in the following formulae the derivative of C_T will appear, there will be always a negative sign. This is due to the fact that the thrust of a rotor is oriented along the $\mathbf{z}_R$ axis with verse opposite to the same axis.
Attention must be paid also when the derivative of C_Π appears because of the verse of rotation of each rotor.

5.3.3 Derivatives Trim Values

In the computation the following relations must be considered.

$$C_{T0j} = \frac{mg}{N_{rot}\cos(\Gamma_j)\cos(\xi_j)\rho A(\Omega_0 R)^2} \tag{5.33}$$

$$C_{\Pi 0j} = \left[\sigma C_{l\alpha}\left(\frac{\theta_c}{6} - \frac{\theta_{tw}}{8} - \frac{\lambda_{i0}}{4}\right)\lambda_{i0} + \frac{\sigma C_d}{8}\right] \tag{5.34}$$

$$\Omega_0 = |\Omega_{0j}| \tag{5.35}$$

j indicates the j-th rotor. The last equation is based on the assumption that, in the trim condition, all the rotors spin at the same rate. In the trim condition, also, the derivatives of the rotor coefficients are assumed equal for all the rotors. Also θ_c is a constant, equal for all the rotors.
In the linear model, the gyroscopic effects are neglected. In hovering the contribute of airframe drag can be ignored. Also, the effects both of the drag coefficient C_H and of the rolling moment coefficient C_Λ are neglected, because they describe, as it appears clear from their definition, second order aerodynamic effects with respect to the thrust and torque coefficients, especially near the hovering flight condition where $\mu = 0$.

5.3.4 Stability Derivatives

The stability matrix $\mathbf{A}$ is a square matrix with 9 rows and 9 columns. In the subsequent argumentation it is explained how the elements of $\mathbf{A}$ are

computed.

Attitude kinematics terms

The first three rows represent the linearized kinematics of the attitude. The only non–zero terms in them are the following.

$$A_{1,7} = A_{2,8} = A_{3,9} = 1 \tag{5.36}$$

This result descends immediately from the relation between derivatives of Euler's angles and angular rates in the *Body Axis* frame, in the hovering flight condition.

X_θ and Y_ϕ derivatives

The next three rows describe the dynamics of velocity in *Body Axis* frame. $A_{4,2}$ and $A_{5,1}$ define the effects of attitude variations combined with gravity acceleration.

$$A_{4,2} = X_\theta = -g \tag{5.37}$$

$$A_{5,1} = Y_\phi = g \tag{5.38}$$

X, Y and Z Derivatives

These derivatives describe the effects of the variations of velocities, angular rates on the velocity dynamics.
Of the X terms, other than X_θ, only X_u and X_q are effective and both derivatives are due to the variation of C_T. X_v has no effect because the drag of rotors would not give a component along the x_B axis. X_w is null because the variation of C_T is null. The rotors drag effects due to yaw rate variations are nullified by the symmetric displacement of the rotors.
To define the derivative X_u, for each rotor the velocity u must be resolved to the *Rotor Axis* frame, to be multiplied by $\frac{\partial C_T}{\partial \mu_z}$: this operation is done

through a multiplication by the term $\mathbf{T}_j(3,1)$ of the matrix $\mathbf{T}_j$. Then this perturbation of the rotor thrust must be transposed back to the *Body Axis* frame and its component directed along the $\mathbf{x}_B$ direction must be isolated. This operation can be done through the multiplication by $\mathbf{T}_j^{-1}(1,3)$. It is worth reminding that a rotation matrix is an orthonormal one: its inverse is equal to its transpose. Thus, $\mathbf{T}_j^{-1}(1,3) = \mathbf{T}_j^T(1,3) = \mathbf{T}_j(3,1)$.
Finally, the derivative X_u is the sum of the contributions of all the rotors. This utilization of the matrix $\mathbf{T}_j$ is the way to insert the tilting angles of the rotors in the definition of the stability derivatives. Indeed, the modification of an unique or two parameters within the rotation matrix permits to insert, severed from the others, the contribute due to any rotor alone. Similar considerations can be applied in the evaluation of all the other derivatives. Obviously the elements of the rotation matrix selected for each derivative depend upon the component of the state vector and upon the direction of the action considered.

$$A_{4,4} = X_u = -\frac{1}{m} \sum_{j=1}^{N_{rot}} \frac{\partial C_T}{\partial \mu_z} \, \rho A \, \Omega_0 \, R \, \mathbf{T}_j(3,1)^2 \tag{5.39}$$

To compute the X_q derivative two effects must be considered: one for the distance of each rotor location from the C.G. along the $\mathbf{z}_B$ direction (component of velocity on rotor qh) and another for the component of velocity due to the rotor arm in the plane $\{(\mathbf{x}_B, \mathbf{y}_B)\}$. Both the velocity components generate variations of thrust along the $\mathbf{y}_B$ direction and along the $\mathbf{z}_B$ direction.

$$\begin{aligned} A_{4,8} = X_q \quad &= -\frac{1}{m} \sum_{j=1}^{N_{rot}} \frac{\partial C_T}{\partial \mu_z} \, \rho A \, \Omega_0 \, R \, (-b \cos \delta_j) \, \mathbf{T}_j(3,1) \, \mathbf{T}_j(3,3) - \\ &-\frac{1}{m} \sum_{j=1}^{N_{rot}} \frac{\partial C_T}{\partial \mu_z} \, \rho A \, \Omega_0 \, R \, h \, \mathbf{T}_j(3,1)^2 \end{aligned} \tag{5.40}$$

For the Y terms the same considerations apply. Only Y_v and Y_p are not null.

$$A_{5,5} = Y_v = -\frac{1}{m} \sum_{j=1}^{N_{rot}} \frac{\partial C_T}{\partial \mu_z} \rho A \, \Omega_0 \, R \, \mathbf{T}_j(3,2)^2 \tag{5.41}$$

$$\begin{aligned} A_{5,7} = Y_p = \quad & -\frac{1}{m} \sum_{j=1}^{N_{rot}} \frac{\partial C_T}{\partial \mu_z} \rho A \, \Omega_0 \, R \times \\ & \times \left[(b \sin(\delta_j)) \, \mathbf{T}_j(3,2) \, \mathbf{T}_j(3,3) + (-h) \, \mathbf{T}_j(3,2)^2 \right] \end{aligned} \tag{5.42}$$

Along the z_B axis the perturbations of forces are generated by variations of climb ratio of the rotors, mostly due to perturbations on w. From equation (5.11) it is clear why the contributions of u, v, r are zero. For symmetry in rotors displacement the effects of p and q are also null.

$$A_{6,6} = Z_w = -\frac{1}{m} \sum_{j=1}^{N_{rot}} \frac{\partial C_T}{\partial \mu_z} \rho A \, \Omega_0 \, R \, \mathbf{T}_j(3,3)^2 \tag{5.43}$$

L, M and N Derivatives

For the roll dynamics the remarkable effects are those due to the lateral velocity v that gives a variation of the thrust of all rotors and those due to the p rate itself that generates opposite variations of C_T on the lateral rotors. For reasons of symmetry, other effects are negligible.

$$\begin{aligned} A_{7,5} = L_v = \quad & -\frac{1}{I_{xx}} \sum_{j=1}^{N_{rot}} \frac{\partial C_T}{\partial \mu_z} \rho A \, \Omega_0 \, R \, \mathbf{T}_j(3,2) \times \\ & \times \left[b \sin(\delta_j) \mathbf{T}_j(3,3) + (-h) \mathbf{T}_j(3,2) \right] \end{aligned} \tag{5.44}$$

h is the height of rotors from the center of gravity of the aircraft: $h < 0$ if the rotors are placed above the C.G. itself.

$$A_{7,7} = L_p = \quad -\frac{1}{I_{xx}} \sum_{j=1}^{N_{rot}} \frac{\partial C_T}{\partial \mu_z} \; \rho A \; \Omega_0 \; R \; \times \\ \times \left[b \sin(\delta_j) \mathbf{T}_j(3,3) - h \mathbf{T}_j(3,2) \right] \tag{5.45}$$

For the pitch dynamics the results are similar to those for the roll dynamics.

$$A_{8,4} = M_u = \quad -\frac{1}{I_{yy}} \sum_{j=1}^{N_{rot}} \frac{\partial C_T}{\partial \mu_z} \; \rho A \; \Omega_0 \; R \; \mathbf{T}_j(3,1) \times \\ \times \left[h \mathbf{T}_j(3,1) + (-b \cos(\delta_j)) \mathbf{T}_j(3,3) \right] \tag{5.46}$$

$$A_{8,8} = M_q = \quad -\frac{1}{I_{yy}} \sum_{j=1}^{N_{rot}} \frac{\partial C_T}{\partial \mu_z} \; \rho A \; \Omega_0 \; R \; \times \\ \times \left[b \cos(\delta_j) \mathbf{T}_j(3,3) + (-h) \mathbf{T}_j(3,1) \right] \tag{5.47}$$

On the dynamics of yaw rate r instead the most important derivative is N_r. The other effects can be supposed negligible for symmetry of rotors displacement and for the alternation of their verses of rotation. N_r is composed by two factors, for any rotor: one for the variation of torque and one for the variation of thrust. In the following formula the matrix $\tilde{\mathbf{T}}_j$ is inserted, because the effect of r on all the rotors is independent of the azimuth position of rotors.

$$A_{9,9} = N_r = \quad -\frac{1}{I_{zz}} \sum_{j=1}^{N_{rot}} \frac{\partial C_T}{\partial \mu_z} \; \rho A \; \Omega_0 \; R \; b^2 \tilde{\mathbf{T}}_j(3,2)^2 + \\ + \frac{1}{I_{zz}} \sum_{j=1}^{N_{rot}} \frac{\partial C_\Pi}{\partial \mu_z} \; \rho A \; \Omega_0 \; sgn(\Omega_{0,j}) \; R^2 \; b \; \tilde{\mathbf{T}}_j(3,2) \tilde{\mathbf{T}}_j(3,3) \tag{5.48}$$

5.3.5 The Stability Matrix

Finally the stability matrix can be written in the proper form.

$$\mathbf{A} = \begin{bmatrix} 0 & 0 & 0 & 0 & 0 & 0 & 1 & 0 & 0 \\ 0 & 0 & 0 & 0 & 0 & 0 & 0 & 1 & 0 \\ 0 & 0 & 0 & 0 & 0 & 0 & 0 & 0 & 1 \\ 0 & X_\theta & 0 & X_u & 0 & 0 & 0 & 0 & 0 \\ Y_\phi & 0 & 0 & 0 & Y_v & 0 & 0 & 0 & 0 \\ 0 & 0 & 0 & 0 & 0 & Z_w & 0 & 0 & 0 \\ 0 & 0 & 0 & 0 & L_v & 0 & L_p & 0 & 0 \\ 0 & 0 & 0 & M_u & 0 & 0 & 0 & M_q & 0 \\ 0 & 0 & 0 & 0 & 0 & 0 & 0 & 0 & N_r \end{bmatrix} \tag{5.49}$$

5.3.6 Control Derivatives

In section (3.2.5) the dynamics of a rotor have been described by the equations of angular motion of the shaft of the electric motor associated to the rotor itself. The speeds of rotors are the quantities that permit to change the state of the aircraft. As described before, however, they do not represent the inputs of the system. The inputs are the voltages of the electromagnetic circuits of motors.

In the non–linear model, the definition of dynamics of motors is included to insert appropriate transients in the rotors speed, eliminating unreal step variations in the angular rates. But, also, these equations are not comprehensive of other effects, as electric transients, regulation of current armature, etc. thus maintaining some degree of uncertainty.

Thus, as control inputs, the small variations of rotors velocities are chosen. The rotors dynamics could be successively inserted, in a more practical way, as transfer functions of the motors. With this hypothesis the study can focus more on the aerodynamic effects of rotors on the state dynamics. That is a result nevertheless interesting, if not only an experimental relation between thrust and motor input is considered.

The components of the control matrix **B** describe the influence of small variations of control inputs on the kinematics and dynamics of the aircraft. The matrix **B** in the present case has 9 rows and 4 columns. The columns are 4 because the aircraft possesses 4 inputs, as discussed in section (3.3.2). These inputs can be listed as:

1. simultaneous variation of all rotors spin rates for vertical flight (*collective* or *throttle* command);
2. opposite variations of spin rates of the "back" rotors and on the "fore" rotors for forward flight (*longitudinal* command);
3. opposite variations of spin rates of rotors on the "right" side and on the "left" side for lateral flight (*lateral* command);
4. opposite variations of spin rates of adjacent rotors for heading control (*directional* or *rudder* command).

In case of perturbation of the control variables, the input vector for the linear model can be defined with the next expression.

$$\mathbf{u} = [u_{col}\ u_{lon}\ u_{lat}\ u_{rud}]^T \tag{5.50}$$

From the 6 D.O.F. model equations it is clear that the inputs do not directly affect the attitude kinematics, in hovering flight, so that the first three rows of the matrix are rows of zeros.

Collective Command Derivatives

From the hovering condition, for symmetric displacement and orientation of the rotors, the collective command exerts its influence only on the vertical direction. Thus the notable derivative is Z_{col}. The value of this derivative can be found making use of equation (5.32). It must be considered only the projection of the thrust of each rotor along the $\mathbf{z}_B$ axis.

$$Z_{col} = \frac{1}{m} \sum_{j=1}^{N_{rot}} \mathbf{T}_j(3,3) \left[-\frac{mg}{N_{rot} \cos(\Gamma_j) \cos(\xi_j)} \frac{2}{\Omega_0} \right] \tag{5.51}$$

Longitudinal Command Derivatives

The prime effect of longitudinal command is a rotation about the $\mathbf{y}_B$ axis. This rotation generates an acceleration along the $\mathbf{x}_B$ axis. This two effects can be described by the derivatives M_{lon} and X_{lon}.
To M_{lon} one contribution is due to the components of rotors thrusts along the $\mathbf{z}_B$ axis and another to those along the $\mathbf{x}_B$ axis.

$$\begin{aligned} M_{lon} = \quad & \frac{1}{I_{yy}} \sum_{j=1}^{N_{rot}} \frac{mg}{N_{rot} \cos(\Gamma_j) \cos(\xi_j)} \frac{2}{\Omega_0} \times \\ & \times [-\mathbf{T}_j(3,3)(-b) \cos(\delta_j) \; sgn\{-\cos(\delta_j)\} - \mathbf{T}_j(3,1) \; h \; sgn\{-\cos(\delta_j)\}] \end{aligned} \tag{5.52}$$

X_{lon} is given by the effect of the components of rotors thrusts along the $\mathbf{x}_B$ axis.

$$X_{lon} = \frac{1}{m} \sum_{j=1}^{N_{rot}} \left[-\mathbf{T}_j(3,1) \frac{mg}{N_{rot} \cos(\Gamma_j) \cos(\xi_j)} \frac{2}{\Omega_0} \; sgn\{-\cos(\delta_j)\} \right] \tag{5.53}$$

Other than this derivatives the N_{lon} derivative must be computed, because there are unbalanced variations of torque and the tilted thrusts affect the yaw dynamics.

$$\begin{aligned} N_{lon} = \quad & \frac{1}{I_{zz}} b \sum_{j=1}^{N_{rot}} \left[-\tilde{\mathbf{T}}_j(3,2) \frac{mg}{N_{rot} \cos(\Gamma_j) \cos(\xi_j)} \frac{2}{\Omega_0} \; sgn\{-\cos(\delta_j)\} \right] + \\ & + \frac{1}{I_{zz}} \sum_{j=1}^{N_{rot}} \left[\mathbf{T}_j(3,3) \; C_{\Pi 0,j} \; \rho \; A \; 2\Omega_0 \; R^3 \; sgn\{\cos(\delta_j)\}(-sgn\{\Omega_{0,j}\}) \right] \end{aligned} \tag{5.54}$$

Lateral Command Derivatives

The effects of a lateral control are similar to those of the longitudinal command. Three derivatives must yet be computed. These are L_{lat}, Y_{lat} and N_{lat}. L_{lat} is analogous to M_{lon}, Y_{lat} to X_{lon} and N_{lat} to N_{lon}.

$$L_{lat} = \frac{1}{I_{xx}} \sum_{j=1}^{N_{rot}} \left[\frac{mg}{N_{rot} \cos(\Gamma_j) \cos(\xi_j)} \frac{2}{\Omega_0} \right] \times$$
$$\times \left[-\mathbf{T}_j(3,3)(-b) \sin(\delta_j)\ sgn\{\sin(\delta_j)\} - \mathbf{T}_j(3,2)h\ (sgn\{\sin(\delta_j)\}) \right] \tag{5.55}$$

$$Y_{lat} = \frac{1}{m} \sum_{j=1}^{N_{rot}} \left[-\mathbf{T}_j(3,2) \frac{mg}{N_{rot} \cos(\Gamma_j) \cos(\xi_j)} \frac{2}{\Omega_0}\ sgn\{-\sin(\delta_j)\} \right] \tag{5.56}$$

$$N_{lat} = \frac{1}{I_{zz}} b \sum_{j=1}^{N_{rot}} \left[-\tilde{\mathbf{T}}_j(3,2) \frac{mg}{N_{rot} \cos(\Gamma_j) \cos(\xi_j)} \frac{2}{\Omega_0}\ sgn\{-\sin(\delta_j)\} \right] +$$
$$+ \frac{1}{I_{zz}} \sum_{j=1}^{N_{rot}} \left[\mathbf{T}_j(3,3)\ C_{\Pi 0,j}\ \rho\ A\ 2\Omega_0\ R^3\ sgn\{-\sin(\delta_j)\} sgn\{-\Omega_{0,j}\} \right] \tag{5.57}$$

Directional Command Derivatives

For symmetry of displacement and tilting of rotors the only effect of this control action is on the yaw rate r. The derivative to compute is N_{rud}. This derivative is sum of two components. One is due to the inclination of the rotors thrusts and the other to the variation of aerodynamic torque of all the rotors. A positive directional command is supposed to give a positive acceleration of r.

$$N_{rud} = \frac{1}{I_{zz}} b \sum_{j=1}^{N_{rot}} \left[-\tilde{\mathbf{T}}_j(3,2) \frac{mg}{N_{rot} \cos(\Gamma_j) \cos(\xi_j)} \frac{2}{\Omega_0} \; sgn\{\xi_j\} \right] + \\ + \frac{1}{I_{zz}} \sum_{j=1}^{N_{rot}} \left[\tilde{\mathbf{T}}_j(3,3) \; C_{\Pi 0,j} \; \rho \; A \; 2\Omega_0 \; R^3 \right] \tag{5.58}$$

5.3.7 The Control Matrix

The control matrix can now be written.

$$\mathbf{B} = \begin{bmatrix} 0 & 0 & 0 & 0 \\ 0 & 0 & 0 & 0 \\ 0 & 0 & 0 & 0 \\ 0 & X_{lon} & 0 & 0 \\ 0 & 0 & Y_{lat} & 0 \\ Z_{col} & 0 & 0 & 0 \\ 0 & 0 & L_{lat} & 0 \\ 0 & M_{lon} & 0 & 0 \\ 0 & N_{lon} & N_{lat} & N_{rud} \end{bmatrix} \tag{5.59}$$

5.4 Numerical Results

The stability matrix and the control matrix for the linear model of the dynamics of a multi–rotor aircraft have been defined in an analytic way. A numeric test can be done to assess the correctness of the results of linearization.

Inserting the data of table (4.3), we can compute the value of any element of the matrix **A**. This result can be compared with the stability matrix obtained after a numerical differentiation executed with $MATLAB^{®}$.

The numerical calculation brings the same result.

$$\mathbf{A}_{analytic} = \begin{bmatrix} 0 & 0 & 0 & 0 & 0 & 0 & 1 & 0 & 0 \\ 0 & 0 & 0 & 0 & 0 & 0 & 0 & 1 & 0 \\ 0 & 0 & 0 & 0 & 0 & 0 & 0 & 0 & 1 \\ 0 & -9.81 & 0 & -0.0048 & 0 & 0 & 0 & 0.0200 & 0 \\ 9.81 & 0 & 0 & 0 & -0.0048 & 0 & -0.0200 & 0 & 0 \\ 0 & 0 & 0 & 0 & 0 & -0.6243 & 0 & 0 & 0 \\ 0 & 0 & 0 & 0 & -1.8190 & 0 & -14.1730 & 0 & 0 \\ 0 & 0 & 0 & 1.8190 & 0 & 0 & 0 & -14.1730 & 0 \\ 0 & 0 & 0 & 0 & 0 & 0 & 0 & 0 & -0.0957 \end{bmatrix} \tag{5.60}$$

$$\mathbf{A}_{numeric} = \begin{bmatrix} 0 & 0 & 0 & 0 & 0 & 0 & 1 & 0 & 0 \\ 0 & 0 & 0 & 0 & 0 & 0 & 0 & 1 & 0 \\ 0 & 0 & 0 & 0 & 0 & 0 & 0 & 0 & 1 \\ 0 & -9.81 & 0 & -0.0048 & 0 & 0 & 0 & 0.0200 & 0 \\ 9.81 & 0 & 0 & 0 & -0.0048 & 0 & -0.0200 & 0 & 0 \\ 0 & 0 & 0 & 0 & 0 & -0.6243 & 0 & 0 & 0 \\ 0 & 0 & 0 & 0 & -1.8190 & 0 & -14.1677 & 0 & 0 \\ 0 & 0 & 0 & 1.8190 & 0 & 0 & 0 & -14.1677 & 0 \\ 0 & 0 & 0 & 0 & 0 & 0 & 0 & 0 & -0.0957 \end{bmatrix} \tag{5.61}$$

Also for the $\mathbf{B}$ matrix, the results of the numeric and analytic differentiation can be compared.

$$\mathbf{B}_{analytic} = \begin{bmatrix} 0 & 0 & 0 & 0 \\ 0 & 0 & 0 & 0 \\ 0 & 0 & 0 & 0 \\ 0 & 0.0025 & 0 & 0 \\ 0 & 0 & 0.0021 & 0 \\ -0.0425 & 0 & 0 & 0 \\ 0 & 0 & 1.5745 & 0 \\ 0 & -1.8180 & 0 & 0 \\ 0 & 0.0426 & 0 & 0.1277 \end{bmatrix} \tag{5.62}$$

$$\mathbf{B}_{numeric} = \begin{bmatrix} 0 & 0 & 0 & 0 \\ 0 & 0 & 0 & 0 \\ 0 & 0 & 0 & 0 \\ 0 & 0.0025 & 0 & 0 \\ 0 & 0 & 0.0021 & 0 \\ -0.0425 & 0 & 0 & 0 \\ 0 & 0 & 1.5745 & 0 \\ 0 & -1.8149 & 0 & 0 \\ 0 & 0.0426 & 0 & 0.1278 \end{bmatrix} \tag{5.63}$$

There is only a small difference in the p and q angular rates dynamics. However, with proper simulations, it can be verified that the numeric responses are indistinguishable. Thus the analytic definition of $\mathbf{B}$ is considered valid (errors are under 0.2%).

5.5 Remarks

In this chapter the analytic development to obtain a linear model of a multi–rotor aircraft dynamics is explained in detail. The aerodynamics of rotor has been accurately considered so that the analysis of dynamic stability can be accomplished with great depth. This linear model can also be utilized properly for control system design.
The problem of linearization of rotors aerodynamic loads is here focused. Although the question has taken relatively little space, this is a very important one for the study of dynamic characteristics of multi–rotor flying vehicles. It is worth noticing that in the specialized literature about multi–rotor aircrafts, this question is almost neglected. Thus the arguments in this and in the following chapters represent a sort of prime attempt in the analytic study of multi–rotor dynamics.

Chapter 6

Aeromechanical Stability Analysis of a Multi–Rotor Vehicle

In this chapter the question of static and dynamic flight stability of a multi–rotor is addressed. All the work is based on the linear modeling developed in chapter (5). A numerical test case is also considered.

6.1 Introduction

Many off–the–shelf multi–rotor vehicles are often provided with a fixed geometry non-planar displacement of rotor discs, such that the thrust generated by the individual rotor is inclined with respect to the local vertical. It is the case when a dihedral angle is provided to each rotor arm and a tilt angle deviates the rotor thrust from the vertical plane that contains the relative rotor arm. It is common knowledge that such design solutions may provide some kind of passive stability, that allows the vehicle to re-level at hover after attitude perturbations [7]. Although the behavior of an isolated rotor has been widely studied in the past years, with results about its inherent dynamic instability [13], there are very few results about the

interaction of two or more rotors. In [3] it was demonstrated that the stability of the longitudinal and lateral motions of a tandem–rotor helicopter largely depends on small differences between the thrusts of the front and rear rotors. In that framework, it was necessary to calculate the rotor thrust derivatives far more accurately than for the single–rotor helicopter. In the end it was shown that, in order to eliminate a divergence in longitudinal dynamic stability, a suitable value of swash–plate dihedral angle was necessary between the two rotors.
In this chapter, the open–loop stability analysis of a fixed–geometry multi–rotor at hover is addressed. In particular, it is investigated how attitude and velocity stability properties are influenced by design parameters such as the blade geometry, the position of the vehicle center C.G. and the rotors displacement and orientation in space. All the demonstration is based on the stability derivatives expressions as given in chapter (5).
After a detailed study of pure static stability, design solutions are proposed in order to cope with unstable oscillations affecting the longitudinal and lateral dynamics. Vertical and directional stability properties are analyzed and, as a further contribution, it is investigated how the combined use of feedback control systems, proper design of tilt angles, and a positive (inward) dihedral angle may drive the vehicle to dynamically stable hovering flight.
The whole argumentation is developed with respect to a quad–rotor configuration.

6.2 Rotors Arrangement

As hinted in section (4.3.2), the values of the dihedral Γ_j and tilting ξ_j angles for all the rotors must be properly assigned. The choice must grant essentially that in flight all the loads generated by the rotors are reciprocally balanced. In a word, in hovering condition, all the horizontal forces due to rotors inclination and all the torques need to make ineffective them-

selves.

To this purpose the rotors must be arranged in the following way. The dihedral angles Γ_j must have the same magnitude and the same sign.

$$\Gamma_j = \bar{\Gamma},\ \forall j = 1, ..., N_{rot} \tag{6.1}$$

To have equal dihedral implies that any rotor generates a component of thrust in $\{(\mathbf{x}_B, \mathbf{y}_B)\}$ plane all directed toward the C.G. or pointing out from it. These components of thrusts are perfectly balanced, in the case of regular azimuthal displacement of rotors.

The tilting angles ξ_j, instead, must possess same magnitude but different sign between adjacent rotors.

$$\begin{cases} \xi_j = \bar{\xi},\ j = 1, ..., 3, ..., N_{rot} - 1 \\ \\ \xi_j = -\bar{\xi},\ j = 2, ..., 4, ..., N_{rot} \end{cases} \tag{6.2}$$

Both the possibilities of sign for $\bar{\xi}$ are acceptable.

With this hypotheses, the assumptions of section (5.3.3) still hold and are maintained in this chapter.

6.3 Stability Analysis

In this section, stability analysis is performed without loss of generality for the multi-rotor configuration depicted in figure (3.6). Note that, with slight modifications, the considerations provided below also hold for vehicle arrangements where 6 or more rotors are symmetrically displaced. Particular attention is dedicated to the rotational stability of the vehicle about the hovering condition, showing how design solutions related to the dihedral angles Γ_j and the tilt angles ξ_j influence the open–loop static stability of roll, pitch, and yaw dynamics. Moreover, some considerations are provided about vertical damping. Finally, the dynamic stability of the

linearized system at hover is addressed, and design solutions are suggested in order to improve the vehicle open-loop behavior.
In what follows, the main stability derivatives are evaluated as components of the **A** stability matrix. For the sake of simplicity it will be assumed that the rotors spin rate at hover Ω_0 and the rotor derivatives of chapter (5.2) do not depend on $\bar{\Gamma}$ and $\bar{\xi}$ and are calculated for the planar case, $\bar{\Gamma} = \bar{\xi} = 0^{\mathbf{o}}$.
Table (6.1) shows relevant vehicle data. In order to evaluate the stability derivatives described in the previous chapter, some additional parameters need to be calculated. From table (6.1) and equation (3.9), the rotor induced velocity results to be $v_{i0} = 4.52$ m/s. Taking into account equation (4.8), with the value obtained for v_{i0}, it is also $\Omega_0 = 216.0$ **rad** $\mathbf{s}^{-1}$, while for the inflow ratio it is $\lambda_{i0} = 0.084$. A more accurate model in which the rotor derivatives, as section (5.3.3), vary with $\bar{\Gamma}$ and $\bar{\xi}$, does not add significant contribution to the calculation of the stability derivatives. In a configuration where $\bar{\Gamma} = \bar{\xi} = 20^{\mathbf{o}}$, for example, it would be easy to show that the evaluation of the derivatives according to the approximate model leads to an error of about 3 % with respect to the exact model. Thus, the assumption of null dihedral and tilting for rotor derivatives computation can be retained.
The derivatives of the rotor aerodynamic coefficients involved in the definition of the stability derivatives are then calculated, with the result that $\partial C_T/\partial \mu_z = 0.04$ and $\partial C_\Pi/\partial \mu_z = 4 \cdot 10^{-4}$.
In this pages, only the most influencing derivatives are investigated. For the multi–rotor configuration provided in table (6.1), in fact, terms such as X_u, X_q, Y_v, and Y_p actually provide a less significant contribution with respect to the derivatives presented in what follows.

6.3.1 Lateral and Longitudinal Stability

The effect of linear velocities u and v on longitudinal and lateral stability is mathematically represented by the derivatives L_v and M_u. Taking into

account the equations (3.20) and (5.44) with the arrangement represented by $\delta_1 = 0$, $\delta_2 = \pi/2$, $\delta_3 = \pi$, and $\delta_4 = (3/2)\pi$, one derives:

$$L_v(\bar{\Gamma}, \bar{\xi}) = -\frac{2\rho A \Omega_0 R}{I_{xx}} \frac{\partial C_T}{\partial \mu_z} \left\{ \cos^2(\bar{\xi}) \sin(\bar{\Gamma}) \left[b\cos(\bar{\Gamma}) - h\sin(\bar{\Gamma}) \right] - h\sin^2(\bar{\xi}) \right\} = \tag{6.3}$$

$$= \cos^2(\bar{\xi})\, L_v(\bar{\Gamma}, 0) + L_v(0, \bar{\xi}) \tag{6.4}$$

where

$$L_v(\bar{\Gamma}, 0) \triangleq -\frac{2\rho A \Omega_0 R}{I_{xx}} \frac{\partial C_T}{\partial \mu_z} \sin(\bar{\Gamma}) \left[b\cos(\bar{\Gamma}) - h\sin(\bar{\Gamma}) \right] \tag{6.5}$$

is the contribution provided by dihedral angle only, and

$$L_v(0, \bar{\xi}) \triangleq \frac{2\rho A \Omega_0 R}{I_{xx}} \frac{\partial C_T}{\partial \mu_z} h \sin^2(\bar{\xi}) \tag{6.6}$$

is the contribution provided by tilt angle only. In the same way, from equations (3.20) and (5.46), it follows:

$$M_u(\bar{\Gamma}, \bar{\xi}) = -\frac{2\rho A \Omega_0 R}{I_{yy}} \frac{\partial C_T}{\partial \mu_z} \left\{ -\cos^2(\bar{\xi}) \sin(\bar{\Gamma}) \left[b\cos(\bar{\Gamma}) - h\sin(\bar{\Gamma}) \right] + h\sin^2(\bar{\xi}) \right\} = \tag{6.7}$$

$$= \cos^2(\bar{\xi})\, M_u(\bar{\Gamma}, 0) + M_u(0, \bar{\xi}) \tag{6.8}$$

where

$$M_u(\bar{\Gamma}, 0) \triangleq \frac{2\rho A \Omega_0 R}{I_{yy}} \frac{\partial C_T}{\partial \mu_z} \sin(\bar{\Gamma}) \left[b\cos(\bar{\Gamma}) - h\sin(\bar{\Gamma}) \right] \tag{6.9}$$

is the contribution provided by dihedral angle only, and

$$M_u(0, \bar{\xi}) \triangleq -\frac{2\rho A \Omega_0 R}{I_{yy}} \frac{\partial C_T}{\partial \mu_z} h \sin^2(\bar{\xi}) \tag{6.10}$$

is the contribution provided by tilt angle only.

The sign of ξ_j $(j = 1, \ldots, 4)$ has no influence on the derivatives reported in the equations (6.4) and (6.4), since ξ_j only appears in cosine or squared sine functions. Provided $\bar{\Gamma} < \tan^{-1}(b/|h|)$, the sign of the two dihedral contributions $L_v(\bar{\Gamma}, 0)$ and $M_u(\bar{\Gamma}, 0)$ is determined only by the sign of $\bar{\Gamma}$.

In both cases, $\bar{\Gamma} = 0$ leads to null dihedral derivatives. According to the convention adopted for the *Body Axis* frame, a positive dihedral angle provides a statically stabilizing effect either along the roll axis, where $L_v(\bar{\Gamma}, 0) < 0$, and the pitch axis, where $M_u(\bar{\Gamma}, 0) > 0$. On the other hand, the effect of the tilt angle is always statically stabilizing in $L_v(0, \bar{\xi})$ and $M_u(0, \bar{\xi})$ if $h < 0$, with the C.G. lying below the plane that contains all the rotor centers.

The stability properties related to L_v and M_u may be clarified by the case when attitude perturbations drive the vehicle to acquire velocity components on the $\{(\mathbf{x}_B, \mathbf{y}_B)\}$ plane, owing to the inclination of the total thrust from the local vertical. The result is the generation of a moment that would lead the vehicle back to the hovering condition.

In the end, from equations (6.4) and (6.8), it is possible to derive the equation:

$$M_u(\bar{\Gamma}, \bar{\xi}) = -\frac{I_{xx}}{I_{yy}} L_v(\bar{\Gamma}, \bar{\xi}) \tag{6.11}$$

The effect of the angular velocities p and q on lateral and longitudinal stability is represented by the derivatives L_p and M_q, respectively. From equations (3.20) and (5.45), it is:

$$L_p(\bar{\Gamma}, \bar{\xi}) = -\frac{2\rho A \Omega_0 R}{I_{xx}} \frac{\partial C_T}{\partial \mu_z} \left\{ \cos^2(\bar{\xi}) \left[b\cos(\bar{\Gamma}) - h\sin(\bar{\Gamma}) \right]^2 + h^2 \sin^2(\bar{\xi}) \right\} =$$

$$= \cos^2(\bar{\xi}) L_p(\bar{\Gamma}, 0) - \frac{2\rho A \Omega_0 R}{I_{xx}} \frac{\partial C_T}{\partial \mu_z} h^2 \sin^2(\bar{\xi}) \tag{6.12}$$

where

$$L_p(\bar{\Gamma}, 0) \triangleq -\frac{2\rho A \Omega_0 R}{I_{xx}} \frac{\partial C_T}{\partial \mu_z} \left[b\cos(\bar{\Gamma}) - h\sin(\bar{\Gamma}) \right]^2 \tag{6.13}$$

is the damping contribution when $\bar{\xi} = 0$. From equations (3.20) and (5.47) it is also:

$$M_q(\bar{\Gamma},\bar{\xi}) = -\frac{2\rho A\Omega_0 R}{I_{yy}}\frac{\partial C_T}{\partial \mu_z}\left\{\cos^2(\bar{\xi})\left[b\cos(\bar{\Gamma}) - h\sin(\bar{\Gamma})\right]^2 + h^2\sin^2(\bar{\xi})\right\} =$$
$$= \cos^2(\bar{\xi})\, M_q(\bar{\Gamma},0) - \frac{2\rho A\Omega_0 R}{I_{yy}}\frac{\partial C_T}{\partial \mu_z}h^2\sin^2(\bar{\xi}) \tag{6.14}$$

provided

$$M_q(\bar{\Gamma},0) \triangleq -\frac{2\rho A\Omega_0 R}{I_{yy}}\frac{\partial C_T}{\partial \mu_z}\left[b\cos(\bar{\Gamma}) - h\sin(\bar{\Gamma})\right]^2 \tag{6.15}$$

is the damping contribution when $\bar{\xi} = 0$. The L_p and M_q derivatives reported in equations (6.12) and (6.15) are always negative definite, providing a damping effect. It is interesting to note that, even when $\bar{\Gamma} = \bar{\xi} = 0$, the system results to be damped. This effect is due to the differential thrust that is generated between the ascending and the descending rotors with respect to the instantaneous axis of rotation that lies on the $\{(\mathbf{x}_B, \mathbf{y}_B)\}$ plane. In particular, the damping contribution increases as $\bar{\Gamma}$ ranges from negative to positive values but decreases the more the tilt angle $\bar{\xi}$ inclines the thrust perturbation of each rotor from the vertical plane that contains the rotor arm, as it can be seen in figure (A.2)).

As a final consideration, the derivatives L_p and M_q are related to each other by the equations (6.12) and (6.14):

$$M_q(\bar{\Gamma},\bar{\xi}) = \frac{I_{xx}}{I_{yy}}L_p(\bar{\Gamma},\bar{\xi}) \tag{6.16}$$

6.3.2 Directional Stability

Now the stability derivative in equation (5.48) for $N_{rot} = 4$ is considered. It results:

$$N_r(\bar{\Gamma},\bar{\xi}) = -\frac{4\rho A\Omega_0 R b^2}{I_{zz}}\frac{\partial C_T}{\partial \mu_z}\sin^2\left(\bar{\xi}\right)+ \\ +\frac{\rho A\Omega_0 R^2 b}{I_{zz}}\frac{\partial C_\Pi}{\partial \mu_z}\cos\left(\bar{\xi}\right)\cos\left(\bar{\Gamma}\right)\sum_{j=1}^{4}\sin\left(\xi_j\right)sgn\left(\Omega_{0,j}\right) \tag{6.17}$$

Note that N_r is null in the case when no tilt angle is provided. On the other hand, the term in equation (6.3.2) that is related to the thrust coefficient derivative $\partial C_T/\partial \mu_z$ is always negative definite for any choice of $\bar{\xi} \neq 0$ (actually providing a damping effect about the $\mathbf{z}_B$ axis). The sign of the term related to the rotor torque coefficient $\partial C_\Pi/\partial \mu_z$ instead depends on the particular configuration adopted for the rotors spin rates $\Omega_{0,j}$ and the relative tilt angles ξ_j. Since $\partial C_\Pi/\partial \mu_z$ is positive in the given hovering condition, the best design solution that maximizes the cost function

$$J_{N_r} = -\sum_{j=1}^{4}\sin\left(\xi_j\right)sgn\left(\Omega_{0,j}\right) \tag{6.18}$$

is represented by the configuration:

$$\sin\left(\xi_j\right)sgn\left(\Omega_{0,j}\right) < 0, \qquad j = 1,\ldots,4 \tag{6.19}$$

for every choice of $\bar{\xi} = |\xi_j|$. In this case, the inequality in equation (6.19) holds if $sgn\left(\xi_j\right) = -sgn\left(\Omega_{0,j}\right)$, with the result that the cost function in equations (6.18) becomes:

$$J^*_{N_r} = -4\sin\left(\bar{\xi}\right) \tag{6.20}$$

As a matter of fact, it should be noted that the rotor torque variation related to $\partial C_\Pi/\partial \mu_z$ does not provide a significant contribution if compared to the effect induced by $\partial C_T/\partial \mu_z$. In fact, at the considered hovering condition, it is $|\partial C_\Pi/\partial \mu_z| << \partial C_T/\partial \mu_z$. Nevertheless, the small damping

contribution obtained by the configuration proposed in equation (6.19) comes at no cost on the vehicle endurance for a given choice of $\bar{\Gamma}$ and $\bar{\xi}$ – that is, the overall thrust required by the equilibrium of forces in equation (4.3) is not altered.
In figure (A.3) the derivative N_r is plotted as a function of $\bar{\xi}$ with the arrangement proposed in equation (6.19). In particular, only the curve for $\bar{\Gamma} = 0^{\mathrm{o}}$ is reported, because the dihedral angle appears in the term related to $\partial C_{\Pi}/\partial \mu_z$ and thus it does not provide a significant contribution.

6.3.3 Vertical Motion Stability

The effect of the linear velocity w on the thrust component directed along the $\mathbf{z}_B$ axis is represented by the derivative Z_w. Taking into account equations (3.20) and (5.43), it is:

$$Z_w = -\frac{4\rho A \Omega_0 R}{m} \frac{\partial C_T}{\partial \mu_z} \cos(\bar{\Gamma})^2 \cos(\bar{\xi})^2 \ . \tag{6.21}$$

The stability derivative in equation (6.21) is always negative definite. According to the convention adopted for the *Body Axis* frame, a negative contribution of Z_w provides static stability along $\mathbf{z}_B$. In other words, if altitude is perturbed from the trim condition, the generation of a velocity component w induces a force ΔZ that opposes the altitude variation. In figure (A.4) the vertical damping Z_w is plotted as a function of the dihedral and the tilt angles.
Note that the inclination of the individual rotor thrust from the $\mathbf{z}_B$ axis is always detrimental for the vertical damping. In fact, the maximum value of $|Z_w|$ is obtained when $\bar{\Gamma} = \bar{\xi} = 0^{\mathrm{o}}$, that represents a planar configuration.

6.3.4 Dynamic Stability

Till now, static stability has been explored for a multi–rotor at hover, with detailed considerations about the influence of dihedral and tilt angles on the stability derivatives. In particular, the speed stability represented by

the L_v and M_u derivatives has been analyzed, with the description of the statically stabilizing momenta induced by perturbations of u and v. If dynamic stability of the linearized system in equation (5.1) is addressed, one should verify whether every real pole of the state matrix $\mathbf{A} = \mathbf{A}(\bar{\Gamma}, \bar{\xi})$, or every real part of any complex pole, is negative. To this aim, it is convenient to write the stability matrix as a function of the stability derivatives defined in chapter (5). It follows:

$$\mathbf{A} = \begin{bmatrix} 0 & 0 & 0 & 0 & 0 & 0 & 1 & 0 & 0 \\ 0 & 0 & 0 & 0 & 0 & 0 & 0 & 1 & 0 \\ 0 & 0 & 0 & 0 & 0 & 0 & 0 & 0 & 1 \\ 0 & X_\theta & 0 & X_u & 0 & 0 & 0 & 0 & 0 \\ Y_\phi & 0 & 0 & 0 & Y_v & 0 & 0 & 0 & 0 \\ 0 & 0 & 0 & 0 & 0 & Z_w & 0 & 0 & 0 \\ 0 & 0 & 0 & 0 & L_v & 0 & L_p & 0 & 0 \\ 0 & 0 & 0 & M_u & 0 & 0 & 0 & M_q & 0 \\ 0 & 0 & 0 & 0 & 0 & 0 & 0 & 0 & N_r \end{bmatrix} \tag{6.22}$$

Now a planar configuration C1, where $\bar{\Gamma} = \bar{\xi} = 0^{\mathbf{o}}$, is considered. Taking into account equation (6.22) and the expressions of the stability derivatives provided above, it results:

$$\mathbf{A}_1 = \begin{bmatrix} 0 & 0 & 0 & 0 & 0 & 1 & 0 & 0 \\ 0 & 0 & 0 & 0 & 0 & 0 & 1 & 0 \\ 0 & 0 & 0 & 0 & 0 & 0 & 0 & 1 \\ 0 & -9.8066 & 0 & 0 & 0 & 0 & 0 & 0 \\ 9.8066 & 0 & 0 & 0 & 0 & 0 & 0 & 0 \\ 0 & 0 & 0 & 0 & -0.5194 & 0 & 0 & 0 \\ 0 & 0 & 0 & 0 & 0 & -10.9171 & 0 & 0 \\ 0 & 0 & 0 & 0 & 0 & 0 & -10.9171 & 0 \\ 0 & 0 & 0 & 0 & 0 & 0 & 0 & 0 \end{bmatrix} \tag{6.23}$$

The eigenvalues of $\mathbf{A}_1$ assume the configuration:

$$\boldsymbol{\eta}_1 = [0,\ 0,\ -0.5194,\ -10.9171,\ -10.9171,\ 0,\ 0,\ 0,\ 0]^T$$

where the three negative real poles are related to the damping effect provided by Z_w, L_p, and M_q, respectively. In particular, the vertical motion of the multi–rotor at hover is described by a first order differential equation, that is $\dot{w} = \Delta Z/m$, with a time constant given by $\tau_w = -1/Z_w$ (about 2 **s** in this case). The time-to-half amplitude is about 1.3 **s**. No damping is provided about the yaw axis.

Now instead it is considered a configuration C2 where $\bar{\Gamma} = 20^{\mathrm{o}}$ and $\bar{\xi} = 10^{\mathrm{o}}$, with the tilt arrangement suggested in equation (6.19). It follows:

$$\mathbf{A}_2 = \begin{bmatrix} 0 & 0 & 0 & 0 & 0 & 0 & 1 & 0 & 0 \\ 0 & 0 & 0 & 0 & 0 & 0 & 0 & 1 & 0 \\ 0 & 0 & 0 & 0 & 0 & 0 & 0 & 0 & 1 \\ 0 & -9.8066 & 0 & -0.0373 & 0 & 0 & 0 & 0 & 0 \\ 9.8066 & 0 & 0 & 0 & -0.0373 & 0 & 0 & 0 & 0 \\ 0 & 0 & 0 & 0 & 0 & -0.4448 & 0 & 0 & 0 \\ 0 & 0 & 0 & 0 & -6.0214 & 0 & -12.6571 & 0 & 0 \\ 0 & 0 & 0 & 6.0214 & 0 & 0 & 0 & -12.6571 & 0 \\ 0 & 0 & 0 & 0 & 0 & 0 & 0 & 0 & -0.3014 \end{bmatrix} \tag{6.24}$$

with the eigenvalues:

$$\boldsymbol{\eta}_2 = [0.1709 \pm 2.1214i,\ 0.1709 \pm 2.1214i,\ -0.4448,\ -13.0362,\ -13.0362,\ -0.3014,\ 0]^T$$

The presence of a tilt angle generates a stable real pole related to the yaw-damping derivative, namely $N_r = -0.3014\ \mathrm{s}^{-1}$, while vertical damping is still provided by $Z_w = -0.4448\ \mathrm{s}^{-1}$. In particular, the motion of the multi-rotor about the yaw axis, that is described by a first order differential equation, $\dot{r} = \Delta N / I_{zz}$, has a time constant given by $\tau_r = -1/N_r \approx 3.3\ \mathrm{s}$. Both the roll and the pitch dynamics are described by a stable, subsidence mode (a large negative real root due to damping) and a mildly unstable, oscillatory mode (due to the speed derivatives L_v and M_u). In this case, the oscillation associated with the unstable dynamics has a period of about 3 s. Time-to-double amplitude is about 4 s and gets worse if dihedral and tilt angles are increased. Because of the speed stability of the rotors, the vehicle is susceptible to gusts whenever it is hovering and, as a result, its position relative to the ground drifts considerably: this makes the task of station-keeping, for which multi–rotor are universally employed, particularly taxing for a pilot if manual control is performed. Finally, it is a result that, if the vehicle is perturbed from trimmed forward flight, the unstable oscillatory mode is made even worse with an increase in the trim advance speed [13].

It can be noticed from figure (A.1) that it is possible to reduce L_v (and M_u) to zero by tilting the rotor-hub axes outwards (*i.e.*, the dihedral angle becomes negative). Let $\bar{\xi}^*$ be the design value of tilt angle obtained, for ex-

ample, from a requirement on the time constant of the yaw damping mode, as in figure (A.3). Provided $\bar{\Gamma}^*$ is the angle that satisfies $L_v(\bar{\Gamma}^*, \bar{\xi}^*) = 0$, it follows from equation (6.4):

$$\cos^2(\bar{\xi}^*)\sin(\bar{\Gamma}^*)\left[b\cos(\bar{\Gamma}^*) - h\sin(\bar{\Gamma}^*)\right] - h\sin^2(\bar{\xi}^*) = 0 \tag{6.25}$$

that can be rearranged to give:

$$2h\,\sin^2(\bar{\Gamma}^*) - b\,\sin(2\bar{\Gamma}^*) + 2h\,\tan^2(\bar{\xi}^*) = 0\ . \tag{6.26}$$

Equation (6.26) provides two real negative solutions:

$$\bar{\Gamma}^* = \tan^{-1}\left\{\frac{b \pm \sqrt{b^2 - 4h^2\tan^2(\bar{\xi}^*)\left[1+\tan^2(\bar{\xi}^*)\right]}}{2h\left[1+\tan^2(\bar{\xi}^*)\right]}\right\} \tag{6.27}$$

provided

$$\bar{\xi}^* \leq \tan^{-1}\left[\sqrt{\frac{1}{2}\left(-1+\sqrt{1+\frac{b^2}{h^2}}\right)}\right] \tag{6.28}$$

Between the two solutions of the equation (6.27), the smallest one represents the suggested design, because it allows to reduce the effort demanded to the motors at hover by the equation (4.3) and to avoid excessive loss of roll, pitch, and vertical damping, according to figures (A.2) and (A.4). In this case, equation (6.27) gives $\bar{\Gamma}_1^* = -65^{\mathrm{o}}$ and $\bar{\Gamma}_2^* = -0.79^{\mathrm{o}}$ for $\bar{\xi}^* = 10^{\mathrm{o}}$. If the design parameters $\bar{\Gamma}_2^*$ and $\bar{\xi}_2^*$ are selected for a third configuration, C3, the vector of eigenvalues results to be:

$$\boldsymbol{\eta}_3 = [-0.0079,\ -0.0079,\ -0.5037,\ -10.5215,\ -10.5215,\ -0.3018,\ 0,\ 0,\ 0]^T$$

where no re–hovering moment is actually generated by changes of speed. In particular, damping is still provided to p, q, r, and w velocities with a fast dynamics of the first–order, as in figure (A.5) for a sample maneuver based on the linearized model). On the other hand, a creeping first–order dynamics with no practical interest characterizes the behavior of u and w

if linear velocity perturbations only are introduced, as figure (A.6) clearly shows).

The slow response of the velocity perturbations u and v is due to the small derivatives X_u and Y_v. Nevertheless, it must be taken into account that the effect of the airframe drag is not considered in the linear analysis, which would strongly increase the force contributions that oppose the motion of the C.G. of the vehicle.

The analysis provided about static and dynamic stability is based on the open loop modeling of the multi–rotor, where no active stabilization system is implemented. The *ad hoc* configuration proposed in equation (6.27), that allows to eliminate the divergent oscillations induced by speed stability, however makes the system very slow in compensating any speed perturbation, with no possibility to oppose attitude variations. As a matter of fact, a stable configuration with positive dihedral is possible if additional damping is artificially provided to longitudinal and later dynamics by a closed–loop control. In many multi–rotor vehicles, this regulation is performed by means of the feedback of p and q on the rotor spin rates, while the same result is obtained for longitudinal stability in many single–rotor helicopters by adding a tailplane [13]. Sufficient extra damping would thus result in the oscillatory mode being stabilized. In the case when attitude information also is used as a feedback term, the system would stabilize at hover after very fast transients and with the capability to avoid the oscillatory behavior. A compromise should be envisaged between the use of passively stable configurations, with tilt and positive dihedral, and the effort demanded by closed-loop controllers, in order to accomplish the desired requirements in terms of both stability and endurance.

6.4 Quad–Rotor Data

In the following table the data employed in the calculations of the previous sections are provided.

Type	Value	Unity	Type	Value	Unity
ρ	1.2247	$\mathbf{kg\ m^{-3}}$	g	9.80665	$\mathbf{m\ s^{-2}}$
m	4	**kg**	I_{xx}	0.044	$\mathbf{kg\ m^2}$
I_{yy}	0.044	$\mathbf{kg\ m^2}$	I_{zz}	0.098	$\mathbf{kg\ m^2}$
N_{rot}	4		R	0.25	**m**
N	2		θ_c	15	$^{\mathbf{o}}$
θ_{tw}	2	$^{\mathbf{o}}$	$C_{l\alpha}$	5.5	$\mathbf{rad^{-1}}$
C_d	0.003		c	0.03	**m**
h	-0.3	**m**	b	0.68	**m**

Table 6.1: Quad–Rotor Data

6.5 Remarks

In this chapter, the open–loop dynamics of a multi–rotor aerial vehicle with fixed geometry has been addressed. In particular, it has been investigated how geometric and aerodynamic parameters influence the capability of the vehicle to passively maintain a stable hovering flight. A non–planar configuration of rotors has been considered, where the thrust of the individual rotor is inclined by design with respect to the local vertical. Two angles define the thrust orientation: a dihedral angle rotates the thrust on the local vertical plane that contains the rotor arm, and a tilt angle rotates the thrust in such a way to generate a component that is orthogonal to that plane. Static stability has been analyzed for a vehicle configuration with four rotors, showing how directional stability is closely related to the tilt angles, while the stability of the longitudinal and lateral axes is mostly influenced by the dihedral angle. As a final contribution, dynamic stability has been tackled and design solutions have been suggested in order to improve the vehicle open–loop behavior and assist eventual feedback controllers in the stabilization task. In this direction, the parameterized linear model has been proven to be a valid instrument for the analysis of different vehicle configurations and a test bench for the design of novel

control strategies.

Chapter 7

Control of a Multi–Rotor Aircraft

In chapter (5) a linear model of a multi–rotor aircraft dynamics has been obtained. In this chapter control laws for attitude stabilization are defined on the base of this linear system. These control laws are validated with numerical simulations. With the same simulations it is also shown whether the speed stability characteristics for a multi–rotor aircraft improve, with respect to the result of the previous chapter for a multi–rotor without active stabilization.
Numeric examples are all referred to the same hexa–copter data already used.

7.1 Control of a Linear System

The dynamic behavior of a multi–rotor around the hovering flight condition can be described by an *LTI* system with the following implicit expression for state vector equation.

$$\dot{\mathbf{x}} = \mathbf{A}\mathbf{x} + \mathbf{B}\mathbf{u}, \quad \mathbf{x}(t_0) = \mathbf{x}_0 \tag{7.1}$$

Once the *state equation* is defined, a control strategy can be chosen. Clas-

sical linear control approaches are PID controllers for $SISO$ systems or the *Optimal Control* theory for $MIMO$ systems [16]. Both the control techniques are discussed in the following, with few theoretic hints, and applied to the attitude stabilization of the multi–rotor. The control laws are then tested in numerical simulations of the non–linear model of dynamics of the aircraft.
In the following treatment all the control laws provide a direct variation of the spin rate of the rotors, without considering the dynamics of the electric motors. This only to show that the linear model is an effective analytic tool for an affordable control system design.

7.1.1 *PID* Control

To design a *PID* controller of a plant, the *transfer function* of this plant is needed. Thus, aiming at the stabilization of the attitude in hovering flight, the $SISO$ systems to be controlled are the attitude perturbation variables ϕ, θ and ψ. Now their transfer functions must be defined.
Considering only the ϕ angle, its state equation can be obtained beginning from the roll rate p dynamics.

$$\dot{p} = L_p p + L_v v + L_{lat} u_{lat} \tag{7.2}$$

Inserting the Laplace's variable s the time derivative disappears.

$$p(s - L_p p) = L_v v + L_{lat} u_{lat} \tag{7.3}$$

Now an assumption is made to obtain a $SISO$ system. The contribute of the velocity v is omitted, supposing less importance of the effects of v, near the hovering flight condition. With this hypothesis the transfer function for roll rate dynamics can be written.

$$p = \frac{L_{lat}}{(s - L_p p)} u_{lat} \tag{7.4}$$

The transfer function of the roll angle perturbation derives from the relation between ϕ and p.

$$\dot{\phi} = p \tag{7.5}$$

$$s\phi = p \tag{7.6}$$

Finally the ϕ transfer function can be expressed.

$$\phi = \frac{L_{lat}}{s(s - L_p p)} u_{lat} \tag{7.7}$$

The transfer function of θ and ψ can be similarly found.

$$\theta = \frac{M_{lon}}{s(s - M_q q)} u_{lon} \tag{7.8}$$

$$\psi = \frac{N_{rud}}{s(s - N_r r)} u_{rud} \tag{7.9}$$

For any transfer function a PID controller can be designed. To do this, the $MATLAB^{®}$ function *pidtune* is utilized. This function for each plant provides the proportional gain K_P, the integral gain K_I and the derivative gain K_D. If $H(s)$ is the regulator transfer function, its expression is the following.

$$H(s) = K_P + \frac{K_I}{s} + K_D s \tag{7.10}$$

For the present case a PD regulator architecture is chosen ($K_I = 0$). For the 3 controllers the gains are shown in table (7.1).
The negative sign of the gains of the θ regulator is due to the fact that a positive longitudinal command u_{lon} gives a positive response of the u velocity but a negative one of the angle θ and of the pitch rate q.

	ϕ [**rad**]	θ [**rad**]	ψ [**rad**]
K_P	204.7194	-177.2922	397.8994
K_D	4.2596	-3.6889	67.4201

Table 7.1: PID Gains

7.1.2 *PID* Regulators Simulation

The PID regulators can be tested with a numerical simulation of the non–linear model of the multi–rotor aircraft. In this simulation the motors dynamics are not included. The simulation starts with non null values of the angles Φ, Θ and Ψ. Precisely, $\Phi(t_0) = 15^{\mathbf{o}}$, $\Theta(t_0) = 15^{\mathbf{o}}$ and $\Psi(t_0) = 15^{\mathbf{o}}$. In figure (B.1) the simulation result is shown. The effectiveness of attitude regulation can be thus witnessed.

Similarly, because, for multi–rotor aircrafts, velocities and attitude are strictly tied, it can be assessed whether the presence of an attitude stabilization system improve the speed stability characteristics of the rotorcraft with respect to the case shown at the end of chapter (6). Figures (B.3) and (B.5) give a positive response.

7.2 Regulation through Optimal Control

Optimal control theory [16, 25] provides a proportional regulator for $MIMO$ LTI systems. This regulator is also known as *linear quadratic regulator* (LQR). This control problem returns a gain matrix $\mathbf{K}$. This matrix is obtained from the minimization of a scalar cost function J.

$$J = \int_0^\infty \left(\mathbf{x}^T\mathbf{Q}\mathbf{x} + \mathbf{u}^T\mathbf{R}\mathbf{u}\right)\mathbf{d}t \tag{7.11}$$

$\mathbf{Q}$ and $\mathbf{R}$ are diagonal arbitrary weighting matrices.

The state dynamics with the presence of the LQR and without pilot inputs can be described by the following equation.

$$\dot{\mathbf{x}} = (\mathbf{A} - \mathbf{BK})\,\mathbf{x}, \quad \mathbf{x}(t_0) = \mathbf{x}_0 \tag{7.12}$$

It is worth noticing that this regulator acts on all the state variables together. Thus, with it, the stabilization action does not work only on the attitude angles but on all the state vector.
The numeric value of $\mathbf{K}$ can be obtained directly through $MATLAB^{®}$.

7.2.1 LQR Simulation

With another simulation the performance of the LQR can be viewed in figure (B.2). For this numeric example the following values have been assigned to the weighting matrices.

$$\mathbf{Q} = \begin{bmatrix} 100 & 0 & 0 & 0 & 0 & 0 & 0 & 0 & 0 \\ 0 & 100 & 0 & 0 & 0 & 0 & 0 & 0 & 0 \\ 0 & 0 & 100 & 0 & 0 & 0 & 0 & 0 & 0 \\ 0 & 0 & 0 & 1 & 0 & 0 & 0 & 0 & 0 \\ 0 & 0 & 0 & 0 & 1 & 0 & 0 & 0 & 0 \\ 0 & 0 & 0 & 0 & 0 & 1 & 0 & 0 & 0 \\ 0 & 0 & 0 & 0 & 0 & 0 & 0.001 & 0 & 0 \\ 0 & 0 & 0 & 0 & 0 & 0 & 0 & 0.001 & 0 \\ 0 & 0 & 0 & 0 & 0 & 0 & 0 & 0 & 0.001 \end{bmatrix} \tag{7.13}$$

$$\mathbf{R} = \begin{bmatrix} 10 & 0 & 0 & 0 \\ 0 & 0.01 & 0 & 0 \\ 0 & 0 & 0.01 & 0 \\ 0 & 0 & 0 & 0.01 \end{bmatrix} \tag{7.14}$$

Differently from *PID* regulation, the control action of the LQR works on all the state variables, so that a stabilizing action is delivered to the velocities and to the angular rates. The speed stability in this case, more

than also in the case of PID regulators, is again enhanced, as it can be seen in figures (B.4) and (B.6).

7.3 Remarks

In this chapter the problem of the attitude stabilization of a multi–rotor aircraft has been dealt with. The results shown here do not represent obviously the very ultimate solution. The objective of the argumentation was to prove the affordability of the mathematical modeling presented in the previous chapters for the designing of control systems for multi–rotor flying vehicles. In this way simple control laws, even though with various approximations, have been found only on the base of analytical computations or with the aid of *ad hoc* tuning algorithms.

Chapter 8

The *Quad–Tilt–Rotor* Aircraft

This chapter deals with the study of a never built configuration of multi–rotor aircraft. All the mathematical instruments of the previous chapters are here utilized to demonstrate whether this innovative machine really grants enhanced flight capabilities with respect to classical multi–rotor platforms.

8.1 Introduction

Recently a patent [1] has been registered in which a new quad–rotor mock–up is described. This new configuration is there named as the *Quad–Tilt–Rotor* aircraft. The features of this aircraft are: tilting rotors, variable pitch propellers and an unique internal combustion engine. The tilting rotors are a mean to increase the number of inputs of the system and, thus, to augment the maneuverability of the aircraft, with respect to classical quad–rotors that are a manifest example of under–actuated systems. The interest in this technology is testified by recent publications [22, 23]. The internal combustion engine is an expedient chosen to possibly increase the flight endurance. More details about this machine are given in following sections.

Before designing a prototype of such a machine, a study has been at-

tempted to understand if actually this machine could grant improvements in terms of maneuverability. Also control strategies and driving actions for a human pilot has been defined [8].
This analysis has been accomplished by means of the dynamic modeling equations described in the previous chapters.
In the next sections a brief mention of the non–linear 6 D.O.F. model is given and, then, the linear model is derived.
The objective of this chapter is the refinement and prosecution of the already cited published work [8]. Starting always from the same mathematical model of dynamics of motion, exploiting the so called technique of *Inverse Simulation*, complex missions are simulated. This technique permits to show more effectively both the performances of this machine and the necessary pilot control actions for any maneuver.
Finally, a study of the controllability property of the *Quad–Til–Rotor* as a linear dynamic system is accomplished. Successively, an approximated study of residual controllability of the system in case of actuator failure is developed, to show if the aircraft can overcome this characteristic of traditional multi–rotor.

8.2 Description of the Aircraft

These pages are focused on the description of a mathematical model of a quad–rotor with tilting rotors and variable pitch propellers, driven by a single internal combustion engine. The model is suitable for describing the dynamics of the vehicle with the purpose of developing feedback control laws for stability and control augmentation. In this framework, structural vibrations and unsteady aerodynamic effects will be neglected.
The dynamics of a conventional multi–rotor configuration is relatively simple: the vehicle is controlled by changing the rate of rotation of the propellers. Most of the times, an even number of rotors is used. The most common configuration, named quad–rotor or quad–copter, features two

pairs of rotors mounted at the ends of a simple cross–shaped structure, or at the corners of a square frame. Two rotors rotate in the clockwise direction and two rotate counter–clockwise, such that at hover each rotor produce a thrust equivalent to one fourth of vehicle weight, with zero pitch and roll moments and perfectly balanced rotor aerodynamic yawing torques, as in figure (8.1).

Yaw control is achieved unbalancing aerodynamic torques acting on the two pairs of rotors (e.g. increasing the speed of clockwise rotors while decreasing the rotation rate of the other two, or viceversa), keeping a constant total thrust. Roll and pitch control moments are obtained by variation of lateral and longitudinal rotor thrust, respectively (e.g. increasing the forward rotor rotation rate while decreasing that of the aft–mounted rotor, a pitch–up moment is obtained). Hexa–copters are also quite popular, where the vehicles may feature either three couples of counter–rotating propellers or six independent ones. In both cases, three of the propellers rotate in one direction, and the remaining three in the opposite one. Note that a conventional quad–rotor is, in terms of control variables, an under–actuated vehicle, where four control variables are present to control 6 mechanical degrees of freedom.

As a major difference, the novel quad–rotor configuration features the possibility of tilting all of the four rotors disks, thus allowing the quad–rotor to move and maneuver with greater flexibility. As an example, it can fly along a horizontal trajectory with zero pitch and roll attitude. Moreover, rotor thrust variation is achieved by varying propeller pitch rather than rotation rate, which results in a faster and linear response. Control along the $\mathbf{z}_B$ *Body Axis* – that is, control of the normal load factor – is achieved by changing simultaneously the pitch of all the rotors. Lateral flight is controlled by tilting fore and aft rotors, whereas longitudinal speed and acceleration are controlled by tilting the lateral rotors. Yaw orientation can be changed by the (indeed little) tilting of a couple of opposite rotors. For each rotor only the tilting around the axis along its own bar is

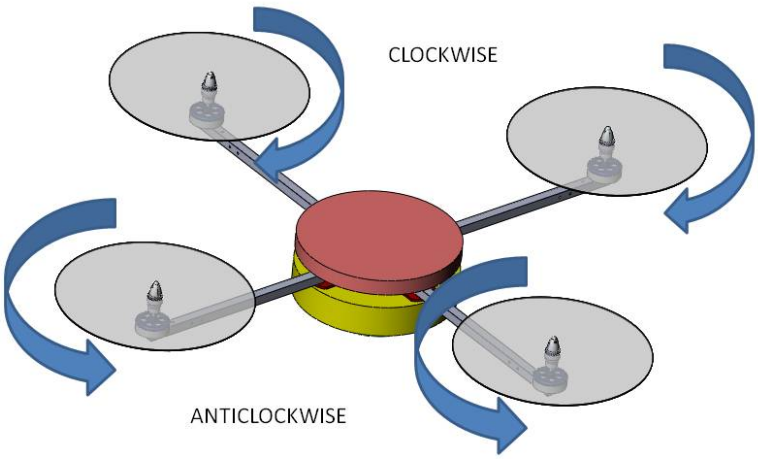

Figure 8.1: Direction of rotation of the 4 rotors.

considered, as in figure (8.2). This machine is also intended to work with constant engine speed, by means of a suitable *RPM* governor [8].

The advantage of such a configuration is the capability to maintain the payload almost always oriented on a fixed plane during the maneuvers of the quad–rotor. Moreover the tilting of all the rotors increases the number of inputs of the vehicle, thought as a dynamic system. This feature transforms it into an over–actuated system, where some sort of control blend needs to be envisaged in order to allow a pilot to fly it as a conventional helicopter.

In this latter respect, the novel quad–rotor will be manually controlled by means of four control inputs, like any other standard *RC* helicopter: one command for vertical acceleration, corresponding to the collective, one command for longitudinal control moment, like the longitudinal cyclic,

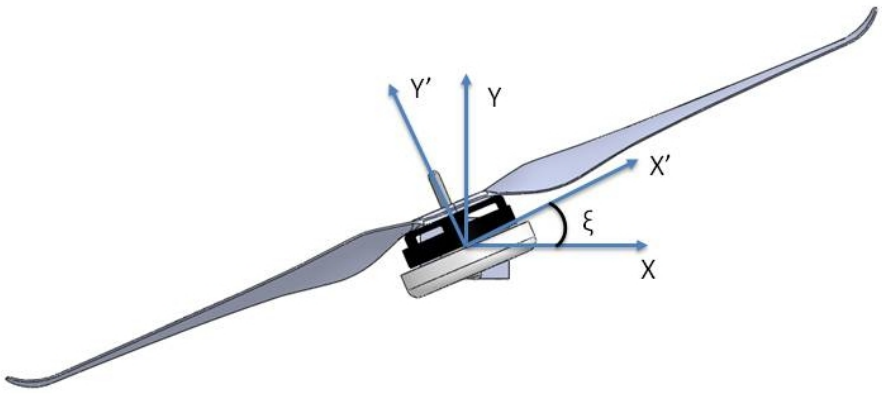

Figure 8.2: Tilting of a rotor

one command for roll control moments, like the lateral cyclic, and one command for heading control, like the tail rotor collective [21]. How to blend the control over the different control variables available will be a major issue in the development of the vehicle control system.

8.2.1 Vehicle Dimensions and Characteristics

A preliminary concept of the novel configuration is presented in figure (8.3). Dimensions and other characteristics of the quad–rotor are sized starting from a survey of available off-the-shelf components. Obviously parts the landing gear and a detailed structure layout will be designed and built according to the actual needs once the configuration is defined in better detail. Brackets will be built out of aluminum alloy commercial tubes or carbon fiber after an adequate evaluation of strength, weight, manufacturing complexity and cost. The engine can be a two stroke engine as the Graupner OS SPEED 91 Hz-R 3C with a maximum output of about 2.65 kW of power (`http://www.graupner.de`). The tank will be located below the engine. The electronic package will be more conveniently located on the top of airframe, which is a mandatory position, in order to protect

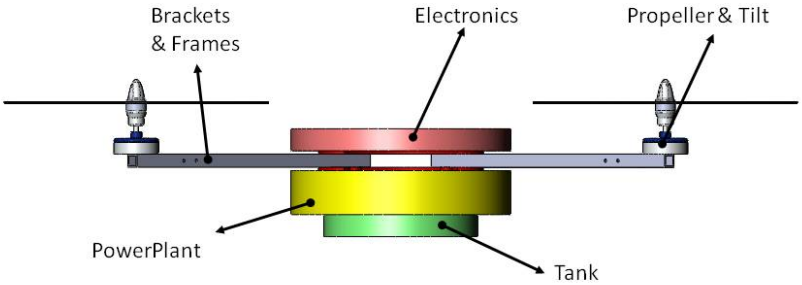

Figure 8.3: Sketch of the Main Parts of the *Quad–Tilt–Rotor*

the electronics from possible shocks from collisions with the ground.
Masses and moments of inertia are estimated by *3D CAD* model with discrete mass distribution. In table (8.1), overall geometric characteristics and split out of total mass are reported. In relation to the estimated geometry and masses, the moments of inertia are obtained and are listed in table (8.2).

8.3 Description of Dynamics of Motion

The mathematical modeling of this machine can be made with all the equations introduced in the previous chapters, both for the non–linear model and for the linear one.
The non–linear model needs only some clarifications about rotors dynamics and control inputs. In this case, the dynamics of the internal combustion

Type	Value	Units
Overall dimension	1360 x 1360 x 250	mm
Variable pitch propellers cluster	50 (x 4)	g
Electronics	250	g
Engine and Transmission	1900	g
Tank (full)	600	g
Aluminium alloy brackets	225 (x 4)	g
Frame	100	g
Overall mass	3950	g

Table 8.1: Quadrotor characteristics

Inertia	Value	Units
I_{xx}	0.044	$kg\ m^2$
I_{yy}	0.044	$kg\ m^2$
I_{zz}	0.098	$kg\ m^2$

Table 8.2: Inertia moments

engine, in terms of its speed Ω, must be considered in the study of the whole system. Moreover, pitch of blades and tilt of rotors are now inputs of the system.

The linear model is discussed in detail successively.

8.3.1 Non-Linear Modeling

The non-linear 6 D.O.F. mathematical model can be written with the expressions of chapters (2) and (3).

The engine equations, as in section (3.2.5), are inserted in place of the electric motors dynamics, remembering that now there is only one engine driving all the rotors. The engine speed Ω must be inserted in state vector. The speed of rotors is then equal to $\Omega\tau$.

The control inputs are different from those of a classical electric driven multi–rotor. A possible choice for them can be the following. Velocities, position and attitude of the vehicle can be controlled through:

1. the pitch of rotors blades θ_c for vertical flight;
2. the tilting of the fore and the aft rotors for lateral flight;
3. the tilting of the other two rotors for longitudinal flight;
4. the tilting of a couple of opposite rotors (or of the two couples), that rotate in opposite sense, for directional control.

For any rotor a tilting input can be modeled with a proper rotation matrix, to give the correct orientation of the air velocity components on the propeller and of all the aerodynamic loads.
Also the throttle of the engine δ_t can be included in the input vector.

Trim

Considering the trim of such an aircraft, in this case all the values for pitch of blades, rotors tilting and throttle deflection must be found. However the method of section (4.3.2) can be still utilized with proper modifications.
For hovering flight, the tilting of rotors can be put equal to $0^{\mathbf{o}}$. Yet again, the thrust of every rotor must be equal to the weight of the aircraft divided by the number of rotors. At this point the engine speed Ω_0 can be chosen arbitrarily. With this value of engine rate the blades pitch can be computed from the expression of C_T. Finally, imposing the equilibrium condition to the engine dynamics equation (3.42), the throttle valve deflection can be obtained.

$$C_{T0} = \frac{mg}{N_{rot}\rho A(\Omega_0 \tau R)^2} \tag{8.1}$$

$$\lambda_{i0} = \sqrt{\frac{C_{T0}}{2}} \tag{8.2}$$

$$v_{i0} = \lambda_{i0}\Omega_0\tau R \tag{8.3}$$

$$\theta_{c0} = 6\left(\frac{C_T}{\sigma C_{l\alpha}} + \frac{\lambda_{i0}}{4} + \frac{\theta_{tw}}{8}\right) \tag{8.4}$$

$$C_{\Pi 0} = C_{T0}\lambda_{i0} + \frac{\sigma C_d}{8} \tag{8.5}$$

$$\delta_t = C_{\Pi 0} N_{rot}\rho A(\Omega_0\tau R)^2 R\tau \frac{\Omega_0}{(P^{max}_{eng,\delta_t} - P^{min}_{eng,\delta_t})} \tag{8.6}$$

The trim values just calculated are those that are inserted in the *Inverse Simulation* algorithm as initial condition for the integration, as explained in the following dedicated section.

8.3.2 Stability Derivatives

Passing to the linear modeling, the development is almost identical to that of chapter (5). It begins again from the linearized rotor aerodynamics equations. The effects of coefficients C_H and C_Λ are yet neglected.
The stability matrix A is now a square matrix with ten rows and ten columns, because of the presence of Ω in state vector.

Attitude Kinematics Terms

The first three rows represent the linearized kinematics of the attitude.

$$A_{1,7} = A_{2,8} = A_{3,9} = 1 \tag{8.7}$$

X_θ and Y_ϕ Derivatives

The next three rows describe the dynamics of velocity in *Body Axis* frame. $A_{4,2}$ and $A_{5,1}$ are defined as in chapter (5).

$$A_{4,2} = X_\theta = -g \tag{8.8}$$

$$A_{5,1} = Y_\phi = g \tag{8.9}$$

X, Y and Z derivatives

These derivatives describe the effects of the variations of velocities, angular rates and engine speed on the velocity dynamics. The gyroscopic effects are neglected and in hovering the contribute of airframe drag can not be considered.

X_w is null because the variation of C_T is null. The p, q and w perturbations give a variation to μ_z for every rotor, but this does not affect the dynamics along the x_B axis itself. The effects of engine speed variations act only on z_B axis.

Along the z_B axis the perturbations of forces are generated by variations of climb ratio of the rotors and by the engine acceleration.

$$A_{6,6} = Z_w = \quad -\frac{1}{m}\frac{\partial C_T}{\partial \mu_z}\rho A\ \Omega\tau R\ N_{rotor} \tag{8.10}$$

$$A_{6,10} = Z_\Omega = -C_T\rho A\ (\tau R)^2\ 2\Omega_0\ N_{rotor} = -\frac{2g}{\Omega_0} \tag{8.11}$$

L, M and N Derivatives

For the roll dynamics the remarkable effects are those due to the p rate itself that generates opposite variations of C_T on the lateral rotors. The lateral rotors, *e.g.*, if r changes, create two rolling moments that acts around the same direction, but the different rotation verses of the same rotors impose opposite signs to the rolling moments themselves, that cancel each other.

h is the height of rotors from the center of gravity of the aircraft: $h < 0$ if the rotors are placed above the C.G. itself.

$$A_{7,7} = L_p = -\frac{1}{I_{xx}} \frac{\partial C_T}{\partial \mu_z} \rho A \ \Omega_0 \tau R \ \ \frac{N_{rot}}{2} \ b^2 \tag{8.12}$$

For the pitch dynamics the results are the same as for the roll dynamics.

$$A_{8,8} = M_q = -\frac{1}{I_{yy}} \frac{\partial C_T}{\partial \mu_z} \rho A \ \Omega_0 \tau R \ \ \frac{N_{rot}}{2} \ b^2 \tag{8.13}$$

On the dynamics of yaw rate r instead more effects are considerable. There is an effect due to w velocity that generates a torque through the load that imparts to the engine. Another effect is a consequence of the engine speed variation itself. p and q variations give a torque for the variation of C_Q on the two rotors that are doing a roll or pitch rotation.

$$A_{9,6} = N_w = -\frac{1}{I_{zz}} \frac{\partial C_\Pi}{\partial \mu_z} \rho A \ \Omega_0 (\tau R)^2 \ N_{rot} \tag{8.14}$$

$$A_{9,7} = N_p = \frac{1}{I_{zz}} \frac{\partial C_\Pi}{\partial \mu_z} \rho A \ \Omega_0 \tau R^2 \ \ \frac{N_{rot}}{2} \tag{8.15}$$

$$A_{9,8} = N_q = -N_p \tag{8.16}$$

$$\begin{aligned} A_{9,10} = N_\Omega = \ & -\frac{1}{I_{zz}} [-N_{rot} C_\Pi \rho A R^3 \tau^2 (2\Omega_0) \tau + \frac{\partial}{\partial \Omega} \frac{(P^{max}_{eng,\delta_t} - P^{min}_{eng,\delta_t}) \delta_t}{\Omega}] \\ & = -\frac{1}{I_{zz}} [-N_{rot} (2\lambda^3_{i0} + \frac{\sigma C_d}{8}) \rho A R^3 \tau^2 (2\Omega_0) \tau - \frac{(P^{max}_{eng,\delta_t} - P^{min}_{eng,\delta_t}) \delta_t}{\Omega^2}] \end{aligned} \tag{8.17}$$

Engine Dynamics Derivatives

A perturbation of the state of the engine is caused by the variation of w and the subsequent variation of C_Π and by a variation of Ω itself.

$$A_{10,10} = Q_\Omega = -N_\Omega \frac{I_{zz}}{I_{shaft}} \tag{8.18}$$

$$A_{10,6} = Q_w = -N_w \frac{I_{zz}}{I_{shaft}} \tag{8.19}$$

The Stability Matrix

Finally the stability matrix can be written in the proper form.

$$\mathbf{A} = \begin{bmatrix} 0 & 0 & 0 & 0 & 0 & 0 & 1 & 0 & 0 & 0 \\ 0 & 0 & 0 & 0 & 0 & 0 & 0 & 1 & 0 & 0 \\ 0 & 0 & 0 & 0 & 0 & 0 & 0 & 0 & 1 & 0 \\ 0 & X_\theta & 0 & 0 & 0 & 0 & 0 & 0 & 0 & 0 \\ Y_\phi & 0 & 0 & 0 & 0 & 0 & 0 & 0 & 0 & 0 \\ 0 & 0 & 0 & 0 & 0 & Z_w & 0 & 0 & 0 & Z_\Omega \\ 0 & 0 & 0 & 0 & 0 & 0 & L_p & 0 & 0 & 0 \\ 0 & 0 & 0 & 0 & 0 & 0 & 0 & M_q & 0 & 0 \\ 0 & 0 & 0 & 0 & 0 & N_w & N_p & N_q & 0 & N_\Omega \\ 0 & 0 & 0 & 0 & 0 & Q_w & 0 & 0 & 0 & Q_\Omega \end{bmatrix} \tag{8.20}$$

8.3.3 Control Derivatives

The matrix **B** in the present case has 10 rows and 9 columns. The columns are 9 because the aircraft possesses 9 inputs: the blades pitch and the tilting angle of the 4 rotors and the throttle valve deflection of the engine.

$$\mathbf{u} = [\theta_{c1}\ \theta_{c2}\ \theta_{c3}\ \theta_{c4}\ \xi_1\ \xi_2\ \xi_3\ \xi_4\ \delta_t]^T \tag{8.21}$$

This choice of the input vector allows the analysis of the controllability of the aircraft in case of actuator failure, as explained in the dedicated following section.
Here again, the inputs do not directly affect the attitude kinematics, in hovering flight, so that the first three rows of the matrix are rows of zeros.

Blades Pitch Derivatives

The pitch variation of the blades of a rotor induces a variation of C_T and C_Π. This brings to:

- a component of thrust in the $\mathbf{z}_B$ direction;

- a moment due to the rotor arm around the $\mathbf{x}_B$ or $\mathbf{y}_B$ direction;
- an acceleration of the engine;
- a moment around $\mathbf{z}_B$ axis due to the variation of torque and the acceleration of engine.

For the fore rotor of the aircraft the non-zero derivatives are listed below.

$$B_{6,1} = Z_{\theta_{c1}} = -\frac{1}{m}\frac{\partial C_T}{\partial \theta_c}\rho A\ (\Omega_0 \tau R)^2 \tag{8.22}$$

$$B_{8,1} = M_{\theta_{c1}} = \frac{1}{I_{yy}}\frac{\partial C_T}{\partial \theta_c}\rho A\ (\Omega_0 \tau R)^2\ b \tag{8.23}$$

$$B_{10,1} = Q_{\theta_{c1}} = -\frac{1}{I_{shaft}}\frac{\partial C_\Pi}{\partial \theta_c}\rho A\ \Omega_0^2 (\tau R)^3 \tag{8.24}$$

$$B_{9,1} = N_{\theta_{c1}} = \frac{1}{I_{zz}}\frac{\partial C_\Pi}{\partial \theta_c}\rho A\ (\Omega_0 \tau)^2 R^3 - Q_{\theta_{c,1}}\frac{I_{shaft}}{I_{zz}} \tag{8.25}$$

For the other rotors the results are similar.

$$B_{6,2} = B_{6,1} = Z_{\theta_{c2}} \tag{8.26}$$

$$B_{7,2} = -B_{8,1}\frac{I_{yy}}{I_{xx}} = L_{\theta_{c2}} \tag{8.27}$$

$$B_{10,2} = B_{10,1} = Q_{\theta_{c2}} \tag{8.28}$$

$$B_{9,2} = B_{9,1} - Q_{\theta_{c2}}\frac{I_{shaft}}{I_{zz}} = N_{\theta_{c2}} \tag{8.29}$$

$$B_{6,3} = B_{6,1} = Z_{\theta_{c3}} \tag{8.30}$$

$$B_{8,3} = -B_{8,1} = M_{\theta_{c3}} \tag{8.31}$$

$$B_{10,3} = B_{10,1} = Q_{\theta_{c3}} \tag{8.32}$$

$$B_{9,3} = -B_{9,1} - Q_{\theta_{c3}} \frac{I_{shaft}}{I_{zz}} = N_{\theta_{c3}} \tag{8.33}$$

$$B_{6,4} = B_{6,1} = Z_{\theta_{c4}} \tag{8.34}$$

$$B_{8,4} = B_{8,1} \frac{I_{yy}}{I_{xx}} = L_{\theta_{c4}} \tag{8.35}$$

$$B_{10,4} = B_{10,1} = Q_{\theta_{c4}} \tag{8.36}$$

$$B_{9,4} = -B_{9,1} - Q_{\theta_{c4}} \frac{I_{shaft}}{I_{zz}} = N_{\theta_{c4}} \tag{8.37}$$

Rotors Tilting Derivatives

The symbols ξ_1, ξ_2, ξ_3 and ξ_4 indicate the four angles of rotors tilting. They are other four control inputs of the system. Considering only small values of the rotors tilting, the variation in vertical thrust, in the hovering flight condition, can be neglected. The tilting angles do not enter directly in the definition of the aerodynamic coefficients rotors. Then, the following hypothesis is applied: the coefficients are not function of the rotor tilting itself around the trim condition. The forces generated in the $\{(\mathbf{x}_B, \mathbf{y}_B)\}$ plane are proportional to the rotor inclination with respect to the vertical direction. Every horizontal force due to rotor tilting generates also two moments.

$$B_{5,5} = \frac{g}{N_{rot}} = Y_{\xi_1} \tag{8.38}$$

$$B_{7,5} = Y_{\xi_1} \frac{m(-h)}{I_{xx}} = L_{\xi_1} \tag{8.39}$$

$$B_{9,5} = Y_{\xi_1} \frac{m\ b}{I_{zz}} = N_{\xi_1} \tag{8.40}$$

$$B_{4,6} = -\frac{g}{N_{rot}} = X_{\xi_2} \tag{8.41}$$

$$B_{8,6} = X_{\xi_2} \frac{m\ h}{I_{yy}} = M_{\xi_2} \tag{8.42}$$

$$B_{9,6} = -X_{\xi_2} \frac{m\ b}{I_{zz}} = N_{\xi_2} \tag{8.43}$$

$$B_{5,7} = \frac{g}{N_{rot}} = Y_{\xi_3} \tag{8.44}$$

$$B_{7,7} = Y_{\xi_3} \frac{m(-h)}{I_{xx}} = L_{\xi_3} \tag{8.45}$$

$$B_{9,7} = -Y_{\xi_3} \frac{m\ b}{I_{zz}} = N_{\xi_3} \tag{8.46}$$

$$B_{4,8} = -\frac{g}{N_{rot}} = X_{\xi_4} \tag{8.47}$$

$$B_{8,8} = X_{\xi_4} \frac{m\ h}{I_{yy}} = M_{\xi_4} \tag{8.48}$$

$$B_{9,8} = X_{\xi_4} \frac{m\ b}{I_{zz}} = N_{\xi_4} \tag{8.49}$$

Engine Speed Derivatives

The input of the engine is the throttle valve deflection. The throttle valve deflection δ_t is the last input of the entire system. Commanding the engine driving torque, two effects derive: one is the acceleration of the engine itself and the other is the yaw rate variation caused by the inertial torque due to the engine acceleration itself. The derivatives to be evaluated are two.

$$B_{9,9} = \frac{(P^{max}_{eng,\delta_t} - P^{min}_{eng,\delta_t})}{\Omega_0} / I_{shaft} = Q_{\delta_t} \tag{8.50}$$

$$B_{8,9} = -Q_{\delta_t} \frac{I_{shaft}}{I_{zz}} = N_{\delta_t} \tag{8.51}$$

The B Matrix

The control matrix can now be written.

$$\mathbf{B} = \begin{bmatrix} 0 & 0 & 0 & 0 & 0 & 0 & 0 & 0 & 0 \\ 0 & 0 & 0 & 0 & 0 & 0 & 0 & 0 & 0 \\ 0 & 0 & 0 & 0 & 0 & 0 & 0 & 0 & 0 \\ 0 & 0 & 0 & 0 & 0 & X_{\xi_2} & 0 & X_{\xi_4} & 0 \\ 0 & 0 & 0 & 0 & Y_{\xi_1} & 0 & Y_{\xi_3} & 0 & 0 \\ Z_{\theta_{c1}} & Z_{\theta_{c2}} & Z_{\theta_{c3}} & Z_{\theta_{c4}} & 0 & 0 & 0 & 0 & 0 \\ 0 & L_{\theta_{c2}} & 0 & L_{\theta_{c4}} & L_{\xi_1} & 0 & L_{\xi_3} & 0 & 0 \\ M_{\theta_{c1}} & 0 & M_{\theta_{c3}} & 0 & 0 & M_{\xi_2} & 0 & M_{\xi_3} & 0 \\ N_{\theta_{c1}} & N_{\theta_{c2}} & N_{\theta_{c3}} & N_{\theta_{c4}} & N_{\xi_1} & N_{\xi_2} & N_{\xi_3} & N_{\xi_4} & N_{\delta_t} \\ Q_{\theta_{c1}} & Q_{\theta_{c2}} & Q_{\theta_{c3}} & Q_{\theta_{c4}} & 0 & 0 & 0 & 0 & Q_{\delta_t} \end{bmatrix} \tag{8.52}$$

8.3.4 Numerical Results

Inserting the data of table (8.4), we can compute the value of any element of the matrix **A**. This result can be compared with the stability matrix obtained after a numerical differentiation executed with $MATLAB^{®}$.
The numerical calculation brings almost the same result.

$$\mathbf{A}_{analytic} = \begin{bmatrix} 0 & 0 & 0\,0\,0 & 0 & 1 & 0 & 0 & 0 \\ 0 & 0 & 0\,0\,0 & 0 & 0 & 1 & 0 & 0 \\ 0 & 0 & 0\,0\,0 & 0 & 0 & 0 & 1 & 0 \\ 0 & -9.81 & 0\,0\,0 & 0 & 0 & 0 & 0 & 0 \\ 9.81 & 0 & 0\,0\,0 & 0 & 0 & 0 & 0 & 0 \\ 0 & 0 & 0\,0\,0 & -0.9478 & 0 & 0 & 0 & -0.0491 \\ 0 & 0 & 0\,0\,0 & 0 & -19.9219 & 0 & 0 & 0 \\ 0 & 0 & 0\,0\,0 & 0 & 0 & -19.9219 & 0 & 0 \\ 0 & 0 & 0\,0\,0 & 0.1550 & -0.0527 & 0.0527 & 0 & 0.0409 \\ 0 & 0 & 0\,0\,0 & -1.4609 & 0 & 0 & 0 & -0.3858 \end{bmatrix} \tag{8.53}$$

$$\mathbf{A}_{numeric} = \begin{bmatrix} 0 & 0 & 0\,0\,0 & 0 & 1 & 0 & 0 & 0 \\ 0 & 0 & 0\,0\,0 & 0 & 0 & 1 & 0 & 0 \\ 0 & 0 & 0\,0\,0 & 0 & 0 & 0 & 1 & 0 \\ 0 & -9.81 & 0\,0\,0 & 0 & 0 & 0 & 0 & 0 \\ 9.81 & 0 & 0\,0\,0 & 0 & 0 & 0 & 0 & 0 \\ 0 & 0 & 0\,0\,0 & -0.9478 & 0 & 0 & 0 & -0.0490 \\ 0 & 0 & 0\,0\,0 & 0 & -19.9219 & 0 & 0 & 0 \\ 0 & 0 & 0\,0\,0 & 0 & 0 & -19.9219 & 0 & 0 \\ 0 & 0 & 0\,0\,0 & 0.1550 & -0.0527 & 0.0527 & 0 & 0.0409 \\ 0 & 0 & 0\,0\,0 & -1.4609 & 0 & 0 & 0 & -0.3858 \end{bmatrix} \tag{8.54}$$

Also for the **B** matrix, the results of the numeric and analytic differentiation can be compared.

$$\mathbf{B}_{analytic} = 10^3 \cdot \begin{bmatrix} 0 & 0 & 0 & 0 & 0 & 0 & 0 & 0 & 0 \\ 0 & 0 & 0 & 0 & 0 & 0 & 0 & 0 & 0 \\ 0 & 0 & 0 & 0 & 0 & 0 & 0 & 0 & 0 \\ 0 & 0 & 0 & 0 & 0 & -0.0025 & 0 & -0.0025 & 0 \\ 0 & 0 & 0 & 0 & 0.0025 & 0 & 0.0025 & 0 & 0 \\ -0.0316 & -0.0316 & -0.0316 & -0.0316 & 0 & 0 & 0 & 0 & 0 \\ 0 & -1.9531 & 0 & 1.9531 & 0.0669 & 0 & 0.0669 & 0 & 0 \\ 1.9531 & 0 & -1.9531 & 0 & 0 & 0.0669 & 0 & 0.0669 & 0 \\ 0 & 0 & 0.0437 & 0.0437 & 0.0681 & 0.0681 & -0.0681 & -0.0681 & -0.0375 \\ -0.2059 & -0.2059 & -0.2059 & -0.2059 & 0 & 0 & 0 & 0 & 0.3535 \end{bmatrix} \tag{8.55}$$

$$\mathbf{B}_{numeric} = 10^3 \cdot \begin{bmatrix} 0 & 0 & 0 & 0 & 0 & 0 & 0 & 0 & 0 \\ 0 & 0 & 0 & 0 & 0 & 0 & 0 & 0 & 0 \\ 0 & 0 & 0 & 0 & 0 & 0 & 0 & 0 & 0 \\ 0 & 0 & 0 & 0 & 0 & -0.0025 & 0 & -0.0025 & 0 \\ 0 & 0 & 0 & 0 & 0.0025 & 0 & 0.0025 & 0 & 0 \\ -0.0316 & -0.0316 & -0.0316 & -0.0316 & 0 & 0 & 0 & 0 & 0 \\ 0 & -1.9531 & 0 & 1.9531 & 0.0669 & -0.0030 & 0.0669 & 0.0030 & 0 \\ 1.9531 & 0 & -1.9531 & 0 & 0.0030 & 0.0669 & -0.0030 & 0.0669 & 0 \\ 0 & 0 & 0.0437 & 0.0437 & 0.0681 & 0.0681 & -0.0681 & -0.0681 & -0.0375 \\ -0.2059 & -0.2059 & -0.2059 & -0.2059 & 0 & 0 & 0 & 0 & 0.3535 \end{bmatrix} \tag{8.56}$$

There is only a small difference in the effects of tilting on the p and q angular rates dynamics. However, with proper simulations, it can be verified that the numeric responses are indistinguishable. Thus the analytic definition of **B** is considered valid.

8.4 Inverse Simulation

Inverse Simulation is a well known and abundantly used technique in the study of flight dynamics. Many articles by now show various applications of this technique to the assessing of handling qualities, control design, model validation, etc. [27].

What Inverse Simulation precisely does, it is to compute the control actions for a system to exhibit a prescribed behavior. For a flying machine this is equal to calculate the control actions a pilot must exert to make the aircraft follow a precise trajectory. In this work Inverse Simulation is

applied to the *Quad–Tilt–Rotor* non–linear model to verify if this aircraft can perform maneuvers not feasible for a classical quad–rotor.

Inverse Simulation Algorithm

The theoretical treatment of Inverse Simulation is exhaustively described in [9].
An application of Inverse Simulation similar is documented in a parallel work [19]. The algorithm there outlined is the same utilized here. Briefly the Inverse Simulation algorithm and some hints about its implementation in $MATLAB^{®}$ are now described.
In general, there are two types of Inverse Simulation algorithms. One is the *Integration Method*. The other is the *Differentiation Method*. The algorithm used here belongs to the first type. The Inverse Simulation problem starts from the declaration of the state vector equation.

$$\dot{\mathbf{X}} = \boldsymbol{f}(\mathbf{X}, \mathbf{U}) \tag{8.57}$$

To this equation it is associated the *output equation*.

$$\mathbf{y}(t) = \mathbf{g}(\mathbf{X}(t)) \tag{8.58}$$

$\mathbf{y}(t)$ is the analytic definition of the trajectory that the aircraft must follow. It is a function $\mathbf{g}$ of some element of the state vector $\mathbf{X}(t)$.
The mission time ΔT is divided in small intervals equal to Δt. The first step now is to find a constant input vector $\mathbf{U}^*$ that satisfies the following condition.

$$\mathbf{y}^*(\Delta t) = \mathbf{g}(\mathbf{X}(\Delta t)) \tag{8.59}$$

This input vector $\mathbf{U}^*$ allows the evolution of the state vector during the interval Δt to reach the desired output of the previous equation, from the initial condition $\mathbf{X}(0)$.

The equation (8.59) can be solved only with a numerical method. In $MATLAB^{®}$ this is done through a *sequential quadratic programming* (*SQP*) algorithm.

The components of $\mathbf{U}$ for the Inverse Simulation problem differ from those utilized till now in the modeling, as in equation (8.21). In place of the blades pitches θ_{cj}, with $j = 1, ..., N_{rot}$, the parameters Σ_j are inserted. Σ_j is a non–dimensional parameter that identifies the thrust of the j-th rotor through the following expression.

$$T_j = \Sigma_j \frac{mg}{N_{rot}} \tag{8.60}$$

The *SQP* algorithm computes through the Σ_j parameters the thrusts of all the rotors. Then, from all the thrusts, the pitch of all the rotors θ_{cj} can be computed. Expression (8.60) allows to have an initial value of parameters Σ_j. In hovering flight, $\Sigma_j = 1$.

Once the input vector $\mathbf{U}^*$ is defined, the integration of the state equation is effected on a time interval equal or inferior to Δt, again with a *Runge–Kutta* method of numerical integration.

$$\mathbf{X}(\Delta t) = \mathbf{X}(0) + \int_0^{\Delta t} \boldsymbol{f}(\mathbf{X}, \mathbf{U}) \mathbf{d}t \tag{8.61}$$

This last value of the state vector $\mathbf{X}(\Delta t)$ is chosen as the new starting point for the successive step of Inverse Simulation along another time interval Δt. All the process is repeated till the end of the predefined maneuver.

Very shortly, this is how Inverse Simulation works.

The implementation in $MATLAB^{®}$ allows some useful expedient in the algorithm.

The usage of the *SQP* algorithm permits to fix some constraint on the state element or on someone of the inputs that do not appear in the output vector $\mathbf{y}(t)$.

For example, in the next simulations, it is imposed that the engine rate Ω can not depart from its trim value Ω_0.

Another important aspect of the entire process is the definition of the output function $\mathbf{y}(t)$, that is to say the flight path of the aircraft. This function must satisfy some conditions in terms of continuity [9, 27] in the time domain. To this purpose, often the output functions were defined by means of polynomial functions of time t. This is done also in [19]. Instead in this work all the output functions are defined with trigonometric functions, as explained in the following.

Five maneuvers are here considered for the Inverse Simulation problem. All these missions can not be performed by a traditional electric driven multi–rotor. Because all these maneuvers develop in few seconds, it is neglected the mass variation of the aircraft due to fuel consumption.

The initial condition of all the maneuvers is that of hovering flight with null attitude ($\Phi_0, \Theta_0, \Psi_0 = 0^{\mathbf{o}}$). The time of the mission is indicated with ΔT.

8.4.1 U–Turn Maneuver

After the hovering initial condition, the aircraft accelerates along the $\mathbf{x}_B$ axis until it reaches a velocity equal to V_{max}, always with null attitude. Then, maintaining the same total velocity and the angle Φ equal to zero, turns to its right. The turn ends when an heading angle Ψ of $180^{\mathbf{o}}$ is achieved and the aircraft continues its reversed forward flight.

The output function for this maneuver is defined in terms of the three components of inertial velocity $\dot{\mathbf{P}}_E$.

$$\dot{\mathbf{P}}_E = [N \ E \ D]^T = [V_x \ V_y \ V_z]^T \tag{8.62}$$

For this simulation ΔT is put equal to 20 $\mathbf{s}$.

It is introduced now the non–dimensional time $\tilde{t}$.

$$\tilde{t} = 2\frac{t-1}{\Delta T - 2} \tag{8.63}$$

At time $t_1 = 1$ **s**, the acceleration begins and then it ends at $t_2 = \Delta T/4$. The relative non–dimensional times $\tilde{t_1}$ and $\tilde{t_2}$ can be easily computed. In this non–dimensional time interval, the following auxiliary variable can be defined.

$$\epsilon_1 = \left[1 - \cos^2\left(\frac{(\tilde{t} - \tilde{t_1})}{(\tilde{t_2} - \tilde{t_1})}\frac{\pi}{2}\right)\right]\pi \tag{8.64}$$

In the same time interval V_x and V_y can be defined.

$$\begin{cases} V_x = \left[1 - \sqrt{\dfrac{1}{1+\tan^2(\epsilon_1)}}\right]\dfrac{V_{max}}{2}, \ \epsilon_1 <= \frac{\pi}{2} \\ \\ V_x = \left[1 + \sqrt{\dfrac{1}{1+\tan^2(\epsilon_1)}}\right]\dfrac{V_{max}}{2}, \ \epsilon_1 > \frac{\pi}{2} \end{cases} \tag{8.65}$$

$$V_y = 0 \ \mathbf{m\ s^{-1}} \tag{8.66}$$

The second phase of the maneuver starts from $t = \Delta T/4$ and ends in $t = \Delta T$. This phase is characterized by the increase of the heading angle Ψ from $0^{\mathbf{o}}$ to $180^{\mathbf{o}}$. For this phase another auxiliary ϵ_2 variable can be computed between $\tilde{t_3}$ and $\tilde{t_2}$.

$$\tilde{t_3} = 2\frac{\Delta T - 1}{\Delta T - 2} \tag{8.67}$$

The trend of the heading angle is defined in the following manner.

$$\begin{cases} \Psi = \left[1 - \sqrt{\dfrac{1}{1+\tan^2(\epsilon_2)}}\right]\dfrac{\pi}{2}, \ \epsilon_2 <= \dfrac{\pi}{2} \\ \\ \Psi = \left[1 + \sqrt{\dfrac{1}{1+\tan^2(\epsilon_2)}}\right]\dfrac{\pi}{2}, \ \epsilon_2 > \dfrac{\pi}{2} \end{cases} \tag{8.68}$$

Remembering that the angles Φ and Θ are always null, the velocities V_x and V_y can be easily obtained.

$$\begin{cases} V_x = V_{max}\cos(\Psi) \\ \\ V_y = V_{max}\sin(\Psi) \end{cases} \tag{8.69}$$

For the whole maneuver it is imposed that $V_z = 0\ \mathbf{m\ s^{-1}}$. The *SQP* algorithm implementation permits moreover to fix a constraint on the angles Φ and Θ, so that they could remain near the null value.

U–Turn Simulation Results The results of the Inverse Simulation are shown in appendix. V_{max} is put equal to $0.5\ \mathbf{m\ s^{-1}}$. In the graphs of figure (C.1) the V_x and V_y velocities and angle Ψ are plotted as given by the previous formulae. In figure (C.2) the same quantities as tracked by the *Quad–Tilt–Rotor* are depicted. All the trends adhere perfectly. Finally in figures (C.3) and (C.4) the pitch of propellers and the tilting of the rotors are shown.

8.4.2 Straight Flight with 360^o Yaw–Turn

The desired output of this maneuver is defined in terms of inertial velocities V_x, V_y, V_z and of the heading angle Ψ. The other attitude angles are put equal to zero.

V_y, V_z are always equal to zero, too.

The velocity V_x, in a first phase, is brought to its maximum value V_{max} and in a second phase returns to the initial zero value. The first phase starts for at time $t_1 = 1\ s$ and ends at time $t_2 = \Delta T/2$.

Utilizing again the non–dimensional time $\tilde{t}$ and the auxiliary variables ϵ and χ, the inertial velocity V_x can be defined.

$$\begin{cases} \chi_1 = \left[1 - \sqrt{\dfrac{1}{1+\tan^2(\epsilon_1)}}\right]\dfrac{\pi}{2},\ \epsilon_1 <= \dfrac{\pi}{2} \\ \\ \chi_1 = \left[1 + \sqrt{\dfrac{1}{1+\tan^2(\epsilon_1)}}\right]\dfrac{\pi}{2},\ \epsilon_1 > \dfrac{\pi}{2} \\ \\ V_x = V_{max}\cos\left(\dfrac{\chi_1}{2} - \dfrac{\pi}{2}\right) \end{cases} \tag{8.70}$$

In a second phase of the maneuver, between $t_2 = \Delta T/2$ and $t_3 = \Delta T - 1$, the velocity V_x is decreased to zero in a specular fashion.

$$\begin{cases} \chi_2 = \left[1 - \sqrt{\dfrac{1}{1+\tan^2(\epsilon_2)}}\right]\dfrac{\pi}{2},\ \epsilon_2 <= \dfrac{\pi}{2} \\ \\ \chi_2 = \left[1 + \sqrt{\dfrac{1}{1+\tan^2(\epsilon_2)}}\right]\dfrac{\pi}{2},\ \epsilon_2 > \dfrac{\pi}{2} \\ \\ V_x = V_{max}\left[1 - \cos\left(\dfrac{\chi_2}{2} - \dfrac{\pi}{2}\right)\right] \end{cases} \tag{8.71}$$

The function that describes the desired trend of Ψ is obtained in a similar way. This angle passes from 0^o to 360^o in a time interval between $t_1 = \Delta T/3$ and $t_2 = 3\Delta T/2$.

$$\begin{cases} \Psi = \left[1 - \sqrt{\dfrac{1}{1+\tan^2(\epsilon_1)}}\right]\pi,\ \epsilon_1 <= \dfrac{\pi}{2} \\ \\ \Psi = -\left[1 - \sqrt{\dfrac{1}{1+\tan^2(\epsilon_1)}}\right]\pi,\ \epsilon_1 > \dfrac{\pi}{2} \end{cases} \tag{8.72}$$

Straight Flight with 360^o Yaw–Turn Simulation Results In appendix (D) the results of simulation are shown.

In this case, $V_{max} = 0.5\ \mathbf{m\ s^{-1}}$ and $\Delta T = 15\ \mathbf{s}$.

The maneuver is perfectly effected.

8.4.3 360° Yaw–Turn

This maneuver is identical to the preceding, with V_x equal to zero during the whole time interval ΔT. This maneuver has been simulated to the purpose of comparing its result with a similar maneuver obtained through direct simulation, as shown in [8]. There the yaw–turn has been accomplished only approximately, without a perfect control on velocities and the attitude angles. With Inverse Simulation, instead, it is possible to assess what is the proper control action to impart to the aircraft. The results are shown in appendix (E) and are also in this case satisfactory.

8.4.4 Straight Flight with Rolling Tilt

In this maneuver the aircraft reaches a condition of forward flight. Then it effects a rotation around the roll axis $\mathbf{x}_B$ till a value of Φ equal to 90°, prosecuting the forward flight.
The acceleration is accomplished in a time interval between $t_1 = 1$ s and $t_2 = \Delta T/2$.

$$\begin{cases} V_x = \left[1 - \sqrt{\dfrac{1}{1+\tan^2(\epsilon_1)}}\right] \dfrac{V_{max}}{2}, \ \epsilon_1 <= \dfrac{\pi}{2} \\ V_x = \left[1 + \sqrt{\dfrac{1}{1+\tan^2(\epsilon_1)}}\right] \dfrac{V_{max}}{2}, \ \epsilon_1 > \dfrac{\pi}{2} \end{cases} \tag{8.73}$$

For t between t_2 and $t_3 = \Delta T$ the rolling motion occurs.

$$\begin{cases} \chi = \left[1 - \sqrt{\dfrac{1}{1+\tan^2(\epsilon_2)}}\right] \dfrac{\pi}{2}, \ \epsilon_2 <= \dfrac{\pi}{2} \\ \chi = \left[1 + \sqrt{\dfrac{1}{1+\tan^2(\epsilon_2)}}\right] \dfrac{\pi}{2}, \ \epsilon_2 > \dfrac{\pi}{2} \\ \Phi = \Phi_{max} \cos(\chi) \end{cases} \tag{8.74}$$

Straight Flight with 90^{o} Rolling Tilt Simulation Results For this maneuver ΔT is put equal to 10 **s** and $V_{max} = 1$ **m** $\mathbf{s}^{-1}$. Φ_{max} is equal 90^{o}. In appendix (F) the relative diagrams are presented. This maneuver, too, is exactly performed.

Hovering with Not Null Attitude

The definition of the output function **y** for this maneuver derives from that of the previous one, with V_x equal to zero during the whole time interval ΔT. This simulation responds to the question whether the *Quad–Tilt–Rotor* could hover with an attitude different from one with null Φ and Θ.

The variation of attitude begins at time $t_1 = 1$ **s** and ends at $t_2 = \Delta T$.

$$\begin{cases} \Phi = \left[1 - \sqrt{\dfrac{1}{1+\tan^2(\epsilon)}}\right] \dfrac{\Phi_{max}}{2}, \ \epsilon <= \dfrac{\pi}{2} \\ \\ \Phi = \left[1 + \sqrt{\dfrac{1}{1+\tan^2(\epsilon)}}\right] \dfrac{\Phi_{max}}{2}, \ \epsilon > \dfrac{\pi}{2} \end{cases} \tag{8.75}$$

In appendix (G) the graphical results are inserted. Here Φ_{max} is put equal to 30^{o} and $\Delta T = 10$ **s**. The hovering flight condition with a not null attitude can be reached.

Final Considerations on Inverse Simulation

The Inverse Simulation has proven to be an excellent instrument to the analysis of flight dynamics of multi–rotor platforms. In this section, with this technique, the enhanced performance capabilities of the *Quad–Tilt–Rotor* have been assessed, with respect to classical quad–rotor normal operations.

This section does not address a theoretical discussion about mathematical or numerical concerns of Inverse Simulation. For similar questions the references cited in the previous pages can be consulted.

8.5 Complete State Controllability Analysis

For a dynamic system one important property, that is related to the design of the control systems in the state space, is the *complete state controllability* of the system itself. For the definition of complete state controllability of a system several texts are available in literature [16, 18]. If the property is verified, then the system, with an apt control action, can be brought from any initial condition in the state space to any other point in the state space in a finite time.

In the case of a *LTI* system, as one described by equations (5.1), a mathematical definition can be derived for the complete controllability. It can be stated that the so called *controllability matrix* $\mathbf{P}$ must have rank equal to the dimension of the state vector. The matrix $\mathbf{P}$ is defined in the next expression.

$$\mathbf{P} = [\mathbf{B} \mid \mathbf{AB} \mid \cdots \mid \mathbf{A}^{n-1}\mathbf{B}] \tag{8.76}$$

The condition for the complete controllability is, in formula, $\rho(\mathbf{P}) = n$, where n is the number of component of the vector x.

Because for the system under study the $\mathbf{A}$ and $\mathbf{B}$ matrices have been defined, the complete state controllability can be checked. Computing the matrix and its rank with $MATLAB^{®}$, the result is that $\rho(\mathbf{P}) = 10 = dim(\mathbf{x})$. This means that the aircraft is completely controllable in terms of attitude, velocity, angular rate and engine speed, by the chosen 9 control inputs.

Now, being the *Quad–Til–Rotor* not more an under–actuated system as a classical quad-rotor, it is interesting to investigate the *residual controllability* of the aircraft in case of an actuator failure. As a failure it is considered the inaccessibility to one command, so that the related control input is maintained equal to that in the trim condition. In a word, to the system linearized mathematical description, a component of the control vector $\mathbf{u}$ and, consequently, a column of the $\mathbf{B}$ matrix are eliminated.

With the new matrix $\mathbf{B}$ the matrix $\mathbf{P}$ can be newly computed and its rank.

8.5.1 Results

In table (8.3) the results of the Controllability analysis previously described are listed for various cases of virtual block of one or more actuators.

Blocked Inputs	$\rho(\mathbf{P})$
ξ_4	10
θ_{c4}	10
ξ_4, θ_{c4}	10
θ_{c3}, θ_{c4}	10
θ_{c2}, θ_{c3}, θ_{c4}	9
ξ_3, ξ_4	10
ξ_2, ξ_3, ξ_4	10
ξ_1, ξ_2, ξ_3, ξ_4	9

Table 8.3: Residual Controllability Test

The case with all tilting actuators blocked is interesting, because the system results not completely controllable. This is due probably for the presence of the engine speed in the state vector, though this quantity may not have significance from the point of view of the control and guidance of the aircraft.

8.6 Data for Simulations

In table (8.4) the data utilized for the simulations are shown.

8.7 Remarks

An innovative configuration of quad–rotor, the *Quad–Tilt–Rotor* aircraft, has been presented in this chapter.

Type	Value	Units	Type	Value	Units
R	0.25	**m**	θ_{tw}	0	**rad**
I_{rotor}	10^{-4}	**kg m**^{2}	$C_{l\alpha}$	5.5	**rad**$^{-1}$
C_d	0.003		τ	1	
m	4	**kg**	I_{xx}	0.044	**kg m**^{2}
I_{yy}	0.044	**kg m**^{2}	I_{zz}	0.098	**kg m**^{2}
I_{gear}	0.01	**kg m**^{2}	A_x	0.5	**m**^{2}
A_y	0.5	**m**^{2}	A_z	0.8	**m**^{2}
ρ	1.2235	**kg m**$^{-3}$	Ω_0	400	**rad s**$^{-1}$
P^{min}_{eng,δ_t}	0	**kW**	P^{max}_{eng,δ_t}	1.47	**kW**
b	0.68	**m**	h	-0.3	**m**
N	2		N_{rot}	4	
g	9.81	**m s**$^{-2}$	Δt	0.01	**s**

Table 8.4: *Quad–Tilt–Rotor* Simulations Data

Of this aircraft an accurate mathematical modeling of dynamics has been defined.

This model, by means of Inverse Simulation technique, has been exploited to simulate some maneuvers that clearly highlighted the increased maneuvering capabilities of this aircraft with respect to a traditional quad–rotor.

Also a linearized model of dynamics has been obtained by an analytic differentiation of the equations of motion.

Through the linearized model an analysis of controllability of the machine in case of actuator failure is accomplished, that showed in what damage situations the aircraft is still controllable.

All the development of this chapter represents a paradigmatic example of how a mathematical model of dynamics is a really effective tool for the study of complex systems like multi–rotor platforms.

Bibliography

[1] Avanzini G., Giulietti F. *Quadcopter configuration with tilting rotors*, Pat. WO2013098736 A2, request No. PCT/IB2012/057589, Dec. 2012.

[2] A. R. S. Bramwell, *Helicopter Dynamics*, Edward Arnold Ltd., 1976

[3] Bramwell, A.R.S., *The Longitudinal Stability and Control of the Tandem-Rotor Helicopter*, Aeronautical Research Council Reports and Memoranda, No. 3223, London, Jan. 1960.

[4] S. Bouabdallah, R. Siegwart, *Full Control of a Quadrotor*, IEEE/RSJ International Conference on Intelligent Robots and Systems, TuA5.5, San diego, CA, USA, Oct 29 - Nov 2, 2007

[5] M. Cutler, N. Kemal Ure, B. Michini, and J. P. How. *Comparison of fixed and variable pitch actuators for agile quadrotors*, AIAA Guidance, Navigation, and Control Conference (GNC), Portland, OR, August 2011. (AIAA-2011-6406)

[6] Dreier, M.E., *Introduction to Helicopter Flight and Tilt Rotor Flight Simulation*, AIAA Education Series, USA, Feb. 2007, Chs. 2, 4, and 11.

[7] Efraim H., and Shapiro H., *Special Quadrotor Structure with Inherent Negative Velocity Feedback*, Proc. of the 32nd Israeli Conference

on Mechanical Engineering (ICME 2012), Tel-Aviv, Israel, 17-18 Oct. 2012.

[8] Ferrarese, G., Giulietti, F., and Avanzini, G., *Modeling and Simulation of a Quad-Tilt Rotor Aircraft*, Proc. of the 2nd IFAC Workshop on Research, Education and Development of Unmanned Aerial Systems, Compiegne, France, 20-22 Nov. 2013, pp. 64-70.

[9] Hess R.A., Gao C., Wang S.H., *Generalized technique for inverse simulation applied to aircraft maneuvers* AIAA Journal of Guidance, Control and Dynamics 1991, Vol. 14, No. 5, Sep.-Oct. 1991, pp. 920-926

[10] Gabriel M. Hoffmann, Haomiao Huang, Steven L. Waslander, Claire J. Tomlin, *Quadrotor Helicopter Flight Dynamics and Control: Theory and Experiment*, AIAA Guidance, Navigation and Control Conference and Exhibit, August 2007, Hilton Head, South Carolina, AIAA 2007-6461

[11] G. Legnani, M. Tiboni, R. Adamini, D. Tosi *MECCANICA DEGLI AZIONAMENTI, Vol.1 - Azionamenti elettrici*, Societá Editrice Esculapio, Bologna, Italia, 2008

[12] Leishman J.G., *Principles of Helicopter Aerodynamics*, Second Edition, Cambridge Aerospace Series, USA, Apr. 2006, Ch. 2.

[13] McLean D., *Automatic Flight Control Systems*, Prentice Hall International Ltd, UK, Nov. 1990, Chs. 2 and 13.

[14] Mettler Bernard, *Identification Modeling and Characteristics of Miniatures Rotorcraft*, Kluwer Academics Publisher, Nowell, MA, USA, September 2002.

[15] Newman Simon, *The Foundations of Helicopter Flight*, Butterworth-Heinemann, 1994.

[16] Katsuhiko Ogata, *Modern Control Engineering*, Prentice Hall International Editions, 1997

[17] Padfield Gareth D., *Helicopter Flight Dynamics*, Blackwell Science Ltd., 1996.

[18] M.E. Penati, G. Bertoni, *Automazione e Sistemi di Controllo*, Societá Editrice Esculapio, Italia, 1996

[19] Irene A. Piacenza, Fabrizio Giulietti, Giulio Avanzini, *Inverse simulation of unconventional maneuvers for a quadcopter with tilting rotors*, Proc. of the 2nd IFAC Workshop on Research, Education and Development of Unmanned Aerial Systems, Compiegne, France, 20-22 Nov. 2013, pp. 64-70.

[20] P. Pounds, R. Mahony, Joel Gresham, *Towards Dynamically-Favourable Quad-Rotor Aerial Robots*, Proceedings Australasian Conference on Robotics and Automation Canberra, Australia, 2004

[21] R.W. Prouty, *Helicopter Performance, Stability, and Control*, Krieger Publishing Company, Malabar, Florida, 2002

[22] Markus Ryll, Heinrich H. Bülthoff, Paolo Robuffo Giordano, *First Flight Tests for a Quadrotor UAV with Tilting Propellers*, IEEE International Conference on Robotics and Automation (ICRA 2012), IEEE, Piscataway, NJ, USA, 4606-4613.

[23] Fatih Senkul, Erdinç Altuğ, *Modeling and Control of a Novel Tilt–Roll Rotor Quadrotor UAV*, 2013 International Conference on Unmanned Aircraft Systems (ICUAS), May 28-31, 2013, Grand Hyatt Atlanta, Atlanta, GA

[24] Peter D. Talbot, Bruce E. Tinling, William A. Decker, Robert T. Chen, *A Mathematical Model of a Single Main Rotor Helicopter for*

Piloted Simulation NASA Technical Memorandum 84281, Ames Research Center, Moffett Field, California, 94035, September 1982.

[25] Tibaldi Marco, *Progetto di Sistemi di Controllo*, Ed. Pitagora, Italia, 1995

[26] Mark B. Tischler, Robert K. Remple, *Aircraft and Rotorcraft System Identification*, AIAA Education Series, 2006

[27] Douglas Thomson, Roy Bradley, *Inverse simulation as a tool for flight dynamics research – Principles and applications* Progress in Aerospace Sciences, Vol. 42, No. 3, May 2006, pp. 174-210.

[28] J. Verbeke, D. Hulens, H. Ramon, T. Goedemé, J. De Schutter *The Design and Construction of a High Endurance Hexacopter suited for Narrow Corridors*, 2014 International Conference on Unmanned Aircraft Systems (ICUAS), May 27-30, 2014. Orlando, FL, USA

Appendix A

Aeromechanical Stability Analysis Results

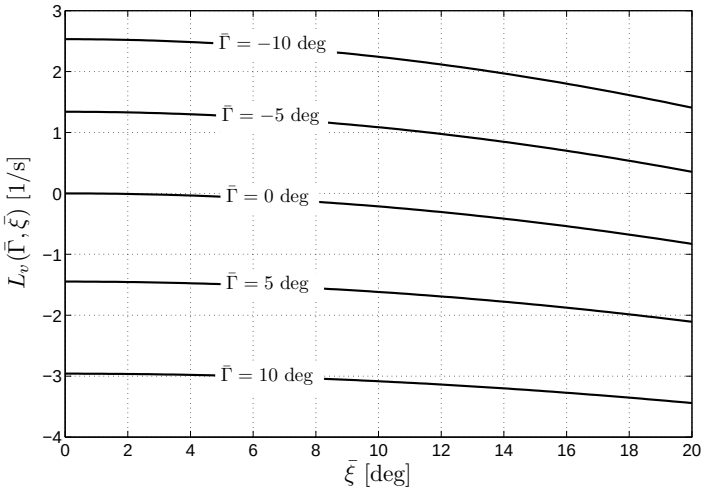

Figure A.1: L_v Derivative

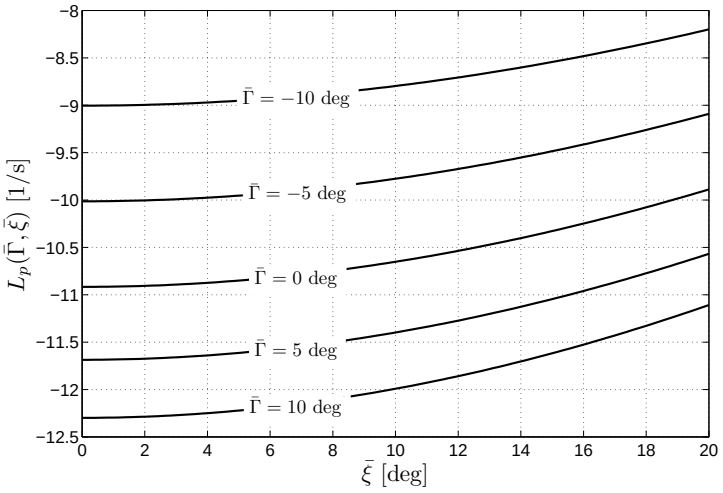

Figure A.2: L_p Derivative

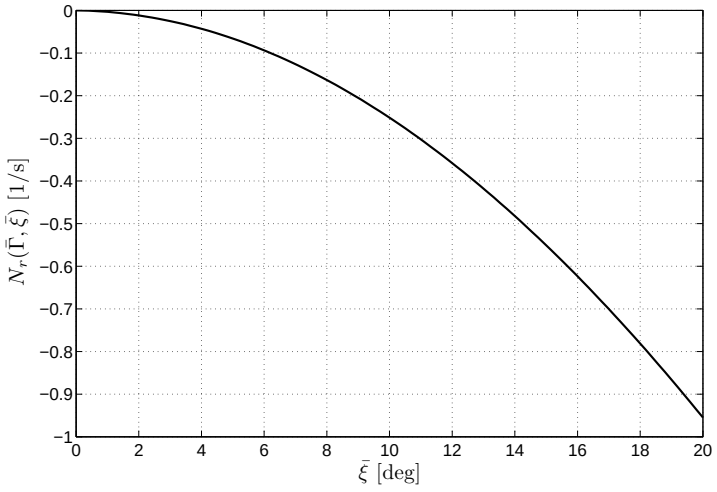

Figure A.3: N_r Derivative

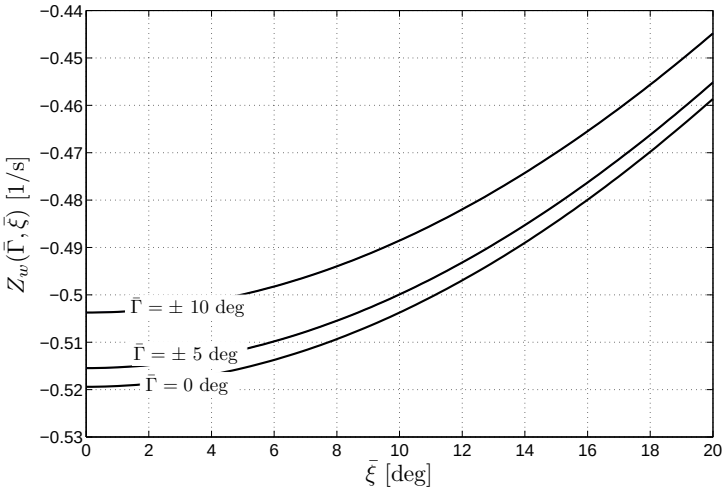

Figure A.4: Z_w Derivative

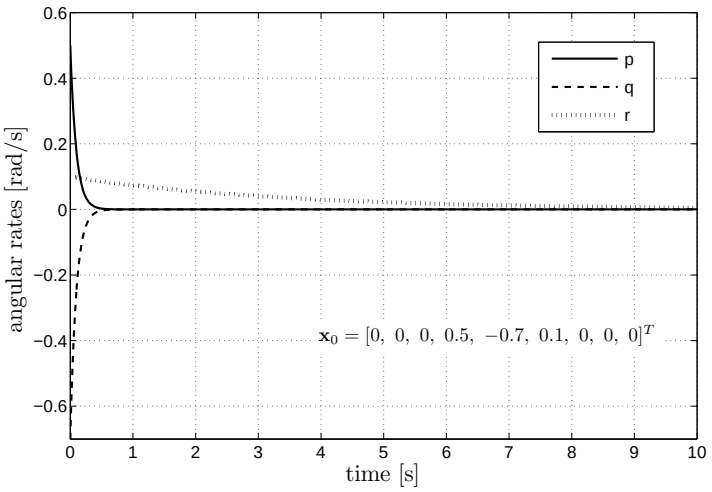

Figure A.5: Vehicle Angular Rates (C3 configuration)

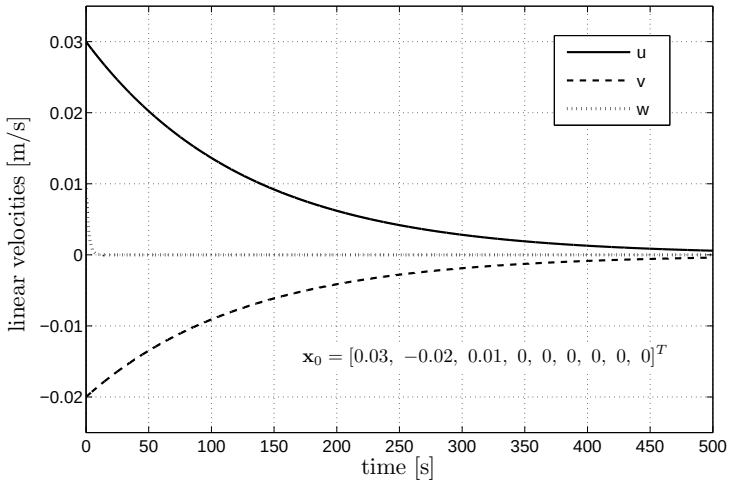

Figure A.6: Vehicle Translational Velocities (C3 configuration)

Appendix B

Control Systems Simulation

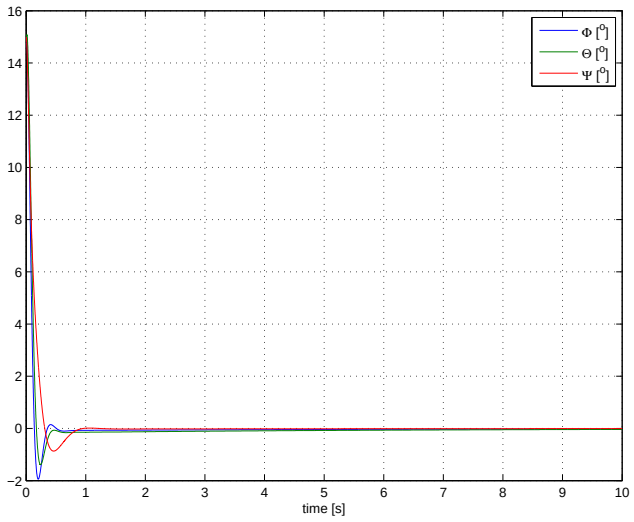

Figure B.1: *PID* Regulation of Attitude

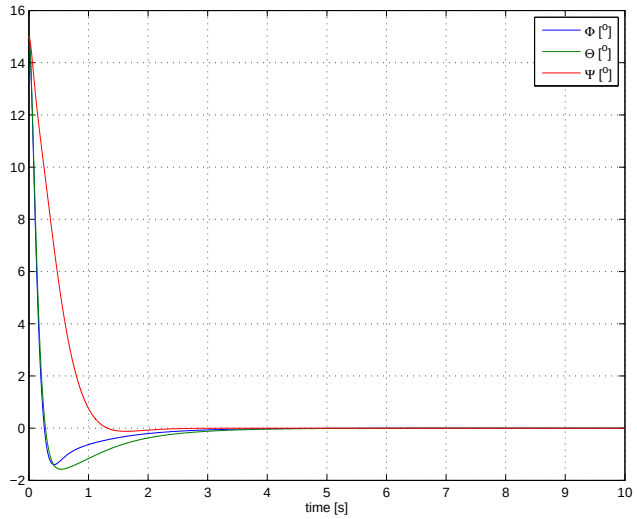

Figure B.2: *LQ* Regulation of Attitude

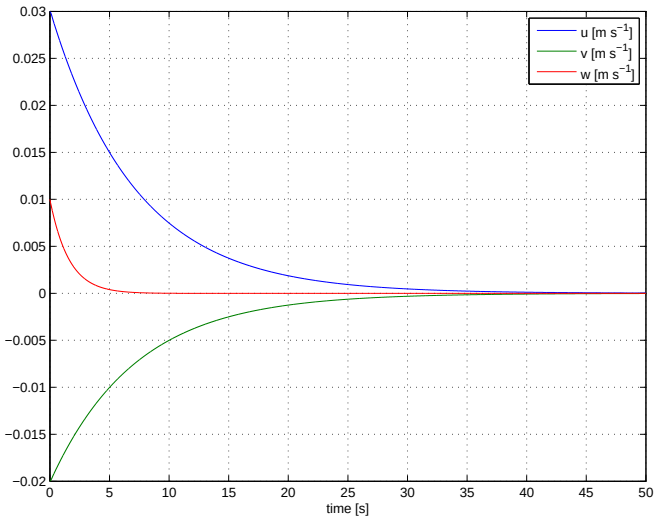

Figure B.3: *PID* Regulation of Velocity

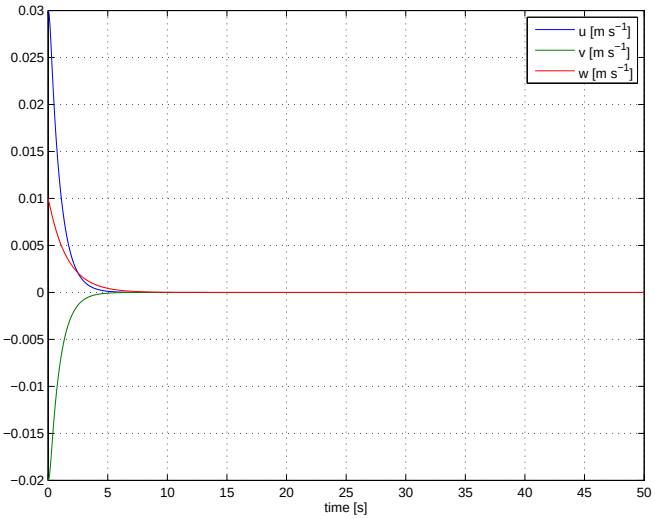

Figure B.4: *LQ* Regulation of Velocity

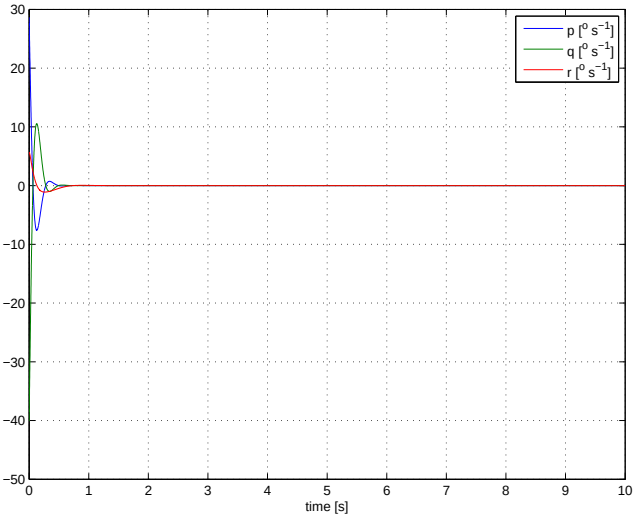

Figure B.5: *PID* Regulation of Angular Rtae

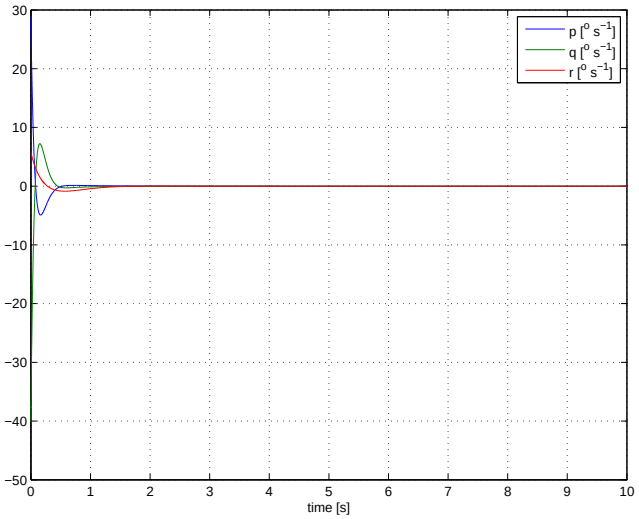

Figure B.6: *LQ* Regulation of Angular Rate

Appendix C

U–Turn Maneuver

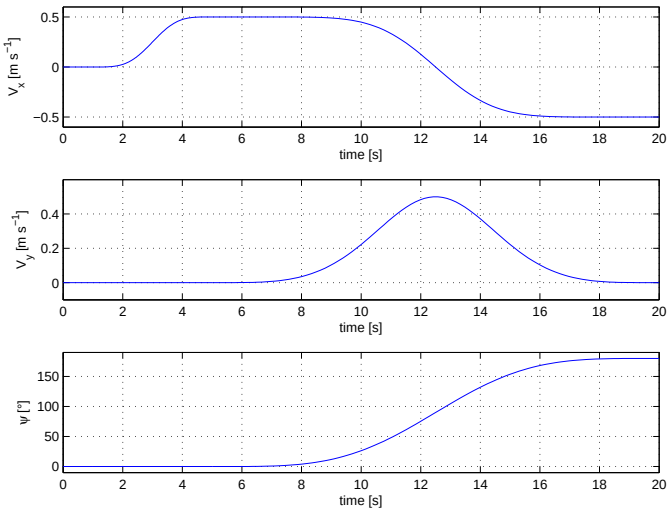

Figure C.1: U–Turn Maneuver: Desired Trajectory

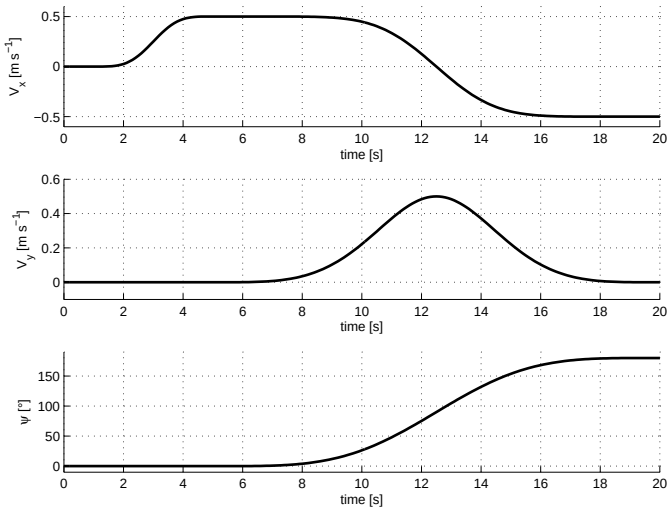

Figure C.2: U–Turn Maneuver: Tracked Trajectory

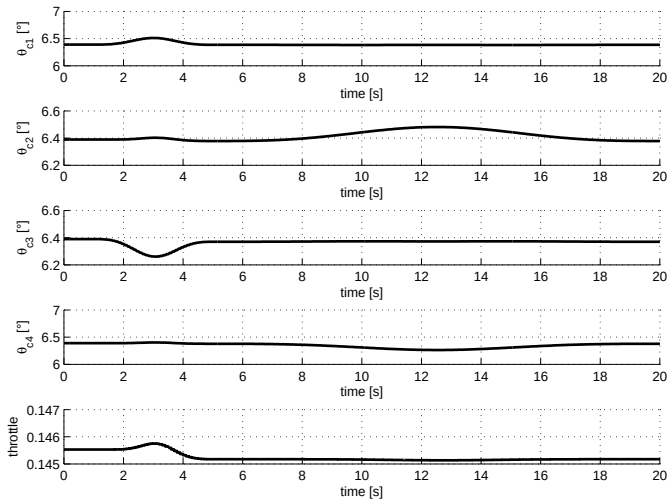

Figure C.3: U–Turn Maneuver: Rotors Pitch and Throttle

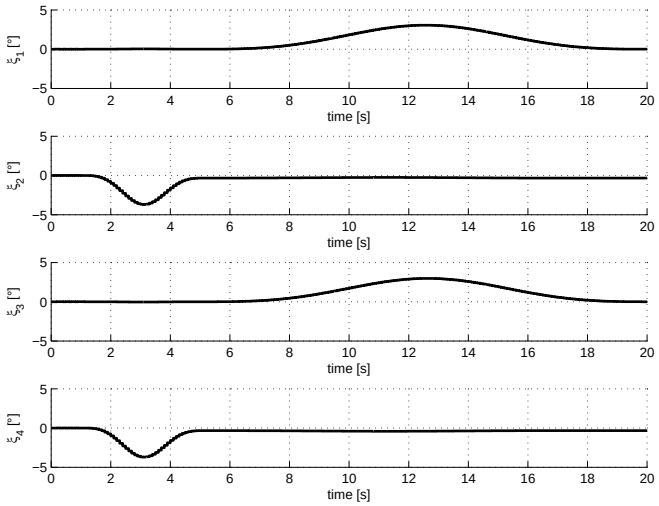

Figure C.4: U–Turn Maneuver: Rotors Tilting

Appendix D

Straight Flight with 360° Yaw–Turn

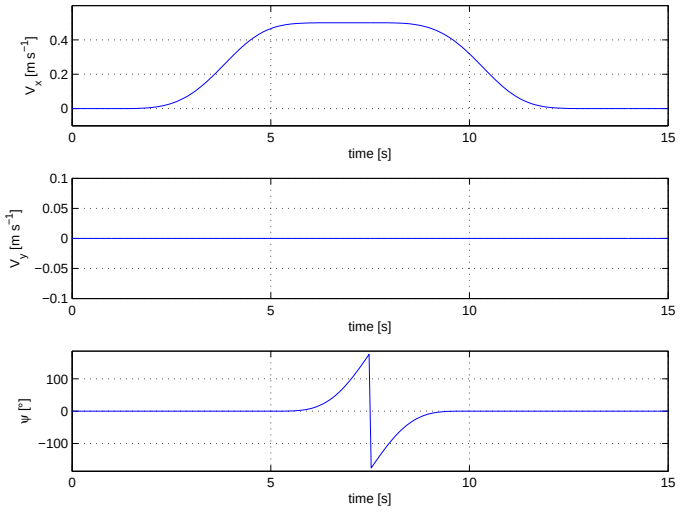

Figure D.1: Straight Flight with 360° Yaw–Turn: Desired Trajectory

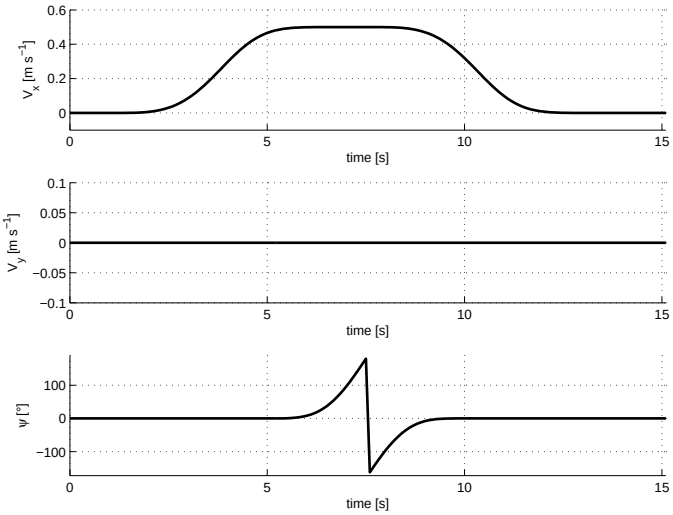

Figure D.2: Straight Flight with 360° Yaw–Turn: Tracked Trajectory

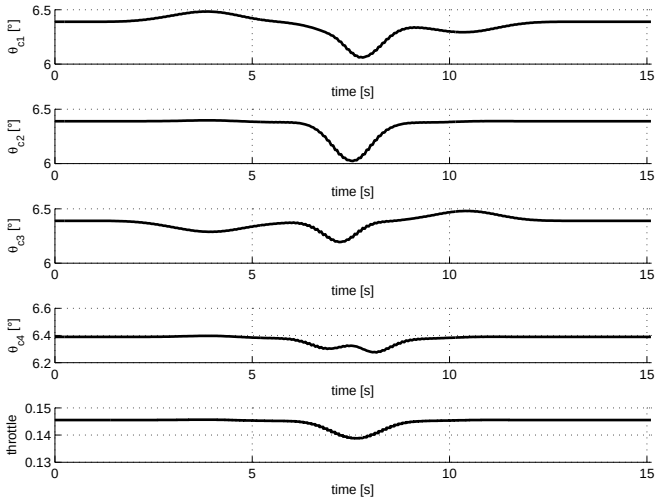

Figure D.3: Straight Flight with 360° Yaw–Turn: Rotors Pitch and Throttle

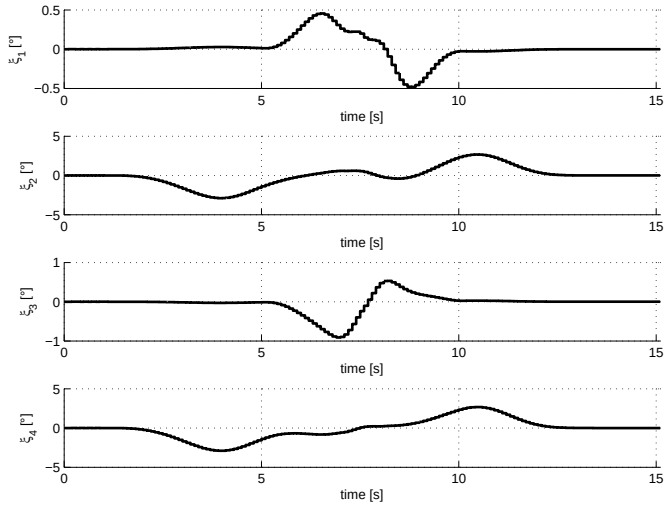

Figure D.4: Straight Flight with 360° Yaw–Turn: Rotors Tilting

Appendix E

360^{o} Yaw–Turn

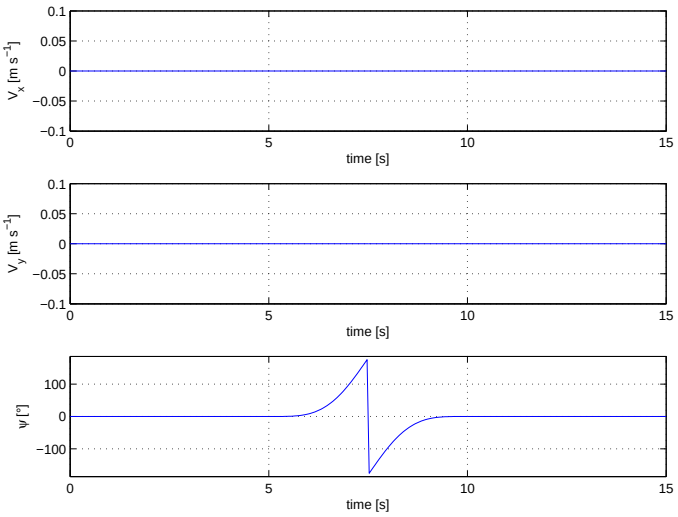

Figure E.1: 360^{o} Yaw–Turn: Desired Trajectory

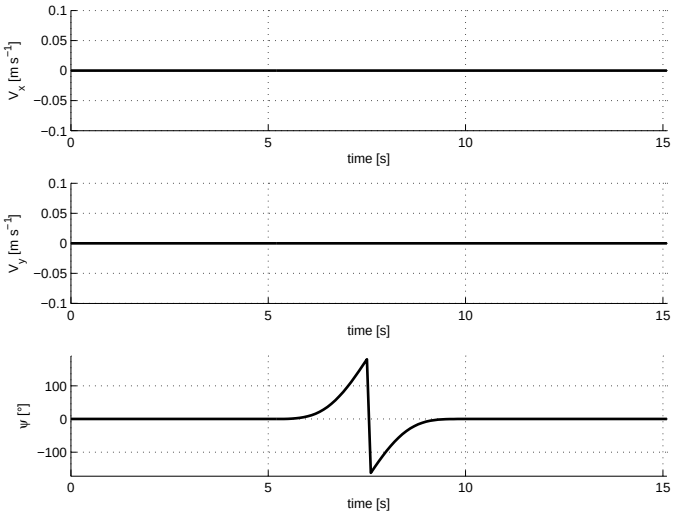

Figure E.2: 360° Yaw–Turn: Tracked Trajectory

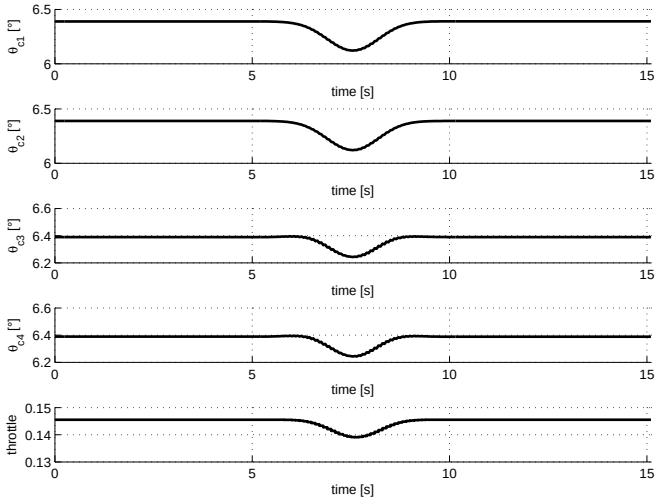

Figure E.3: 360° Yaw–Turn: Rotors Pitch and Throttle

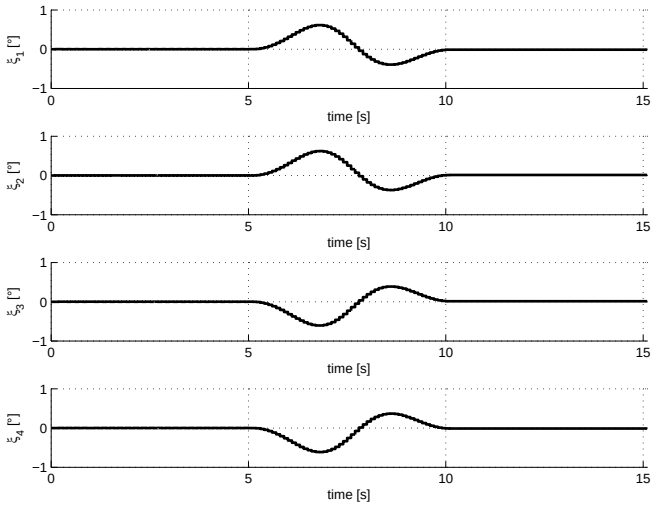

Figure E.4: 360° Yaw–Turn: Rotors Tilting

Appendix F

Straight Flight with Rolling Tilt

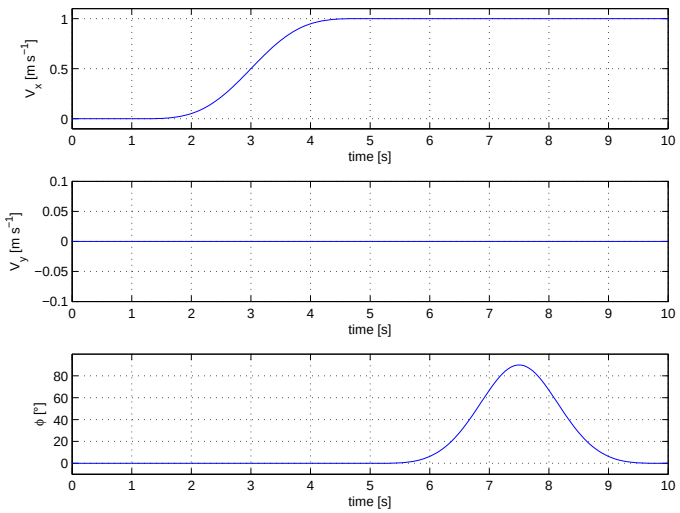

Figure F.1: Straight Flight with Rolling Tilt: Desired Trajectory

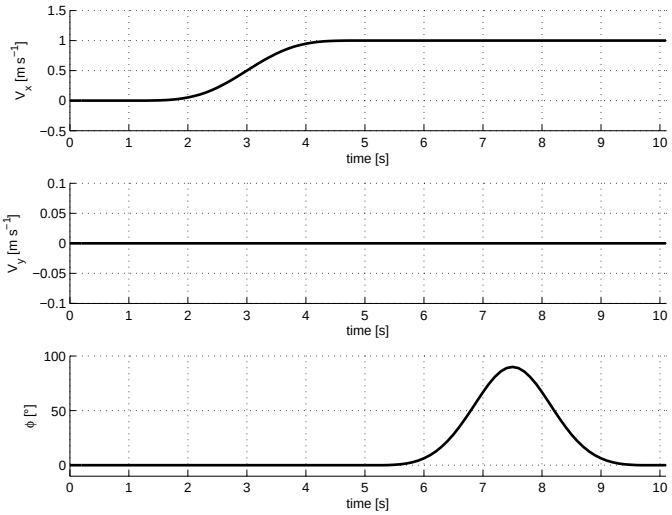

Figure F.2: Straight Flight with Rolling Tilt: Tracked Trajectory

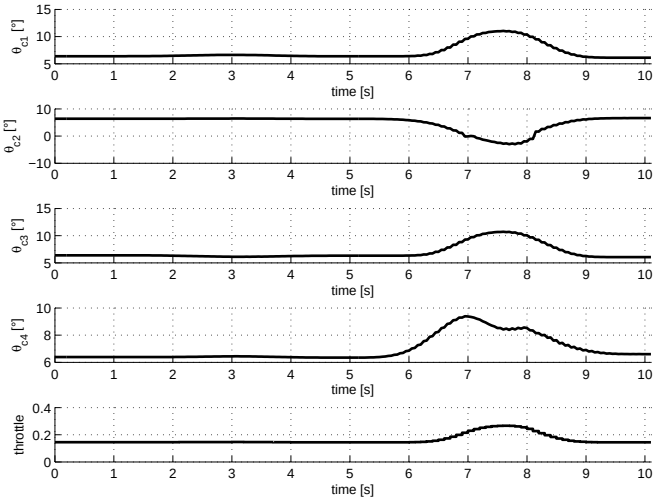

Figure F.3: Straight Flight with Rolling Tilt: Rotors Pitch and Throttle

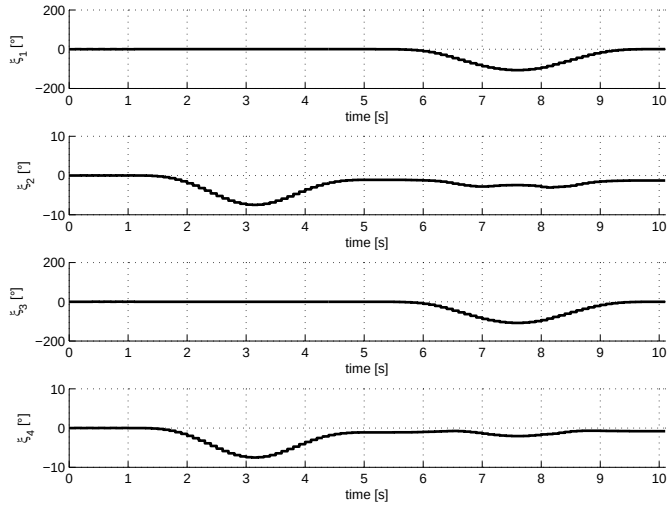

Figure F.4: Straight Flight with Rolling Tilt: Rotors Tilting

Appendix G

Hovering with Not Null Attitude

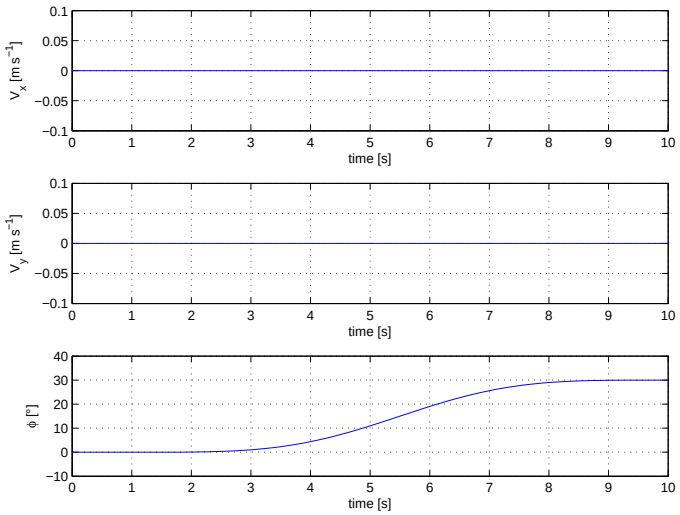

Figure G.1: Hovering with Not Null Attitude: Desired Trajectory

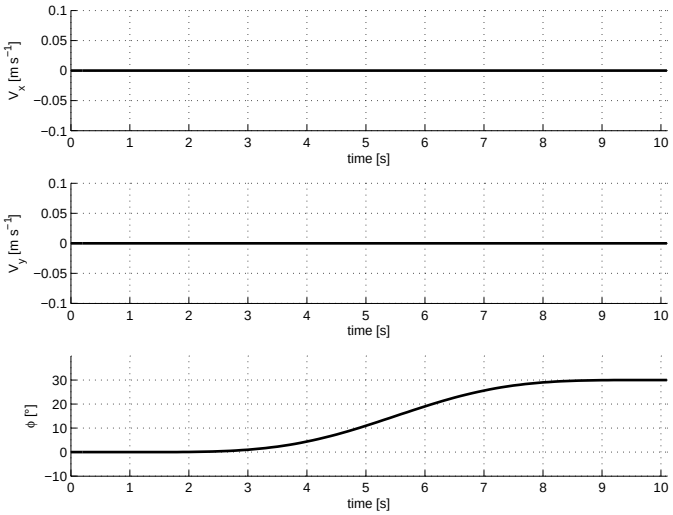

Figure G.2: Hovering with Not Null Attitude: Tracked Trajectory

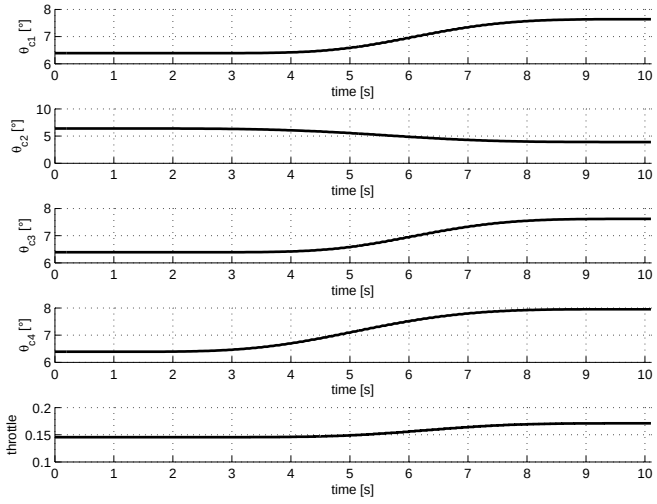

Figure G.3: Hovering with Not Null Attitude: Rotors Pitch and Throttle

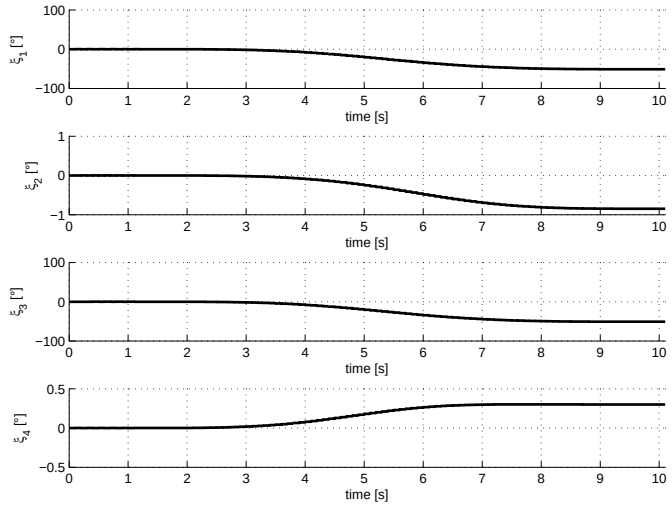

Figure G.4: Hovering with Not Null Attitude: Rotors Tilting